

ไฮโดรฟอร์มิลเลชันและไฮดรอกซีเมทิลเลชันของซิส-1,4-พอลิบิวทาไดอินน้ำหนักระดับสูง  
ด้วยตัวเร่งปฏิกิริยา



นางสาว ศศิโสสม อิมเอิบสิน

สถาบันวิทยบริการ  
จุฬาลงกรณ์มหาวิทยาลัย

วิทยานิพนธ์นี้เป็นส่วนหนึ่งของการศึกษาตามหลักสูตรปริญญาวิทยาศาสตรดุษฎีบัณฑิต

สาขาวิชาเคมีเทคนิค ภาควิชาเคมีเทคนิค

คณะวิทยาศาสตร์ จุฬาลงกรณ์มหาวิทยาลัย

ปีการศึกษา 2546

ISBN 974-17-4172-3

ลิขสิทธิ์ของจุฬาลงกรณ์มหาวิทยาลัย

CATALYTIC HYDROFORMYLATION AND HYDROXYMETHYLATION OF  
HIGH MOLECULAR WEIGHT C/S-1,4-POLYBUTADIENE



Miss Sasisom Im-erbsin

สถาบันวิทยบริการ  
จุฬาลงกรณ์มหาวิทยาลัย  
A Dissertation Submitted in Partial Fulfillment of the Requirements  
for the Degree of Doctor of Philosophy in Chemical Technology

Department of Chemical Technology

Faculty of Science

Chulalongkorn University

Academic year 2003

ISBN 974-17-4172-3

Thesis Title           CATALYTIC HYDROFORMYLATION AND HYDROXYMETHYLATION  
                                  OF HIGH MOLECULAR WEIGHT *CIS*-1,4-POLYBUTADIENE

By                         Miss Sasisom Im-erbsin

Field of Study         Chemical Technology

Thesis Advisor        Professor Pattarapan Prasassarakich, Ph.D.

Thesis Co-advisor    Professor Garry L. Rempel, Ph.D.

---

Accepted by the Faculty of Science, Chulalongkorn University in Partial  
Fulfillment of the Requirements for the Doctor's Degree

..... Dean of the Faculty of  
Science  
(Professor Piamsak Menasveta, Ph.D.)

THESIS COMMITTEE

..... Chairman  
(Associate Professor Tharapong Vitidsant)

..... Thesis Advisor  
(Professor Pattarapan Prasassarakich, Ph.D.)

..... Thesis Co-advisor  
(Professor Garry L. Rempel, Ph.D.)

..... Member  
(Professor Ratana Jiratananon, Ph.D.)

..... Member  
(Associate Professor Nuanphun Chantarasiri, Ph.D.)

..... Member  
(Associate Professor Somkiat Ngamprasertsith, Ph. D.)

ศศิโสม อิมเอิบสิน : ไฮโดรฟอร์มมิเลชันและไฮดรอกซีเมทิลเลชันด้วยตัวเร่งปฏิกิริยาของซิส-1,4-พอลิบิวทาไดอีนน้ำหนักโมเลกุลสูง (CATALYTIC HYDROFORMYLATION AND HYDROXYMETHYLATION OF HIGH MOLECULAR WEIGHT CIS-1,4-POLYBUTADIENE) อ. ที่ปรึกษา : ศ. ดร. ภัทรพรณ ประศาสน์สารกิจ, อ.ที่ปรึกษาร่วม : Prof. Garry L. Rempel หน้า 136 ISBN 974-17-4172-3

ไฮโดรฟอร์มมิเลชัน และไฮดรอกซีเมทิลเลชัน จัดเป็นกระบวนการพอลิเมอไรเซชันภายหลังเพื่อเติมหมู่ฟังก์ชัน เช่น หมู่แอลดีไฮด์ และ หมู่ไฮดรอกซีบนสายพอลิเมอร์ พอลิเมอร์ที่ว่องไวสามารถใช้สำหรับการกราฟต์ ปฏิกิริยาเชื่อมขวาง หรือปฏิกิริยาดัดแปรอื่นๆ งานวิจัยนี้เป็นการศึกษาไฮโดรฟอร์มมิเลชันของยางสังเคราะห์พอลิบิวทาไดอีนน้ำหนักโมเลกุลสูงโดยใช้  $\text{HRh}(\text{CO})(\text{PPh}_3)_3$  เป็นตัวเร่งปฏิกิริยาในตัวทำละลายมอนอคลอโรเบนซีน ระดับการเปลี่ยนแปลงตรวจสอบด้วย  $^1\text{H}$  NMR สเปกโทรสโกปี จากการออกแบบการทดลองเชิงตัวประกอบแบบ  $2^4$  แฟกทอ-เรียล อุณหภูมิ ความดัน และความเข้มข้นของตัวเร่งปฏิกิริยาเป็นตัวแปรที่สำคัญ การศึกษาจลนพลศาสตร์เชิงรายละเอียดทำในเครื่องปฏิกรณ์แบบกะ และเครื่องปฏิกรณ์แบบกะที่มีการควบคุมด้วยคอมพิวเตอร์ เพื่อติดตามปริมาณของแก๊สสังเคราะห์ที่ถูกใช้ไปในระหว่างช่วงปฏิกิริยา ผลจลนพลศาสตร์เสนอปฏิกิริยาไฮโดรฟอร์มมิเลชันเป็นอันดับหนึ่งกับความเข้มข้นของตัวเร่งปฏิกิริยา ความเข้มข้นของพันธะคู่คาร์บอน และความดันรวมของไฮโดรเจนและคาร์บอนมอนอกไซด์ที่อัตราส่วนหนึ่งต่อหนึ่ง ศึกษาผลของความเข้มข้นของคาร์บอนมอนอกไซด์ในแก๊สสังเคราะห์ การเติมไตรฟีนิลฟอสฟิน และความเร็วของการกวนด้วย งานวิจัยนี้เสนอและอภิปรายกลไกของกระบวนการเร่งปฏิกิริยา

ไฮดรอกซีเมทิลเลชันเกิดขึ้นด้วยปฏิกิริยาต่อเนื่องไฮโดรจิเนชันของไฮโดรฟอร์มมิเลตพอลิบิวทาไดอีน โดยใช้  $\text{Ru}(\text{CH}=\text{CH}(\text{Ph}))\text{Cl}(\text{CO})(\text{PCy}_3)_2$  ภายใต้ภาวะความดันและอุณหภูมิสูง สมบัติเชิงความร้อนไฮโดรฟอร์มมิเลตและไฮดรอกซีเมทิลเลตพอลิบิวทาไดอีนถูกตรวจสอบ ผลที่ได้พบว่าไฮโดรฟอร์มมิเลชันสามารถเพิ่มค่าอุณหภูมิล้าวยแก้วของผลิตภัณฑ์ อย่างไรก็ตามความต้านทานความร้อนของไฮโดรฟอร์มเมตและไฮดรอกซีเมทิลเลตพอลิบิวทาไดอีนลดลง เนื่องจากความไม่เสถียรของหมู่ฟังก์ชันบนสายพอลิเมอร์

ภาควิชา	เคมีเทคนิค	ลายมือชื่อนิสิต.....
สาขาวิชา	เคมีเทคนิค	ลายมือชื่ออาจารย์ที่ปรึกษา.....
ปีการศึกษา	2546	ลายมือชื่ออาจารย์ที่ปรึกษาร่วม.....

## 4273830923 : MAJOR CHEMICAL TECHNOLOGY

KEY WORD: HYDROFORMYLATION / HYDROXYMETHYLATION / *CIS*-1,4-POLYBUTADIENE / RHODIUM CATALYST

SASISOM IM-ERBSIN : CATALYTIC HYDROFORMYLATION AND HYDROXYMETHYLATION OF HIGH MOLECULAR WEIGHT *CIS*-1,4-POLYBUTADIENE.

THESIS ADVISOR : PROF. PATTARAPAN PRASASSARAKICH, Ph.D. THESIS

COADVISOR : PROF. GARRY L. REMPEL, Ph.D. pp. 136 ISBN 974-17-4172-3.

Catalytic hydroformylation and hydroxymethylation of unsaturated polymers is a post polymerization process to introduce reactive functionalized groups such as aldehyde groups or hydroxyl groups, onto backbone polymers. This reactive polymer can be used for grafting, crosslinking or further modification reactions. The hydroformylation of high molecular weight *cis*-1,4-polybutadiene in the presence of  $\text{HRh}(\text{CO})(\text{PPh}_3)_3$  as catalyst and monochlorobenzene as solvent was studied. The degree of conversion was examined using  $^1\text{H-NMR}$  spectroscopy. From a  $2^4$  factorial experimental design, temperature, catalyst concentration and total pressure appear to be significant factors. A detailed kinetic study was carried out in a Parr batch reactor and a computer controlled batch reactor by monitoring the amount of synthesis gas consumed during the reaction time. The kinetic results indicate that the hydrofomylation is first order with respect to each of catalyst concentration, and carbon-carbon double bond concentration and  $\text{H}_2/\text{CO}$  pressure (1:1 ratio) in the pressure range of 13.8 and 30 bar. Effects of CO concentration in synthesis gas, added triphenylphosphine, and stirring speed were also studied. Mechanistic aspects of the catalytic process are discussed.

Hydroxymethylation was achieved by subsequent hydrogenation of hydroformylated polybutadiene using  $\text{Ru}(\text{CH}=\text{CH}(\text{Ph}))\text{Cl}(\text{CO})(\text{PCy}_3)_2$  under fairly severe conditions. The thermal properties of the hydroformylated and hydroxymethylated polybutadiene were characterized. The results show that the hydroformylation can increase the glass transition temperature of the polymer. However, the thermal stability of hydroformylated and hydroxymethylated polybutadiene does not significantly change.

Department	Chemical Technology	Student's signature.....
Field of study	Chemical Technology	Advisor's signature.....
Academic year	2003	Co-advisor's signature.....

## ACKNOWLEDGEMENTS

I wish to express my gratitude to advisor, Prof. Pattarapan Prasassarakich and co-advisors, Prof. Garry L. Rempel, for their valuable support, constant encouragement and deep appreciation for their guidance throughout this work. Also, sincere thanks go to members of thesis committee: Prof. Ratana Jiratananon, Assoc. Prof. Tharapong Vitidsant, Assoc. Prof. Nuanphun Chantarasiri and Assoc. Prof. Somkiat Ngamprasertsith for all useful advices.

Special thanks to all people in the associated institutions and companies for their kind assistance and collaboration:

Golden Jubilee Scholarship (Thailand Research Fund) and Natural Science and Engineering Research Council of Canada (NSERC) for financial support during Ph.D. program.

Dr. Neil T. McManus for his warm supports, brilliant suggestion and kind advices during this study.

Technicians of the Department of Chemical Technology, Chulalongkorn University and the Department of Chemical Engineering, University of Waterloo, Canada for their helps.

Dr. Kitikorn Charmondusit, Miss Napida Hinchiranun, and Mr. Aungsuthon Mahittikul for wise discussions, good memories and friendships.

Dr. Rungnapa Tangtongkul for guiding on modeling work.

All colleagues and my friends for contributed suggestion, assistance, and worthy friendships.

Finally, I wish to express great gratitude to all my family members, especially, my mother and father, for their love and encouragement throughout the tenure of my Ph.D. program.

# CONTENTS

	PAGE
ABSTRACT (in Thai).....	iv
ABSTRACT (in English).....	v
ACKNOWLEDGMENTS.....	vi
CONTENTS.....	vii
LIST OF TABLES.....	xi
LIST OF FIGURES.....	xii
LIST OF SCHEMES.....	xvii
NOMENCLATURE.....	xviii
CHAPTER I: INTRODUCTION.....	1
1.1 Chemical Modification of Diene-Based Polymers.....	1
1.2 Polybutadiene.....	3
1.3 Catalytic Hydroformylation and Hydroxymethylation.....	4
1.3.1 Hydroformylation and Hydroxymethylation of C=C.....	5
1.3.2 Hydroformylation and Hydroxymethylation of Polymers.....	10
1.4 Objective and Scope.....	16
CHAPTER II: EXPERIMENTAL AND DATA ANALYSIS.....	17
2.1 Materials.....	17
2.2 Catalyst and Ligand Preparation.....	17
2.2.1 HRh(CO)(PPh <sub>3</sub> ) <sub>3</sub> .....	19
2.2.2 Rh <sub>4</sub> (CO) <sub>12</sub> .....	21
2.2.3 Rh <sub>6</sub> (CO) <sub>16</sub> .....	22
2.2.4 [Rh(COD)Cl] <sub>2</sub> .....	22
2.2.5 Rh(COD) <i>acac</i> .....	22
2.2.6 P(OC <sub>6</sub> H <sub>4</sub> C(CH <sub>3</sub> ) <sub>3</sub> ) <sub>3</sub> .....	23
2.2.7 RuHCl(CO)(PCy <sub>3</sub> ) <sub>2</sub> .....	23
2.2.8 Ru(CH=CHPh)Cl(CO)(PCy <sub>3</sub> ) <sub>2</sub> .....	24
2.3 Parr Batch Reactor System.....	26
2.3.1 Description of Parr Batch Reactor System.....	26
2.3.2 Bomb Assembly Procedure.....	27

## CONTENTS (continued)

	PAGE
2.3.3 Hydroformylation reaction in A Parr reactor.....	28
2.3.4 Experimental Design.....	28
2.3.5 Kinetic Study.....	30
2.4 Computer Controlled Batch Reactor System (Gas Uptake Apparatus).....	30
2.4.1 Description of Gas Uptake Apparatus.....	30
2.4.2 Assembly the Reactor for Gas Uptake Apparatus.....	33
2.4.3 Hydroformylation in Gas Uptake Apparatus.....	33
2.4.4 Kinetic Studies and Univariate Experiment.....	34
2.5 Characterization.....	35
2.5.1 Fourier Transform – Infrared Spectroscopic Analysis.....	35
2.5.2 <sup>1</sup> H and <sup>13</sup> C Nuclear Magnetic Resonance Spectroscopic Analysis.....	35
2.6 Thermal Analysis and Film Properties.....	36
2.6.1 Thermogravimetric Analysis (TGA).....	36
2.6.2 Differential Scanning Calorimetry (DSC).....	36
2.6.3 Swelling Measurement and Resistance to Solvent.....	36
2.7 Determination of Degree of hydroformylation and hydroxymethylation.....	37
<b>CHAPTER III: HYDROFORMYLATION OF HIGH MOLECULAR WEIGHT</b>	
<i>CIS</i> -1,4-POLYBUTADIENE IN A PARR BATCH REACTOR.....	38
3.1 Product Identification for Hydroformylated PBD.....	39
3.2 Hydroformylation Catalyzed by Various Rh Complexes.....	43
3.3 The 2 <sup>4</sup> Experimental Design.....	44
3.4 Kinetics of Hydroformylation by using Parr Batch Reactor.....	47
3.4.1 Effect of Stirring Speed.....	50
3.4.2 Effect of Temperature.....	50
3.4.3 Effect of %CO in Synthesis.....	52
3.4.4 Effect of Catalyst Concentration.....	54



## CONTENTS (continued)

	PAGE
3.4.5 Effect of Total Pressure.....	55
3.4.6 Effect of Added PPh <sub>3</sub> .....	56
3.5 Reaction Mechanism and Rate Law.....	57
<b>CHAPTER IV: HYDROFORMYLATION OF HIGH MOLECULAR WEIGHT CIS-1,4-POLYBUTADIENE USING A COMPUTER CONTROLLED BATCH REACTOR SYSTEM.....</b>	
	<b>60</b>
4.1 Kinetics of Hydroformylation of <i>Cis</i> -1,4-Polybutadiene using a Gas Uptake Apparatus.....	61
4.2 Hydroformylation Catalyzed by Various Rh Complexes.....	62
4.3 Kinetics of Hydroformylation in the presence of Rh <sub>4</sub> (CO) <sub>12</sub> .....	64
4.4 Kinetics of the Hydroformylation of <i>Cis</i> -1,4-Polybutadiene in the presence of HRh(CO)(PPh <sub>3</sub> ) <sub>3</sub> .....	68
4.4.1 Effect of Stirring Speed.....	68
4.4.2 Effect of Polymer Concentration.....	71
4.4.3 Effect of Temperature.....	72
4.4.4 Effect of Total Pressure of Synthesis Gas.....	74
4.4.5 Effect of %CO in synthesis gas.....	75
4.4.6 Effect of Catalyst Concentration.....	76
4.4.7 Effect of PPh <sub>3</sub> addition.....	77
4.4.8 Effect of Solvent Type.....	78
4.5 Reaction Mechanism and Rate Law.....	79
<b>CHAPTER V: HYDROXYMETHYLATION OF HIGH MOLECULAR WEIGHT CIS-1,4-POLYBUTADIENE.....</b>	
	<b>85</b>
5.1 Product Identification for Hydroxymethylated PBD.....	86
5.2 Hydroxymethylation of High Molecular Weight of <i>Cis</i> -1,4-Polybutadiene.....	91
5.3 Mechanism of Hydroxymethylation and Hydrogenation.....	92
<b>CHAPTER VI: PHYSICAL PROPERTIES OF HYDROFORMYLATED AND HYDROXYMETHYLATED POLYBUTADIENE.....</b>	
	<b>95</b>

## CONTENTS (continued)

	PAGE
6.1 Differential Scanning Calorimetry (DSC).....	96
6.2 Thermogravimetric Analysis (TGA).....	101
6.3 Swelling Properties of Hydroformylated PBD Film.....	105
CHAPTER VII: CONCLUSION AND RECOMMENDATIONS.....	109
7.1 Conclusion.....	109
7.1.1 Hydroformylation of High Molecular Weight <i>Cis</i> -1,4-PBD in a Parr Batch Reactor.....	109
7.1.2 Hydroformylation of High Molecular Weight <i>Cis</i> -1,4-PBD using a Computer Controlled Batch Reactor.....	110
7.1.3 Hydroxymethylation of High Molecular Weight <i>Cis</i> -1,4-PBD.....	110
7.1.4 Physical Properties of Hydroformylated and Hydroxymethylated PBD.....	111
7.2 Recommendations.....	112
REFERENCES.....	113
APPENDICES.....	118
APPENDIX I.....	119
APPENDIX II.....	120
APPENDIX III.....	130
APPENDIX IV.....	132
APPENDIX V.....	133
VITA.....	136

## LIST OF TABLES

TABLE		PAGE
1.1	Industrial oxo process.....	9
1.2	Comparison of hydroformylation of polydiene by $\text{HRh}(\text{CO})(\text{PPh}_3)_3$ .....	14
2.1	Rhodium complexes under hydroformylation condition.....	17
2.2	The summarized condition for hydroformylation of polybutadiene in $2^4$ factorial design: temperature (A), pressure (B), polymer concentration (C), and catalyst concentration (D).....	29
3.1	The results of hydroformylation of PBD using Rh (I) complexes.....	43
3.2	Results for hydroformylation of polybutadiene in $2^4$ factorial design: temperature (A), pressure (B), polymer concentration (C), and catalyst concentration (D).....	44
3.3	Kinetic results of univariate experiment.....	49
4.1	Investigation of hydroformylation of <i>cis</i> -1,4-PBD using various Rh complexes.....	63
4.2	Kinetic results of PBD hydroformylation catalyzed by $\text{Rh}_4(\text{CO})_{12}$ in gas uptake apparatus.....	64
4.3	Kinetic results of univariate experiments in the presence of $\text{HRh}(\text{CO})(\text{PPh}_3)_3$ .....	69
4.4	Effect of solvent on the PBD hydroformylation.....	79
4.5	Model parameter estimates.....	81
4.6	Model analysis of variance results.....	81
5.1	IR absorption of functional groups in polybutadiene, hydroformylated, and hydroxymethylated polybutadiene.....	87
5.2	Peak assignment of $^1\text{H}$ NMR spectrum of hydroformylated (Figure 5.2a) and hydroxymethylated (Figure 5.2b) polybutadiene.....	89
5.3	Results of hydroformylation and hydroxymethylation of high molecular weight <i>cis</i> -1,4-polybutadiene.....	91
6.1	DSC and TGA results of PBD, hydroformylated PBD, and hydroxymethylated PBD.....	99
6.2	The solvent resistance of hydroformylated PBD film with various %CHO..	106

## LIST OF FIGURES

FIGURE	PAGE
2.1 $^1\text{H}$ -NMR spectra of $\text{HRh}(\text{CO})(\text{PPh}_3)_3$ .....	20
2.2 $^{31}\text{P}$ -NMR spectra of $\text{HRh}(\text{CO})(\text{PPh}_3)_3$ .....	20
2.3 $^1\text{H}$ -NMR spectra of $\text{Ru}(\text{CH}=\text{CHPh})\text{Cl}(\text{CO})(\text{PCy}_3)_2$ .....	25
2.4 $^{31}\text{P}$ -NMR spectra of $\text{Ru}(\text{CH}=\text{CHPh})\text{Cl}(\text{CO})(\text{PCy}_3)_2$ .....	25
2.5 Flow diagram of computer controlled batch reactor system (Gas uptake apparatus) (Mohammadi, 1987).....	32
3.1 FT-IR spectra of a) <i>cis</i> -1,4-polybutadiene b) hydroformylated <i>cis</i> -1,4-polybutadiene, $[\text{C}=\text{C}] = 370 \text{ mM}$ ; $[\text{Rh}] = 326 \mu\text{M}$ ; $\text{P}_{\text{H}_2/\text{CO}} = 13.8 \text{ bar}$ , $\text{H}_2:\text{CO} = 1:1$ ; $\text{T} = 40^\circ\text{C}$ ; Time = 24 h.....	40
3.2 $^1\text{H}$ -NMR spectra of a) <i>cis</i> -1,4-polybutadiene b) <i>cis</i> -1,4-hydroformylated polybutadiene, $[\text{C}=\text{C}] = 370 \text{ mM}$ ; $[\text{Rh}] = 326 \mu\text{M}$ ; $\text{P}_{\text{H}_2/\text{CO}} = 13.8 \text{ bar}$ ; $\text{H}_2:\text{CO} = 1:1$ ; $\text{T} = 40^\circ\text{C}$ ; Time = 15 h.....	41
3.3 $^{13}\text{C}$ -NMR spectra of a) <i>cis</i> -1,4-polybutadiene b) <i>cis</i> -1,4-hydroformylated polybutadiene, $[\text{C}=\text{C}] = 370 \text{ mM}$ ; $[\text{Rh}] = 326 \mu\text{M}$ ; $\text{P}_{\text{H}_2/\text{CO}} = 13.8 \text{ bar}$ ; $\text{H}_2:\text{CO} = 1:1$ ; $\text{T} = 40^\circ\text{C}$ ; Time = 15 h.....	42
3.4 The normal probability plot for the $2^4$ factorial design for the hydroformylation of polybutadiene.....	45
3.5 Plots of a) Main effects for hydroformylation of polybutadiene: temperature ( $\bullet$ ), pressure ( $\blacksquare$ ), polymer concentration ( $\blacktriangle$ ) and catalyst concentration ( $\times$ ), b) AB interaction and c) AD interaction for hydroformylation of polybutadiene.....	46
3.6 Conversion profile for hydroformylation ( $\bullet$ ) and hydrogenation ( $\blacksquare$ ) of polybutadiene, $[\text{C}=\text{C}] = 370 \text{ mM}$ ; $[\text{Rh}] = 326 \mu\text{M}$ ; $\text{P}_{\text{H}_2/\text{CO}} = 68.9 \text{ bar}$ ; $\text{H}_2:\text{CO} = 1:1$ ; $\text{T} = 70^\circ\text{C}$ .....	48
3.7 The first order $\ln(1-x)$ plot for hydroformylation of polybutadiene, $[\text{C}=\text{C}] = 370 \text{ mM}$ ; $[\text{Rh}] = 326 \mu\text{M}$ ; $\text{P}_{\text{H}_2/\text{CO}} = 68.9 \text{ bar}$ ; $\text{H}_2:\text{CO} = 1:1$ ; $\text{T} = 70^\circ\text{C}$ .....	48
3.8 Effect of stirring speed on rate constant, $[\text{C}=\text{C}] = 370 \text{ mM}$ ; $[\text{Rh}] = 326 \mu\text{M}$ ; $\text{P}_{\text{H}_2/\text{CO}} = 41.3 \text{ bar}$ ; $\text{H}_2:\text{CO} = 1:1$ ; $\text{T} = 70^\circ\text{C}$ .....	50

## LIST OF FIGURES (continued)

FIGURE	PAGE
3.9	Effect of temperature on rate constant (●) and conversion at 10 h (■), [C=C] = 370 mM; [Rh] = 326 μM; P <sub>H<sub>2</sub>/CO</sub> = 55.1 bar; H <sub>2</sub> :CO = 1:1.....51
3.10	Arrhenius plot for the hydroformylation of polybutadiene: [C=C] = 370 mM; [Rh] = 326 μM; P <sub>H<sub>2</sub>/CO</sub> = 55.1 bar; H <sub>2</sub> :CO = 1:1.....51
3.11	Effect of %CO in synthesis gas on rate constant (●) and conversion at 10 h (■), [C=C] = 370 mM; [Rh] = 326 μM; P <sub>H<sub>2</sub>/CO</sub> = 41.3 bar; T = 70°C.....52
3.12	Effect of catalyst concentration on rate constant at H <sub>2</sub> :CO of 3:1 (●) and 1:1 (■), [C=C] = 370 mM; P <sub>H<sub>2</sub>/CO</sub> = 41.3 bar; T = 70°C.....54
3.13	Effect of total pressure on rate constant at H <sub>2</sub> :CO of 3:1 (●) and 1:1 (■), [C=C] = 370 mM; [Rh] = 326 μM; H <sub>2</sub> :CO = 1:1; T = 70°C..... 55
3.14	Effect of added triphenyl phosphine on rate constant (●) and conversion at 10 h (■), [C=C] = 370 mM; [Rh] = 326 μM; P <sub>H<sub>2</sub>/CO</sub> = 41.3 bar; H <sub>2</sub> :CO = 1:1; T = 70°C.....56
4.1	Conversion profile (●) and 1 <sup>st</sup> order reaction plot (o) for hydroformylation of PBD using HRh(CO)(PPh <sub>3</sub> ) <sub>3</sub> : [C=C] = 370 mM, [Catalyst] = 327 μM, Solvent = MCB, P = 41.3 bar, and T = 70 °C.....61
4.2	Conversion profile of hydroformylation using various rhodium complexes, [C=C] = 370 mM; P <sub>H<sub>2</sub>/CO</sub> = 41.3 bar; H <sub>2</sub> :CO = 1:1; T = 80°C.....63
4.3	Effect of temperature on rate constant (●) and conversion at 2 h (■) in the presence of Rh <sub>4</sub> (CO) <sub>12</sub> , [C=C] = 370 mM; [Rh] = 75 μM; P <sub>H<sub>2</sub>/CO</sub> = 41.3 bar; H <sub>2</sub> :CO = 1:1.....66
4.4	Effect of total pressure on rate constant (●) and conversion at 2 h (■) in the presence of Rh <sub>4</sub> (CO) <sub>12</sub> , [C=C] = 370 mM; [Rh] = 75 μM; H <sub>2</sub> :CO = 1:1; T = 50°C.....66
4.5	Effect of catalyst concentration on rate constant (●) and conversion at 2 h (■) in the presence of Rh <sub>4</sub> (CO) <sub>12</sub> , [C=C] = 370 mM; P <sub>H<sub>2</sub>/CO</sub> = 41.3 bar; H <sub>2</sub> :CO = 1:1; H <sub>2</sub> :CO = 1:1; T = 50°C.....67

### LIST OF FIGURES (continued)

FIGURE		PAGE
4.6	a) Effect of stirring speed on rate constant (●) and conversion at 2 h (■) by using Gas Uptake Apparatus, [C=C] = 370 mM; [Rh] = 326 μM; P <sub>H<sub>2</sub>/CO</sub> = 41.3 bar; H <sub>2</sub> :CO = 1:1; T = 70°C  b) Effect of stirring speed on reaction rate in Gas Uptake Apparatus (●) and Parr reactor (■), [C=C] = 370 mM; [Rh] = 326 μM; P <sub>H<sub>2</sub>/CO</sub> = 41.3 bar; H <sub>2</sub> :CO = 1:1; T = 70°C.....	70
4.7	Effect of polymer concentration on rate constant (●) and %conversion at 2 h (■), [Rh] = 326 μM; no added PPh <sub>3</sub> ; P <sub>H<sub>2</sub>/CO</sub> = 41.3 bar; H <sub>2</sub> :CO = 1:1; T = 70°C.....	71
4.8	Effect of temperature on rate constant (●) and conversion at 10 h (■), [C=C] = 370 mM; [Rh] = 326 μM; no added PPh <sub>3</sub> ; P <sub>H<sub>2</sub>/CO</sub> = 41.3 bar; H <sub>2</sub> :CO = 1:1.....	72
4.9	a) Arrhenius plot for the hydroformylation of polybutadiene b) Eyring plot for PBD hydroformylation, [C=C] = 370 mM; [Rh] = 326 μM; no added PPh <sub>3</sub> ; P <sub>H<sub>2</sub>/CO</sub> = 41.3 bar; H <sub>2</sub> :CO = 1:1.....	73
4.10	Effect of total pressure on rate constant (●) and conversion at 2 h (■), [C=C] = 370 mM ; [Rh] = 326 μM; no added PPh <sub>3</sub> ; H <sub>2</sub> :CO = 1:1; T = 70°C.....	74
4.11	Effect of %CO in synthesis on rate constant (●) and conversion at 2 h (■), [C=C] = 370 mM ; [Rh] = 326 μM; no added PPh <sub>3</sub> ; P = 41.3 bar; T = 70°C.....	75
4.12	Effect of catalyst concentration on rate constant (●) and conversion at 2 h (■), [C=C] = 370 mM; no added PPh <sub>3</sub> ; P <sub>H<sub>2</sub>/CO</sub> = 41.3 bar; H <sub>2</sub> :CO = 1:1; T = 70°C.....	76
4.13	Effect of PPh <sub>3</sub> addition on rate constant (●) and conversion at 2 h (■), [C=C] = 370 mM; [Rh] = 326 μM; P <sub>H<sub>2</sub>/CO</sub> = 41.3 bar; H <sub>2</sub> :CO = 1:1; T = 70°C.....	77

## LIST OF FIGURES (continued)

FIGURE	PAGE
4.14 Effect of solvent types in synthesis on rate constant; monochlorobenzene (●), benzene (o), and toluene (■), [C=C] = 370 mM ; [Rh] = 326 μM; no added PPh <sub>3</sub> ; P = 41.3 bar; H <sub>2</sub> :CO = 1:1; T = 70°C.....	78
4.15 Residual plot from non-linear regression.....	81
4.16 Comparison of the conversion profiles of experiment with model prediction for 2 <sup>3</sup> factorial design experiments	
(a) Conversion profile at various polymer concentration, [Rh] = 326 μM; no added PPh <sub>3</sub> ; P <sub>H<sub>2</sub>/CO</sub> = 41.3 bar; H <sub>2</sub> :CO = 1:1; T = 70°C.....	82
(b) Conversion profile at various pressure, [C=C] = 370 mM ; [Rh] = 326 μM; no added PPh <sub>3</sub> ; H <sub>2</sub> :CO = 1:1; T = 70°C.....	82
(c) Conversion profile at various %CO of synthesis gas, [C=C] = 370 mM ; [Rh] = 326 μM; no added PPh <sub>3</sub> ; P = 41.3 bar; T = 70°C.....	83
(d) Conversion profile at various catalyst concentration, [C=C] = 370 mM; no added PPh <sub>3</sub> ; P <sub>H<sub>2</sub>/CO</sub> = 41.3 bar; H <sub>2</sub> :CO = 1:1; T = 70°C.....	83
(e) Conversion profile at various PPh <sub>3</sub> /Rh by mole, [C=C] = 370 mM; [Rh] = 326 μM; P <sub>H<sub>2</sub>/CO</sub> = 41.3 bar; H <sub>2</sub> :CO = 1:1; T = 70°C.....	84
5.1 FT-IR spectra of a) 10 % hydroformylated <i>cis</i> -1,4-polybutadiene b) hydroxymethylated <i>cis</i> -1,4-polybutadiene, [C=C] = 247 mM; [Ru] = 161 μM; P <sub>H<sub>2</sub></sub> = 41.3 bar; T = 150°C; Solvent = MCB; Time = 4 h.....	88
5.2 <sup>1</sup> H-NMR spectra of a) 10 % hydroformylated <i>cis</i> -1,4-polybutadiene b) hydroxymethylated <i>cis</i> -1,4-polybutadiene, [C=C] = 247 mM; [Ru] = 161 μM; P <sub>H<sub>2</sub></sub> = 41.3 bar; T = 150°C; Solvent = MCB; Time = 4 h.....	90
6.1 DSC thermograms of a) PBD and b) 20% hydroformylated PBD.....	98
6.2 Glass transition temperature of high molecular weight <i>cis</i> -1,4-PBD and hydroformylated PBD at various %CHO contents.....	99
6.3 DSC thermograms of 20% hydroxymethylated PBD.....	100

## LIST OF FIGURES (continued)

FIGURE		PAGE
6.4	TG curves of a) PBD and b) 18% hydroformylated PBD.....	102
6.5	a) The initial decomposition temperature ( $T_{id}$ ) and b) the maximum decomposition temperature ( $T_{max}$ ) with various %CHO contents in PBD.....	103
6.6	TG curves of a) PBD and b) 20% hydroxymethylated PBD.....	104
6.7	%Swelling of hydroformylated PBD film (75% CHO) with time.....	106
6.8	%Swelling of hydroformylated PBD film with various %CHO in (a) water..... (b) ethanol..... (c) MCB.....	107 107 108


  
 สถาบันวิทยบริการ  
 จุฬาลงกรณ์มหาวิทยาลัย



## LIST OF SCHEMES

SCHEME		PAGE
1.1	Obtained chemicals from aldehydes.....	5
3.1	Possible rhodium species in solution under hydroformylation conditions (S= solvent).....	53
3.2	Mechanism of hydroformylation of polybutadiene using $\text{HRh}(\text{CO})(\text{PPh}_3)_3$ ...	57
5.1	Mechanism for NBR hydrogenation catalyzed by $\text{Ru}(\text{CH}=\text{CH}(\text{Ph}))\text{Cl}(\text{CO})(\text{PCy}_3)_2$ .....	93
5.2	Mechanism for CPIP hydrogenation catalyzed by $\text{Ru}(\text{CH}=\text{CH}(\text{Ph}))\text{Cl}(\text{CO})(\text{PCy}_3)_2$ .....	93
5.3	Mechanism for PBD hydroxymethylation catalyzed by $\text{Ru}(\text{CH}=\text{CH}(\text{Ph}))\text{Cl}(\text{CO})(\text{PCy}_3)_2$ .....	94

  
 สถาบันวิทยบริการ  
 จุฬาลงกรณ์มหาวิทยาลัย

## NOMENCLATURES

acac	:	Acetylacetonate
BR	:	Butadiene Rubber
Co	:	Cobalt
DMTA	:	Dynamic Mechanical Analysis
DSC	:	Differential Scanning Calorimeter
EPDM	:	Ethylenepropylenediene Monomer
EtOH	:	Ethanol
FT-IR	:	Fourier Transform Infrared Spectroscopy
$k_{rds}$	:	Limiting Reaction Rate Constant
$[\eta]$	:	Intrinsic Viscosity
MCB	:	Monochlorobenzene
MW	:	Molecular Weight
NBR	:	Nitrile Butadiene Rubber
NMR	:	Nuclear Magnetic Resonance Spectroscopy
NR	:	Natural Rubber
$P(n\text{-Bu})_3$	:	Tributylphosphine
PBD	:	Polybutadiene
$PCy_3$	:	Tricyclohexylphosphine
PIP	:	Polyisoprene
PP	:	Polypropenamer
$PPh_3$	:	Triphenylphosphine
PTFE	:	Polytetrafluoroethylene
PVC	:	Poly(vinyl chloride)
Rh	:	Rhodium
Ru	:	Ruthenium
SBR	:	Styrene-Butadiene Rubber
$T_g$	:	Glass Transition Temperature
TGA	:	Thermogravimetric Temperature
THF	:	Tetrahydrofuran

**NOMENCLATURES (continued)**

$T_{id}$	:	Initial Decomposition Temperature
TMA	:	Thermomechanical Analysis
$T_{max}$	:	Maximum Decomposition Temperature
TPPTS	:	Tris(m-sulfonatophenyl)phosphine
TSH	:	<i>p</i> -Toluenesulfonyl Hydrazide



สถาบันวิทยบริการ  
จุฬาลงกรณ์มหาวิทยาลัย

# CHAPTER I

## INTRODUCTION

### 1.1 Chemical Modification of Diene-Based Polymers

Diene polymers such as natural rubber (NR), polyisoprene (PIP), polybutadiene (PBD), nitrile butadiene rubber (NBR), and styrene-butadiene rubber (SBR) are some of the most important commercial polymers. Due to the carbon-carbon double bond in the polymer backbone, these polymers can be reacted with other chemicals to produce alternative materials. In fact, the diene polymers are easily degraded due to the carbon-carbon double bond. Thus, this degradation can change the physical properties of polymers; for example, tensile strength, solubility, resistance to chemicals, etc.

Chemical modification of polymers includes such reactions as crosslinking, grafting, degradation, oxidation, isomerization, cyclization, etc. Its principal utility is to produce desirable physical and chemical properties within the polymer that are often difficult or impossible to achieve using standard polymerization techniques. Polymers generally used as substrates for chemical modifications are unsaturated polymers or polymers containing olefinic unsaturation within the polymer structure. One of the most interesting methods for the chemical modification of polymers is to introduce a functional group onto the backbone of polymers. McManus and Rempel (1995) have reviewed the catalytic chemical modification reactions such as hydrogenation, hydrosilylation, hydrocyanation, hydrocarboxylation, hydroformylation, and hydroxymethylation for diene based polymers and copolymers.

The important factors involved in the catalytic chemical modification of polymers are: (i) the reactivity of the substance; (ii) the nature of the catalyst; (iii) the reaction conditions employed; and (iv) the presence of functional groups in the polymer substance (Mohammadi, 1987). Naturally, the reactivity of C=C unsaturation in the parent polymers is lower than of the simple alkene. This can be explained by the nature of the polymer which has a higher steric hindrance. Moreover, each polymer may consist of different types of isomer present in the polymer with each isomer having different reactivity.

In general, catalytic systems are classified into two types, heterogeneous and homogeneous catalytic systems. The heterogeneous system involves a mixture of solid catalyst and liquid/gas reactant. The performance of the catalyst usually depends on the available active surface area of the catalyst since the chemical reaction proceeds via chemisorption of the reacting species on the catalyst surface. In comparison, a homogeneous system involves a single-phase reaction in which the catalyst is dissolved in the liquid phase. Important factors for the reactivity of the catalyst are the stability of the active species presented in the catalytic cycle, the activity and stability of catalyst under reaction condition, and the presence of side reactions.

For both catalytic systems, the reaction rate commonly depends on some conditions such as temperature, pressure, reactant concentration, and stirring speed. In the case of heterogeneous catalytic systems, the ease of separation of products from the reaction system is the superior advantage when compared with a homogeneous catalyst. However, in the case of polymer modification reactions, the reaction system has a high viscosity. Accordingly, it is very difficult to separate the supported catalyst from such a reaction system. Although a high thermal stability of catalyst is found, severe reaction conditions are generally needed to achieve the reaction. With high temperature, interactions occurring between the catalyst and polymer may lead to degradation and crosslinking of the polymer during the desired modification reaction.

The homogeneous catalytic system shows some advantages over the heterogeneous system for chemical modification reactions. The advantages include (i) the activity is achieved at relatively milder conditions; (ii) increased selectivity; (iii) ease of controlling modification; and (iv) ease of study. In the case of the heterogeneous catalytic system, many of the metal atoms beneath the active catalytic surface do not contribute the catalytic activity. Thus, in terms of activity per metal atom, homogeneous catalysts are generally much more active. Heterogeneous catalysts are insoluble solid catalysts, which usually have different types of sites. Even in the pure metallic state the individual metal atoms may be oriented in a number of different environments. The variation of these sites can cause difference in steric and electronic properties which may yield a variety of products. On the other hand, a homogeneous catalyst generally has only one type of active site. Thus, the selectivity and control of the reaction is generally better.

Transition metal complexes have been extensively used as homogenous catalysts. Due to Lewis-base ligands, especially phosphines and carboxylates, the modification of transition metal complexes can be easily achieved and can lead to a major improvement in catalytic reactivity, selectivity and stability.

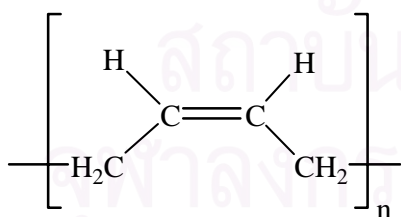
## 1.2 Polybutadiene

Polybutadiene (PBD) or butadiene rubber (BR) is one of the most important commercial polymers after poly(styrene-butadiene) and natural rubber in terms of tonnage consumed. It is produced from the 1,3-butadiene monomer containing four carbon atoms, and six hydrogen atoms ( $C_4H_6$ ). The four carbon atoms are in a chain containing two double bonds.

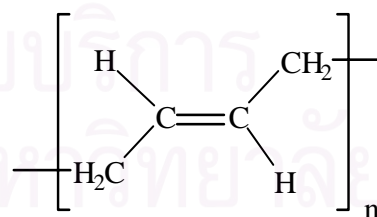


1,3-butadiene

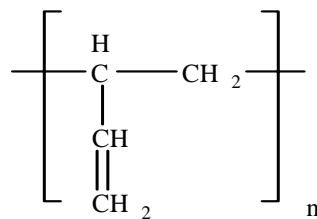
Polybutadiene is made primarily by solution polymerization or emulsion polymerization. Considering polymerization of butadiene, there are four basically stereoregular forms of polybutadiene: *cis*-1,4-, *trans*-1,4- and 1,2-polybutadiene (Barlow, 1993).



*cis*-1,4-polybutadiene



*trans*-1,4-polybutadiene



1,2-polybutadiene

By using different catalysts and/or solvents for polymerization, polybutadiene can be formed used with varying proportions of the above forms. Cis and trans forms are predominantly used in a number of applications. The trans form emerges as a fibrous material, while the cis form is a rubber. The 1,2-content of the polybutadiene also significantly influences its properties. It has been found that the 1,2- (vinyl) content of the polybutadiene rubber directly affects abrasion properties.

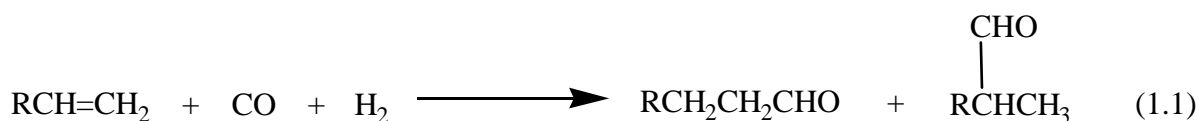
The properties of polybutadiene rubber show some superiority to both natural rubber and poly(styrene-butadiene) vulcanizates: abrasion resistance and groove cracking resistance of tyres, low-temperature flexibility, heat aging resistance, high resilience at low deformations, ozone resistance in static and dynamic, and ability to accept higher levels of filler and oil with less deterioration in properties.

It has been indicated that *cis*-polybutadiene or polybutadiene rubber is a useful blending material in the tyre industry. Because of its abrasion properties and low heat build-up and its cost. More than a half of polybutadiene produced is used for blending with poly(styrene-butadiene) in passenger-car tyres and with natural rubber in truck tyres. It is also used as the toughening rubber in high-impact polystyrene. Furthermore, it is used for producing playballs, children's toys, etc (Morton, 1973).

### 1.3 Catalytic Hydroformylation and Hydroxymethylation

Hydroformylation is one of the oldest homogeneous catalytic processes still in use today and it is responsible for producing the large amounts of aldehyde materials resulting from a homogeneous transition metal-catalyzed reaction. Earliest, Otta Roelen (of Ruhrchemie in Germany) successfully discovered the reaction to produce aldehydes from alkenes and CO/H<sub>2</sub> mixtures by using a homogenous catalyst; HCo(CO)<sub>4</sub> (Crabtree, 1988; Spessard et al., 1966; Bhaburi et al., 1979; Trzeciak and Ziolkowski, 1999). The catalytic hydroformylation of alkene is a reaction called the

'oxo process'; the C=C bond is reacted with H<sub>2</sub> and CO resulting in the formation of straight and branched chain aldehydes as shown by Eq. 1.1.

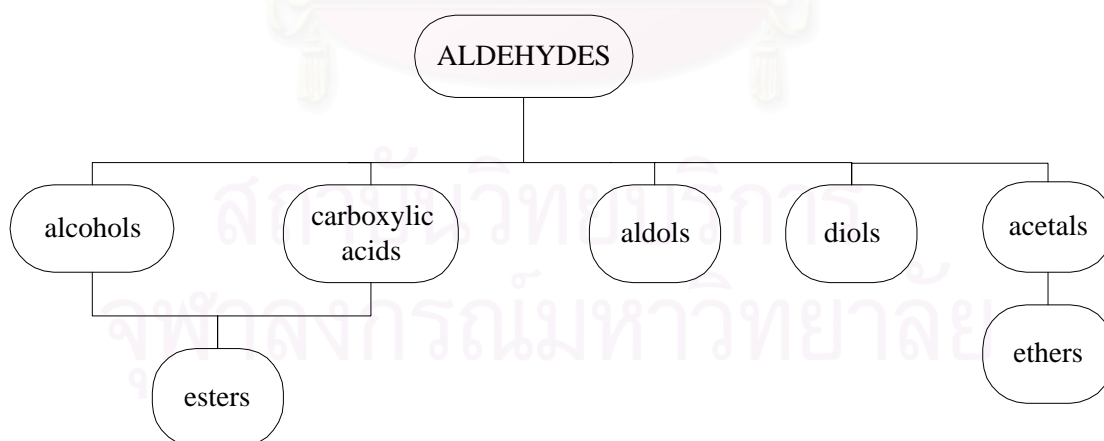


The aldehyde product resulting from hydroformylation of olefins can be reacted in a further reaction by addition of H<sub>2</sub> to give alcohol as shown in Eq 1.2.



### 1.3.1 Hydroformylation and Hydroxymethylation of C=C

The hydroformylation of C=C in alkene leads to straight and branched chain aldehydes illustrated in Eq. 1.1 and 1.2. Aldehydes are considered as industrially important raw materials. Typical chemicals obtainable from aldehydes are shown in Scheme 1.1 (Trzeciak and Ziolkowski., 1999).



**Scheme 1.1** Obtained chemicals from aldehydes (Trzeciak and Ziolkowski, 1999).

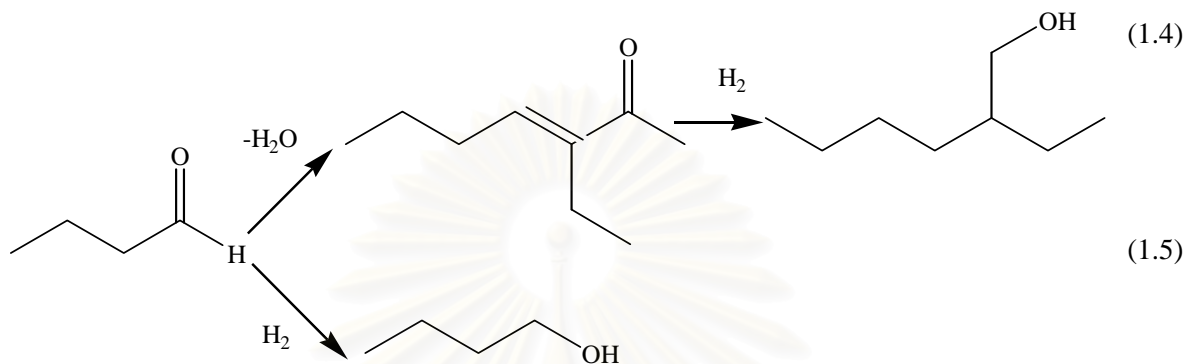
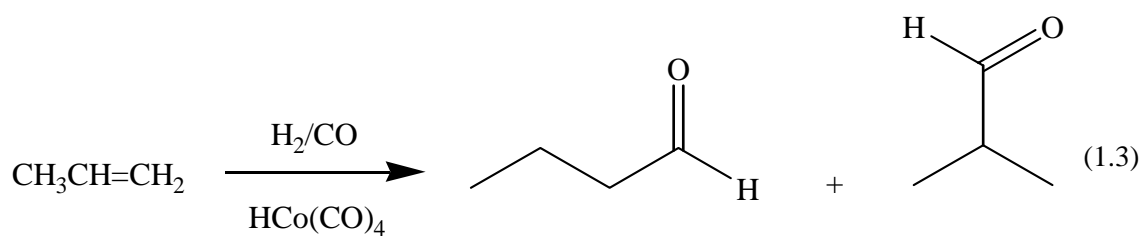
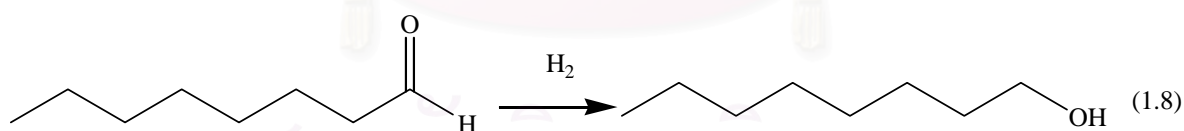
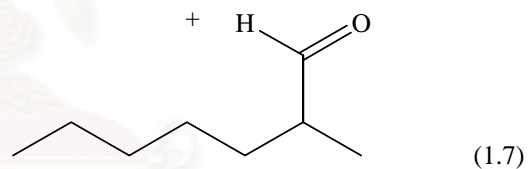
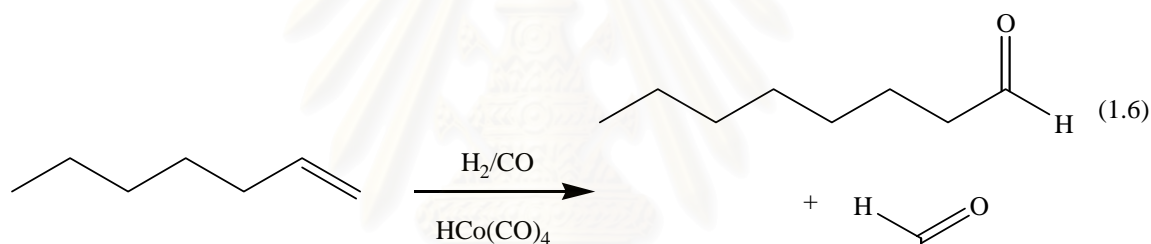
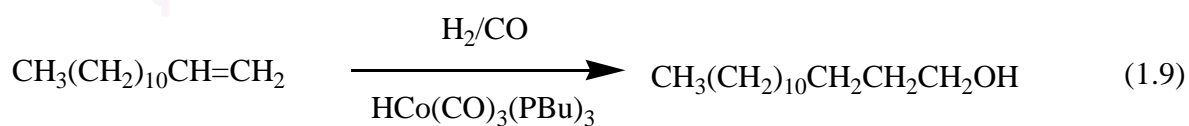
The most common feedstock for hydroformylation is propene. It can be transformed into butanal and 2-methylpropanal, the former being the much more



valuable product (Eq. 1.3). Butanal may undergo aldol condensation followed by hydrogenation to give 2-ethyl-1-hexanol (Eq. 1.4) or hydrogenated in a separate step using a heterogeneous catalyst to give 1-butanol (Eq. 1.5), a useful solvent. The hexanol is used to make a diester of phthalic acid, which then serves as an agent (called a plasticizer) for making the normally rigid plastic and flexible polyvinylchloride (PVC). Hydroformylation converts  $C_7$ - $C_9$  alkenes to aldehyde with one more carbon, which are then hydrogenated to give straight-chain alcohols, also useful as plasticizers (Eq. 1.6, 1.7, and 1.8). Alcohols containing 12 to 16 carbons result from hydroformylation-hydrogenation of corresponding alkenes with one less carbon atom. These alcohols serve as the basis for surfactant (detergent) compounds with several domestic and industrial uses (Eq. 1.9) (Crabtree, 1988; Spessard et al., 1996).

The earliest commercial catalyst for the hydroformylation was  $Co_2(CO)_8$  which is reacted with  $H_2$  under hydroformylation condition to give the active species,  $HCo(CO)_4$ . The reaction can be employed at temperature of 150 to 180°C and a total pressure of 200 to 300 bar at 50/50  $H_2/CO$ . Referring to hydroformylation of propene (Eq. 1.3), either straight chain (anti-Markovnikov) or branch chain (Markovnikov) aldehydes can be formed as butanal and 2-methylpropanal, respectively. In fact, butanal which is a straight chain aldehyde is much more valuable commercially. With  $HCo(CO)_4$ , a yield of 80% aldehydes can be obtained at the above mentioned conditions and the ratio of straight to branch chain aldehydes is about 3:1 to 4:1.

Later, a modified homogeneous cobalt based hydroformylation catalyst was developed by addition of phosphines, such as  $P(n-Bu)_3$ . This catalyst can give higher activity and selectivity under a pressure range of 50 – 150 bar. The product ratio is 7:1 of straight to branch chain aldehyde. It is believed that the steric bulk of the phosphine both encourages the formation of the less hindered straight chain aldehyde and also activates the migratory insertion in catalytic cycle.

Hydroformylation of propene:Hydroformylation of C<sub>7</sub>-C<sub>9</sub> alkenes:Hydroformylation of C<sub>11</sub>-C<sub>15</sub> alkenes:

As development of hydroformylation catalyst, the use of rhodium catalysts offers many advantages over cobalt systems (Trzeciak and Ziolkoski, 1999). The advantages of rhodium complexes are:

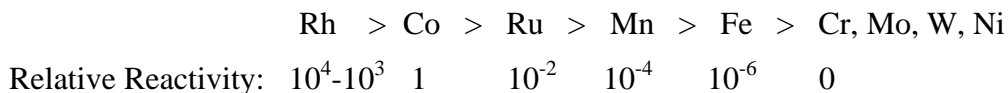
1. Rhodium based catalysts are more active and selective.
2. Modified rhodium catalysts are more selectivity than the non-modified one and requires less energy consumption.
3. Water-soluble systems of rhodium can give higher selectivity and environmental friendly.

The Rh-carbonyl cluster compound,  $\text{Rh}_4(\text{CO})_{12}$ , is a very active hydroformylation catalyst, but has very poor selectivity toward the ratio of linear to branch hydroformylation product and also serves as a good alkene hydrogenation catalyst. To get more activity and selectivity, the rhodium system was modified by addition of phosphine to obtain the more highly phosphine-substituted rhodium carbonyl hydride species,  $\text{RhH}(\text{CO})(\text{PPh}_3)_3$ . This catalyst is active at low pressure and moderate temperature (10–50 bar, 60–120°C). With this catalyst, linear to branch aldehyde product with a ratio as high as 12 to 1 can be obtained. In the presence of excess  $\text{PPh}_3$ , the ratio of straight chain aldehydes, the desired product, to the branch chain aldehydes can be optimized to as high as 30:1. This can be described by the steric hindrance effect of the bulky  $\text{PPh}_3$  ligand.

When it comes to an industrial process, it depends on what the desired product is. If linear aldehydes are the desired product, the rhodium-phosphine catalyst should be used because it can give very high selectivity toward the linear aldehydes. In contrast, if alcohols are the goal, then the use of a phosphine-modified Co catalyst is preferred due to occurrence of hydroformylation and hydrogenation by the same catalyst.

As mentioned above that the optimal phosphine for Rh-based catalysis appears to be  $\text{PPh}_3$ , not  $\text{PBu}_3$  which is used in the phosphine-modified Co process. This can be explained in that  $\text{PBu}_3$  is too good at donating electron density to the metal in case of Rh, and the intermediate catalytic species are too stable for effective catalysis.  $\text{PPh}_3$  is more suitable for modified rhodium-based catalyst for hydroformylation and have higher activity.

In addition, some other metals may serve as hydroformylation catalysts, such as Ru, Mn, Fe, Cr, etc. However, the best effective hydroformylation catalysts are Rh and Co. The overall effectiveness of these metals with respect to their reactivity is as follows (Spessard et al., 1996):



Although hydroformylation catalyzed by Ru complexes is significant slower than by Co and Rh complexes, there was a report that ruthenium complexes was used for hydroformylation of hex-1-ene under total pressure (100 bar) of H<sub>2</sub> and CO (1:1) and 120°C. The reaction achieved a yield 80% aldehydes with no side reactions, and the ratio of straight to branch aldehyde is about 2.4 (Sanchez-Delgado, 1976). Today, the effective hydroformylation catalysts used commercially are Co and Rh complexes and these catalysts are summarized in Table 1.

**Table 1.1** Industrial oxo process (Trzeciak and Ziolkowski, 1999).

Company	Precursor and active form of catalyst	Modifying ligand L	T (°C) P (bar)	n/iso
BASF, Rurchemie	Co(CO) <sub>8</sub> , HCo(CO) <sub>4</sub>	None	150-180°C 200-300 bar	2-4
Shell	Co <sub>2</sub> (CO) <sub>8</sub> , HCo(CO) <sub>3</sub> L	Phosphines	160-200°C 50-150 bar	7
Ruhrchemie	Rh <sub>4</sub> (CO) <sub>12</sub> , HRh(CO) <sub>4</sub>	None	100-140°C 200-300 bar	ca. 1
Union Carbide, Davy Powergass, Johnson- Matthey, LPO	(acac)Rh(CO) <sub>2</sub> , (acac)Rh(CO)PPh <sub>3</sub> , HRh(CO)(PPh <sub>3</sub> ) <sub>3</sub>	PPh <sub>3</sub>	60-120°C 10-50 bar	ca. 11.5
Ruhrchemie, Rhone Poulenc	[RhCl(1,3-cod)] <sub>2</sub> , HRh(CO)(TPPTS) <sub>3</sub>	TPPTS	110-130°C 40-60 bar	≥ 19

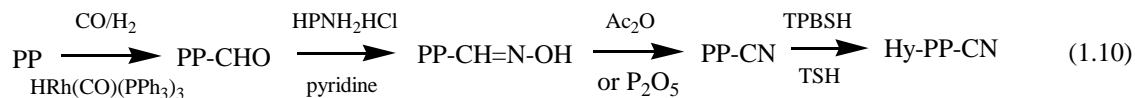
### 1.3.2 Hydroformylation and Hydroxymethylation of Polymers

Catalytic hydroformylation of unsaturated polymers is a process whereby aldehyde groups are introduced into the polymer backbone by treating with H<sub>2</sub> and CO in the presence of a catalyst. The common catalysts generally employed for this process is a Co or Rh complex. The most effective catalysts for the hydroformylation of C=C in polymer are Rh complexes. Hydridocarbonyltris(tripheylphosphine)-rhodium, HRh(CO)(PPh<sub>3</sub>)<sub>3</sub> is a catalyst which is effective for hydroformylation of polymers under the moderate conditions of pressure and temperature (10-50 bar and 60-120 °C) (Trzeciak and Ziolkowski, 1999).

Most studies reported for the hydroformylation of diene polymers, i.e. polybutadiene (PBD) and poly(styrene-butadiene) (SBR), involve rhodium catalysts. However, the earliest study showed that the hydroformylation of 1,4-polybutadiene and high-styrene SBR could be achieved at high pressure and temperature using a cobalt catalyst, [Co(CO)<sub>4</sub>]<sub>2</sub>. The reaction was carried out under a total pressure (H<sub>2</sub>:CO at 1:1) of 165 bar and temperature of 145°C for 3 h. The % double bond conversion could reach up to 100%. However, there was considerable gel formation during this process due to crosslinking of the polymer. Even under milder condition, i.e. 125°C, 2 h, 165 bar, there was gel formation and lower double bond conversion was obtained. The reason for this is the instability of hydroformylated product with crosslinking occurring due to the reactions of the aldehyde group, and probable main chain degradation during the reaction. All of this maybe caused from the use of severe conditions (Ramp, 1966).

During the discovery of rhodium complexes as hydroformylation catalyst, rhodium complexes were developed as a ligand-modified rhodium species, HRh(CO)(PPh<sub>3</sub>)<sub>3</sub>, as shown in Table 1.1. This catalyst is widely used in industrial processes because the catalyst can be easily prepared and is active under mild reaction conditions. Also, it can give high activity and selectivity. The first report of the use of HRh(CO)(PPh<sub>3</sub>)<sub>3</sub> for hydroformylation of a macromolecule was the hydroformylation of polypentenamer (PP) by Sanui et al. (1974). The reaction occurred over the total pressure range of 2-20 bar (H<sub>2</sub>:CO = 1:1) and temperature range of 25-40°C. The maximum conversion in 12 hours was 50%. This hydroformylated polypentanamer can be modified to the aldoxime (-CH=N-OH) and nitrile (-CN) derivatives as shown in Eq. 1.10. Since the nitrile derivative results from reaction of formyl group, the

degree of hydroformylation was estimated from N analysis. Moreover, direct oxidation of the formyl group and hydrolysis of the nitrile group to the carboxylic acid was carried out (Sanui et al., 1974).



where

PP	=	starting polypentenamer
PP-CHO	=	polypentenamer derivative with formyl side groups
PP-CH=NOH	=	polypentenamer derivative with aldoxime side groups
PP-CN	=	polypentenamer derivative with nitrile side groups
TPBSH	=	2,4,6-triisopropylbenzenesulfonyl hydrazine
TSH	=	p-toluenesulfonyl hydrazide
Hy-PP-CN	=	hydrogenated polypentenamer derivative with nitrile sidegroups

Ogata et al. (1976) reported the syntheses of modified polyester having pendant functional groups such as hydroxyl, formyl, aldoxime, aminomethyl, and hydroxymethyl. The hydroformylation was achieved by using  $\text{HRh(CO)(PPh}_3)_3$  under a pressure of 30/15 bar of  $\text{H}_2/\text{CO}$  and a temperature of  $40^\circ\text{C}$ . For the hydroformylation of the polyester, it was possible to achieve up to 90% conversion in 25 hours. The aldoxime groups ( $-\text{CH}=\text{NOH}$ ) can be prepared from the formyl groups by adding sufficient hydroxylamine hydrochloride and pyridine. In addition, there was subsequent reaction to obtain the aminomethyl group ( $-\text{CH}_2\text{NH}_2$ ) with the presence of acetic acid, iron powder, and zinc powder. The formyl group also can be reacted with sodium borohydride and water to give the hydroxymethyl group ( $-\text{CH}_2\text{OH}$ ).

Azuma et al. (1980) reported the preparation of functional polydiene by a two-step process for hydroxymethylation of polypentenamer and *cis*-1,4-polybutadiene. The initial reaction was hydroformylation using  $\text{HRh(CO)(PPh}_3)_3$ . The reaction occurred at reasonable rates at  $40\text{--}50^\circ\text{C}$  and 10-20 bar of a 50/50 mixture of  $\text{H}_2$  and  $\text{CO}$ . The subsequent hydrogenation reaction was carried out using a reducing agent, e.g., sodium borohydride or trimethoxyborohydride. It was shown that higher conversion leads to a problem in solubility due to the crosslinking of the hydroxyl

group with the formyl group. The use of a selective reducing agent for reduction of the formyl groups without hydrogenation at double bonds is critical.

The synthesis and characterization of hydroformylated 1,2-polybutadiene was reported by Mohammadi (1987). The reaction was carried out under a temperature of 60°C and pressure of 20 bar to reach 2-20% hydroformylation using  $\text{HRh}(\text{CO})(\text{PPh}_3)_3$  as catalyst. The subsequent hydrogenation was carried out using  $\text{RuCl}(\text{C}_6\text{H}_5\text{COO})(\text{CO})(\text{PPh}_3)_2$  as the catalyst. The formyl groups and as well as the remaining C=C bonds were completely hydrogenated. The product was characterized using  $^1\text{H}$  and  $^{13}\text{C}$  N.M.R spectroscopic analysis. It was shown that the hydroformylation product from 1,2-polybutadiene was just terminal polyaldehyde; there was no evidence of iso-branched polyaldehyde.

Later, there was a study of the hydroformylation of low molecular weight 1,2- and 1,4-polybutadiene in the presence of  $\text{HRh}(\text{CO})(\text{PPh}_3)_3$  with excess triphenylphosphine. The reaction condition involved a temperature of 80°C and a total pressure of 20 bar ( $\text{H}_2:\text{CO} = 1:1$ ). Under this condition, the conversion rate of 1,2-polybutadiene was ca. 6 times that of 1,4-polybutadiene (Tremont et al., 1990; Mill et al., 1990).

Scott and Rempel (1992) investigated the kinetics of hydroformylation of SBR using  $\text{HRh}(\text{CO})(\text{PPh}_3)_3$ . The characterization of the products by IR and  $^1\text{H}$  N.M.R. spectroscopy showed the formation of internal aldehyde groups from 1,4-units and terminal branched aldehyde groups from 1,2-units of the copolymers. The reaction was achieved at a total pressure of 0.9 bar (1:1 of  $\text{H}_2:\text{CO}$ ) and a temperature of 51°C. The kinetic studies were carried out using a computer-automated batch reactor that was designed to accurately monitor gas consumption while maintaining constant pressure. Furthermore, they postulated a possible reaction mechanism and presented an understanding of the catalyst species in solution.

Bhattacharjee et al. (1992) reported on the hydroformylation of nitrile rubber (NBR) catalyzed by  $\text{HRh}(\text{CO})(\text{PPh}_3)_3$  or  $\text{RhCl}(\text{CO})(\text{PPh}_3)_2$ . They found that the conversion was up to 30% of the double bonds. The reaction was carried out under the following conditions: 100°C and 56 bar of a 50/50  $\text{H}_2/\text{CO}$ . Gel formation was observed when the %hydroformylation was higher at 30%. In kinetic studies, it was found that  $\text{HRh}(\text{CO})(\text{PPh}_3)_3$  was more efficient than  $\text{RhCl}(\text{CO})(\text{PPh}_3)_2$ . Some

properties such as intrinsic viscosity,  $[\eta]$  and the glass transition temperature,  $T_g$  were examined. After hydroformylation,  $[\eta]$  was decreased and  $T_g$  was increased.

Sibtain and Rempel (1991) also investigated this hydroformylation and hydroxymethylation of SBR using  $\text{HRh}(\text{CO})(\text{PPh}_3)_3$  and  $\text{HRuCl}(\text{CO})(\text{PPh}_3)_3$ , respectively. The hydroformylation occurred at  $50^\circ\text{C}$  and 1 bar to yield 1-17% conversion of carbon-carbon unsaturation to aldehyde. Moreover, they reported the development of infrared calibration curves to estimate the degree of hydroformylation by comparison with the conversion calculated from the characterization by  $^1\text{H}$  NMR spectroscopy.

In the same manner, McGrath et al. (1995) reported the synthesis of novel EPDM (ethylenepropylendiene monomer) and polybutadiene polyols. The hydroformylation reaction was accomplished at high pressure (70 bar and 1:1 of  $\text{H}_2:\text{CO}$ ) and a temperature of  $100^\circ\text{C}$ . Subsequently, the aldehyde groups were reduced to hydroxymethyl groups by using a reducing agent, i.e.  $\text{NaBH}_4$ . The reduction generated the polymeric alcohol without further reaction of the remaining double bonds.

As mentioned above, all previous investigations reported the use of low molecular weight polymers having  $M_w$  less than 200,000 for hydroformylation with results of moderate conversion. Recently, Chen et al. (1997) studied the hydroformylation of higher molecular weight styrene-butadiene copolymers ( $M_w \sim 200,000$ ) under more severe reaction conditions ( $40^\circ\text{C}$  and 55 bar of 50/50  $\text{H}_2/\text{CO}$ ) in the presence of various rhodium catalysts and conversions of higher than 50% were achieved.

A comparison of the results for hydroformylation of polymers is summarized in Table 1.2. The aldehyde functionalities are reactive and can be modified to give a variety of different functionalities. The most commonly reported secondary modification is hydrogenation to give a polymer-bound hydroxyl group. There are two methods to reduce the formyl groups: non-catalytic and catalytic hydrogenation.



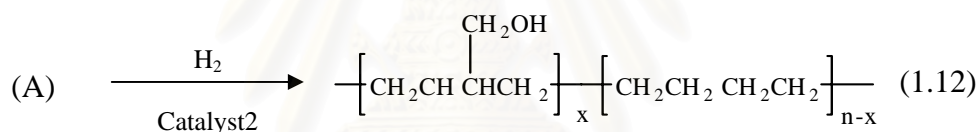
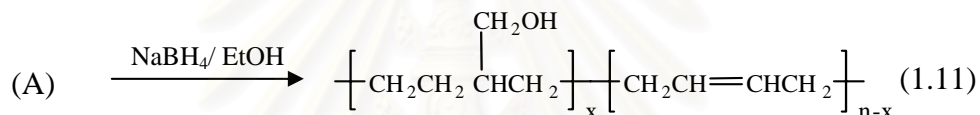
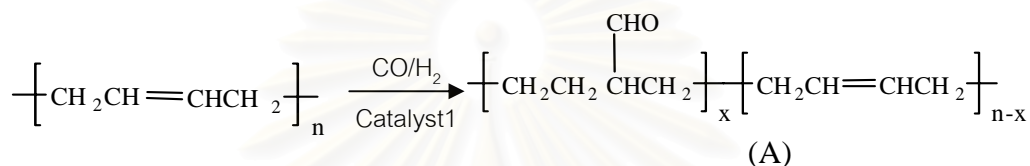
**Table 1.2** Comparison of hydroformylation of polydiene by HRh(CO)(PPh<sub>3</sub>)<sub>3</sub>.

Investigators	Polymer	M <sub>w</sub>	[Rh] <sup>b</sup> (μM)	Condition			Conversion (%)
				Temp (°C)	P <sub>H<sub>2</sub>/CO</sub> <sup>e</sup> (bar)	Time (h)	
This work	<i>cis</i> -1,4-PBD (98%)	2,000,000	326	70	55.1	10	80
Azuma et al.	<i>cis</i> -1,4-PBD (97%)	420,000	1850	40	7	4	27
			3800	40	12	4	20
			925	40	12	4	29
Mohammadii (198&)	1,2-PBD (92%)	30,000 <sup>a</sup>	580	60	2	-	5-40
Tremont et al. (1990)	<i>cis</i> -1,4-PBD	156,800	354 <sup>c</sup>	87	20	23	55
	1,2-PBD (90%)	45,790	354 <sup>c</sup>	87	20	23	69
Sibtain and Rempel (1991)	SBR	-	408	50	1	-	1-17
Scott and Rempel (1992)	SBR (82 % BD)	160,000	2080	51	0.9	~1.5	30
Chen et al. (1997)	SBR (23.5 % ST) SBR (35% ST)	222,800 252,300	437	40	13.8	19	27
			437	40	13.8	16	22
			437	40	55.1	72	80
			437	40	55.1	36	53
Bhattacharjee et al. (1992)	NBR (40% CN)	-	300 <sup>d</sup>	90	56	3	25

<sup>a</sup>Mn<sup>b</sup>[Rh] = [HRh(CO)(PPh<sub>3</sub>)<sub>3</sub>]<sup>c</sup>PPh<sub>3</sub>/[Rh] = 165 (by mole)<sup>d</sup>PP<sub>3</sub>/[Rh] = 200 (by mole)<sup>e</sup>H<sub>2</sub>/CO = 1:1

The reduction of the polyaldehyde by non-catalytic reaction involves using reducing agent such as  $\text{NaBH}_4$  in Ethanol according to Eq. 1.11 (Sanui et al., 1974; Ogata et al., 1976; Azuma et al., 1980; McGrath et al., 1995). In addition, other reducing agents have been used, i.e. Zn in  $\text{CH}_3\text{COOH}$  or  $\text{NaBH}(\text{OCH}_3)_3$  (Ogata et al., 1976; Azuma et al., 1980). In this method, there was no further reaction with  $\text{C}=\text{C}$  bond in the backbone polymers.

In the case of catalytic hydrogenation, ruthenium complexes are commonly used for reducing the formyl groups to give hydroxyl methyl groups. In fact, these complexes can hydrogenate the remaining  $\text{C}=\text{C}$  bonds in the polymer (Eq. 1.12).



Some applications of hydroformylated polymers are as follows: ion exchange resins, chelating polymers, photosensitive polymers, polymer reagents, reactive fiber, degradable polymers (Mohammadi, 1987). In addition, there has been a development of polyaldehydes obtained from unsaturated polymers for use as protective coatings (Mertzweiller et al., 1967; Cull and Mertzweiller, 1967; Mertzweiller et al., 1968), smooth and wrinkle-free films (Cull, 1967), and sizing for glass fibers (Mertzweiller, 1965). Hydroformylation results changing in hydrophobic groups to hydrophilic groups within the polymer. Such products can also possibly be used as membranes (Ogata, 1976). Due to the reactivity of the aldehyde group, the hydroformylated products can be reacted via further reaction to produce nitrile, alcohol, acetate, and amine functionalities (Sanui et al., 1974; Ogata, 1976; Azuma, 1980; Sibtain and Rempel, 1991; McGrath et al., 1995). The most often utilized subsequent reaction is hydrogenation to give a polymer having hydroxy methyl groups. The

hydroxymethylated product can be used as substrate for producing polyurethane (Tremont et al., 1990; Mills et al., 1990).

#### 1.4 Objective and Scope

Up until this time, most studies have reported on the catalytic hydroformylation of polymers having MW less than 500,000. However, higher molecular weight polymers exhibit some superior mechanical properties such as tensile properties. Thus, work on the chemical modification of high molecular weight polymers instead of polymers of lower molecular weight is important.

At present, high molecular weight of *cis*-1,4-polybutadiene can serve as a primary material for hydroformylation, thus serving as a source of information to extend the hydroformylation to other polydienes such as synthetic *cis*-1,4-polyisoprene and natural rubber. Modification of natural rubber (which is a major product in Thailand) can improve its properties and also provide alternative specialty polymers as new valued added products.

The main purpose of this study is to investigate the catalytic process for the hydroformylation of high molecular weight *cis*-1,4-polybutadiene using Rhodium complexes. The determination of significant parameters was achieved by using  $2^4$  experimental design. The parameters were identified to study the effect on degree of hydroformylation. This work also was aimed at a study of the detailed kinetics of hydroformylation of a plausible *cis*-1,4-polybutadiene to obtain an understanding of the reaction which leads to the postulation of a plausible reaction mechanism. The mechanism was proposed and fitted with the kinetic results.

The subsequent reaction called hydroxymethylation was hydrogenation of hydroformylated PBD using Ruthenium complexes. The study was achieved at various formyl loading, which was controlled in hydroformylation step. The physical properties of all products from both reactions were investigated, such as the glass transition temperature ( $T_g$ ), and the initial decomposition temperature ( $T_{id}$ ).

Due to the hydrophilic properties of the hydroformylated and hydroxymethylated products, they can possibly be used in membrane applications. In addition, it was also postulated that the mechanical properties of high molecular weight hydroformylated PBD were superior. Therefore, the film properties such as swelling and resistance to common solvents were investigated.

## CHAPTER II

### EXPERIMENTAL AND DATA ANALYSIS

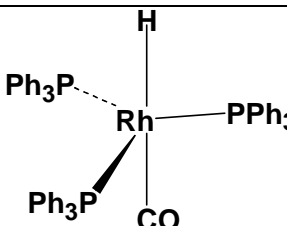
#### 2.1 Materials

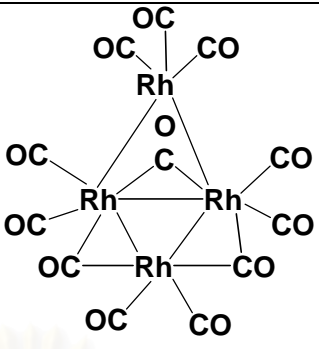
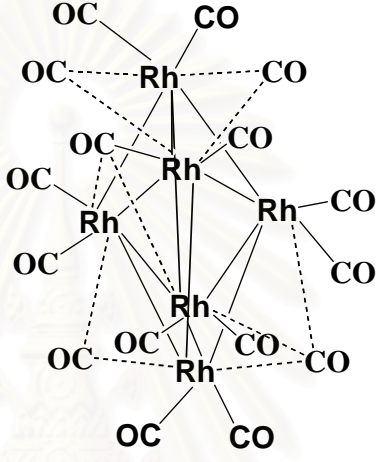
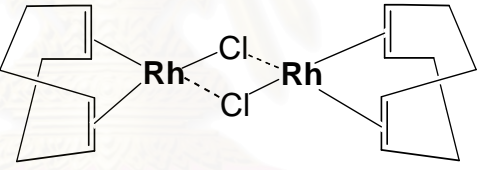
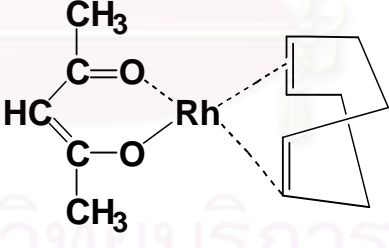
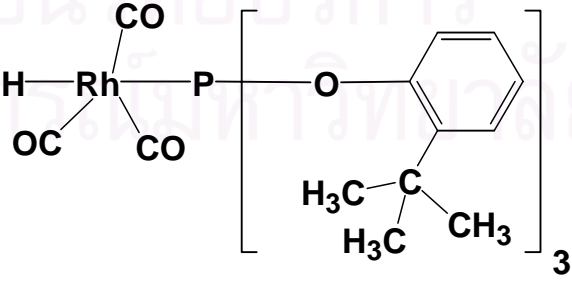
The polymer used in the present study was high molecular weight polybutadiene containing 98 wt% *cis* content, and a weight-average molecular weight of *ca.* 2,000,000-3,000,000 obtained from Aldrich Chemical Co. Analytical grade monochlorobenzene obtained from Fisher Scientific Ltd. was used as received. High purity (98%) synthesis gas of H<sub>2</sub>/CO at ratio of 1/1 was obtained from Praxair Inc.

#### 2.2 Catalyst and Ligand Preparation

The hydroformylation catalysts used in this investigation were HRh(CO)(PPh<sub>3</sub>)<sub>3</sub>, Rh<sub>4</sub>(CO)<sub>12</sub>, Rh<sub>6</sub>(CO)<sub>16</sub>, [RhCl(COD)]<sub>2</sub>, and Rh(COD)acac. For investigation of a new modified rhodium catalyst, the phosphate was prepared as tri(*o*-*t*-butylphenyl)phosphate complexes. The structures of these catalysts are presented in Table 2.1. The catalyst for subsequent hydrogenation was RuCl(CO)(CH=Cl(Ph))(PCy<sub>3</sub>)<sub>2</sub> prepared from RuHCl(CO)(PCy<sub>3</sub>)<sub>2</sub>. All catalysts were prepared according to the literature procedure (reference in Table 2.1). FT-IR and <sup>1</sup>H NMR spectroscopy was used to analyze the catalysts. To confirm their composition, the catalysts were analyzed by elemental analysis at Glueph Laboratories, Ltd (see Appendix I).

**Table 2.1** Rhodium complexes under hydroformylation condition.

Catalyst	Structure	Reference
HRh(CO)(PPh <sub>3</sub> ) <sub>3</sub>		Ahmad et al. (1974)

Catalyst	Structure	Reference
$\text{Rh}_4(\text{CO})_{12}$		Martinengo et al. (1980)
$\text{Rh}_6(\text{CO})_{16}$		Parkinson (1987)
$[\text{RhCl}(\text{COD})]_2$		Chatt and Venanzi (1957)
$\text{Rh}(\text{COD})\text{acac}$		Jongma et al. (1991)
$\text{Rh}(\text{COD})\text{acac}/$ $\text{P}(\text{OC}_6\text{H}_4\text{C}(\text{CH}_3)_3)_3$		Jongma et al. (1991)

### 2.2.1 HRh(CO)(PPh<sub>3</sub>)<sub>3</sub>

Carbonylhydridotris(triphenylphosphine)rhodium (I) was first prepared by reacting hydrazine (N<sub>2</sub>H<sub>4</sub>) with *trans*-carbonylchlorobis(triphenylphosphine)rhodium (I), RhCl(CO)(PPh<sub>3</sub>)<sub>2</sub> in ethanolic solution (Bath and Vaska, 1963). Also, it can be prepared directly from hydrated rhodium trichloride using aqueous formaldehyde as the source of the carbonyl ligand. Rhodium trichloride can be reduced by either triphenylphosphine or tetrahydroborate. This required more precaution because the reduction can produce hydrogen chloride, and in the gas phase, hydrogen chloride reacts with formaldehyde to form the potent carcinogen *bis*(chloromethyl)ether (Jardine, 1982). However, in this study this method was used since it required less time and provided a higher yield (Ahmad et al., 1974).

A solution of 0.26 g (1.0 mmol) rhodium trichloride 3-hydrate in 20 ml of ethanol was added to a vigorously stirred, boiling solution of triphenylphosphine (2.64 g, 10 mmoles) in 100 ml of ethanol. After a delay of 15 seconds, aqueous formaldehyde (10 ml, 40% w/v solution) and a solution of 0.8 g of potassium hydroxide in 20 ml of hot ethanol were added rapidly and successively to the vigorously stirred, boiling reaction mixture. The mixture was heated under reflux for 10 minutes and then allowed to cool to room temperature. The bright yellow, crystalline product was filtered, washed with ethanol, water, ethanol, and *n*-hexane, and dried in *vacuo*. The <sup>1</sup>H-NMR spectra in CD<sub>2</sub>Cl<sub>2</sub> show aromatics, phenyl, and metal hydride as seen in Figure 2.1. The <sup>31</sup>P-NMR spectra in CD<sub>2</sub>Cl<sub>2</sub> shows a singlet of phosphine (Figure 2.2).

สถาบันวิทยบริการ  
จุฬาลงกรณ์มหาวิทยาลัย

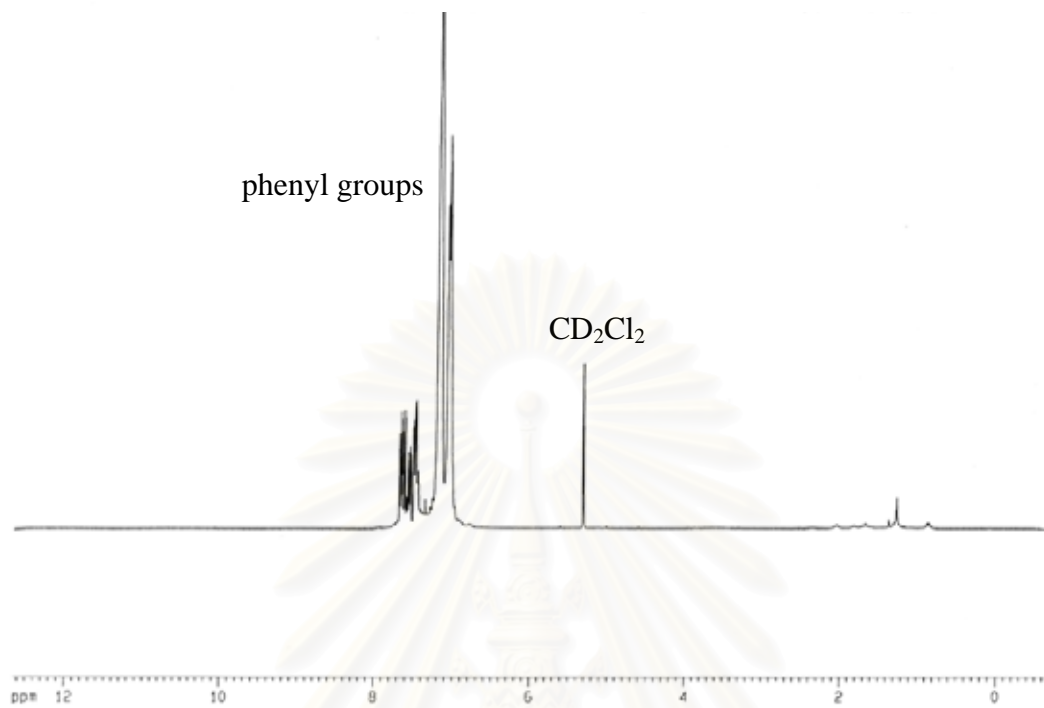


**Figure 2.1**  $^1\text{H}$ -NMR spectra of  $\text{HRh}(\text{CO})(\text{PPh}_3)_3$ .

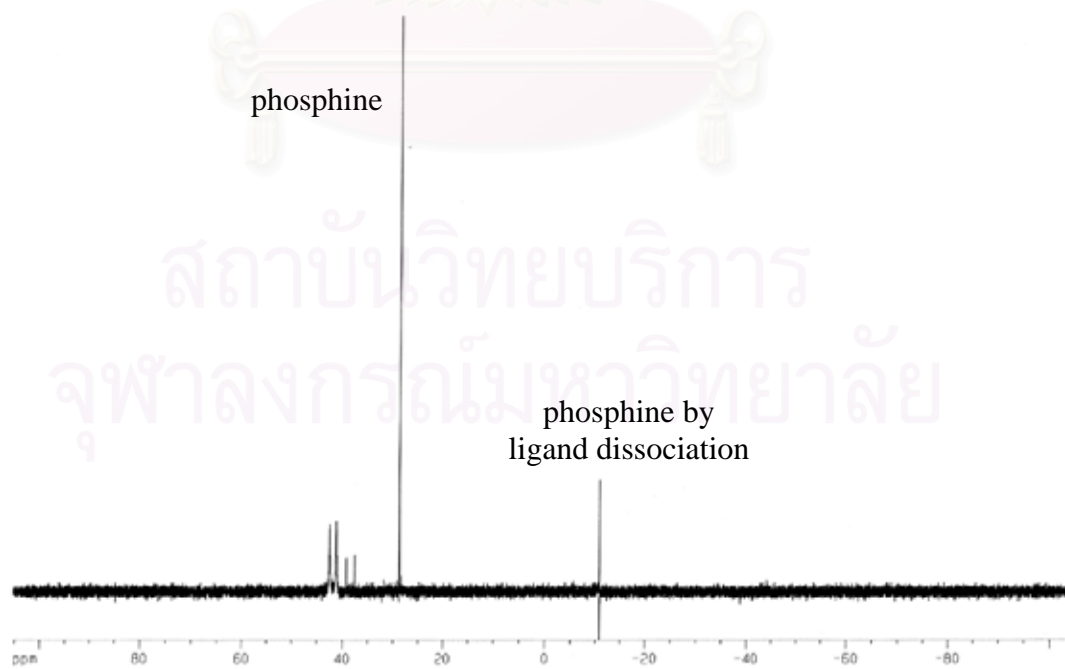


**Figure 2.2**  $^{31}\text{P}$ -NMR spectra of  $\text{HRh}(\text{CO})(\text{PPh}_3)_3$ .

### 2.2.2 $\text{Rh}_4(\text{CO})_{12}$

The preparation of  $\text{Rh}_4(\text{CO})_{12}$  followed the Martinengo's method (Martinengo et al., 1980). Tri- $\mu$ -carbonyl-nonacarbonyltettrarhodium,  $\text{Rh}_4(\text{CO})_9(\mu\text{-CO})_3$ , was prepared from  $\text{RhCl}_3 \cdot 3\text{H}_2\text{O}$ . Copper powder was first activated by washing with a mixture of concentrated hydrochloric acid and acetone and then rinsed with acetone and dried in vacuo. The solvent  $\text{CH}_2\text{Cl}_2$  may be laboratory grade and was distilled with anhydrous sodium carbonate before use. This purified method must be carefully carried out in a well-ventilated hood because carbon monoxide occurs. A two-necked, 1-L flask, equipped with a stopcock on the side neck and a magnetic stirring bar, was charged with activated copper powder (1.5 g, 24 mmole), sodium chloride (0.6 g, 10 mmole), and water (200 mL).

A 100-mL dropping funnel with a pressure-equalizing tube was then placed on the central neck. The funnel was stoppered, and the entire apparatus was pumped in *vacuo* until the water is well degassed. It then was filled through the side stop-cock with carbon monoxide from a CO-line, including a mineral oil bubbler and a pressure-release bubbler with an 80-mm mercury column. The dropping funnel was opened while CO was passed through it, and it was charged with a degassed solution of  $\text{RhCl}_3 \cdot 3\text{H}_2\text{O}$  (2.6 g, Rh 39.6%, 9.0 mmole) in water (50 mL). The funnel was closed, and the solution was dropped into the flask at a rate of about 1 mL/min while the mixture was stirred vigorously. During the addition, care must be taken that the pressure in the flask was never lower, the lack of CO can cause the partial formation of rhodium metal. The best conditions for the reaction are the continuous escape of gas from the pressure-release bubbler. For the same reason, the stirring must be vigorous enough to ensure good contact between the gaseous and aqueous phases. The rate of absorption of the CO was initially slow, but gradually increased, reaching a maximum when about half the  $\text{RhCl}_3$  solution was added.

At the end of the addition, the last traces of the  $\text{RhCl}_3$  solution in the funnel were washed down into the flask with 10 mL of degassed water, and the mixture was stirred for 2 hours. During this time, some  $\text{Rh}_4(\text{CO})_{12}$  begins to separate as an orange powder. The dropping funnel was then opened in a CO stream and charged with a degassed solution of diisodium citrate (0.4 M, 50 mL). The funnel was stoppered, and the solution of citrate was dropped into the yellow mixture over 50 minutes. The



mixture was then stirred for 20 hours, and the resulting orange suspension of the carbonyl was filtered under a carbon monoxide atmosphere. The solid was washed with water to remove all the mother liquor and then dried *in vacuo* at room temperature.

The product was extracted on a filter under CO with the minimum amount of  $\text{CH}_2\text{Cl}_2$  (about 25 mL, in 5-mL portions). The solution was quickly evaporated to dryness *in vacuo* on a water bath at room temperature, and the resulting crystalline mass was dried *in vacuo* for 2 hours to give  $\text{Rh}_4(\text{CO})_{12}$ .

### 2.2.3 $\text{Rh}_6(\text{CO})_{16}$

The hexadecacarbonylhexarhodium,  $\text{Rh}_6(\text{CO})_{16}$  was prepared by treating with CO in methanolic solution according to Parkinson (1987). One gram of  $\text{RhCl}_3 \cdot 3\text{H}_2\text{O}$  in 200 ml of 90% aqueous methanol was reacted in a one litre autoclave under 50 bar of carbon monoxide pressure for four days. The product was then collected by filtration, washed with hot hexane and dried under vacuum.

### 2.2.4 $[\text{Rh}(\text{COD})\text{Cl}]_2$

The preparation of Bis(cycloocta-1:5-diene)- $\mu\mu'$ -dichlorodirhodium,  $[\text{Rh}(\text{COD})\text{Cl}]_2$  was reported by Chatt and Venanzi (1957).

Rhodium trichloride trihydrate (1 g) in ethanol (30 ml) was boiled under reflux with the diene (2 ml) for 3 hr. The solution was cooled, and the orange solid filtered off, washed with ethanol, dried, and recrystallised from acetic acid. It was soluble in dichloromethane, moderately so in chloroform, acetic acid, and acetone, slightly soluble in ether, methanol, ethanol, and benzene, and insoluble in water.

### 2.2.5 $\text{Rh}(\text{COD})\text{acac}$

Rhodium (1,5-cyclooctadiene)-2,4-pentanedionate,  $\text{Rh}(\text{COD})\text{acac}$  was prepared from  $[\text{Rh}(\text{COD})\text{Cl}]_2$  according to Jongma et al. (1991). The dimer (2.48 g, 5 mmole), 2.5 g of  $\text{Na}_2\text{CO}_3$ , 2.5 g of 2,4-pentanedione and 20 ml of water were suspended in 60 ml of  $\text{CH}_2\text{Cl}_2$  and stirred at room temperature for 16 h. The water

layer was extracted with  $\text{CH}_2\text{Cl}_2$ . The combined  $\text{CH}_2\text{Cl}_2$  layers were evaporated till dryness.

### 2.2.6 $\text{P}(\text{OC}_6\text{H}_4\text{C}(\text{CH}_3)_3)_3$

Tri(*o*-*t*-butylphenyl)phosphite was used with  $\text{Rh}(\text{COD})\text{acac}$  to generate  $\text{Rh}(\text{CO})_3\text{P}(\text{OC}_6\text{H}_4\text{C}(\text{CH}_3)_3)_3$ . This catalyst was also mentioned in Jongma's studies (Jongsma et al., 1991). For the preparation of the ligand,  $\text{PCl}_3$  (33.6 ml, 0.38 mol) was added dropwise to 200 ml of *o*-*t*-butylphenol (1.3 mol) at  $50^\circ\text{C}$ . The mixture was then stirred overnight at  $160^\circ\text{C}$ . The product was purified by vacuum distillation and recrystallized from *n*-hexane.

### 2.2.7 $\text{RuHCl}(\text{CO})(\text{PCy}_3)_2$

$\text{RuCl}_3 \cdot 3\text{H}_2\text{O}$  (2.54 g) was dissolved in deoxygenated 2-methoxyethanol (55 ml). The red-brown solution was stirred for 5 minutes. Crystallized tricyclohexylphosphine (8.32 g) was added. The deep red solution was refluxed and stirred for 20 minutes under a nitrogen atmosphere and subsequently deoxygenated triethylamine (6 ml) was added therein. The solution was refluxed for 6 hours under nitrogen. The stirring was stopped and the solution was allowed to cool slowly for about 2 hours. Orange crystals precipitated out from the solution. The solution was filtered using Schlenk apparatus under nitrogen and the crystals were washed with deoxygenated toluene (15 ml) and subsequently dried at room temperature for 48 hours. Since the material is air sensitive, no calculation of yield was attempted. However, previous yields of about 80% based on Ru have been attained using this procedure by other investigators. The  $^{31}\text{P}$ -NMR spectrum in  $\text{C}_6\text{D}_6$ /toluene showed a singlet at 46.9 ppm, with a small additional singlet at 36.1 ppm attributable to the dichloro species  $\text{RuCl}_2(\text{CO})(\text{PCy}_3)_2$ .

Samples of  $\text{RuHCl}(\text{CO})(\text{PCy}_3)_2$  were further recrystallized from toluene. In a typical procedure, the entire sample was dissolved in dry, deoxygenated refluxing toluene (75 ml) under nitrogen. The solution was then allowed to cool slowly to room temperature, then stored in the refrigerator overnight. Orange crystals were slowly formed. The crystals were washed twice with cold deoxygenated toluene (10 ml), then dried under vacuum at  $60^\circ\text{C}$  for 5 hours to remove strongly-bound solvent. The  $^{31}\text{P}$ -

NMR spectrum in  $C_6D_6$ /toluene showed only a singlet at 46.9 ppm with no other peaks. The  $^1H$ -NMR spectrum showed a triplet, attributable to the metal-hydride, centered at  $-24.2$  ppm, and the characteristic absorbencies of the various cyclohexyl protons in the region from 2.5 to 1.2 ppm. Integrations of the hydride to cyclohexyl protons were in the ratio of approximately 1 to 66.

### 2.2.8 $Ru(CH=CHPh)Cl(CO)(PCy_3)_2$

A sample of hydride catalyst,  $RuHCl(CO)(PCy_3)_2$  (approx. 7 g) was dissolved in refluxing, dry, deoxygenated toluene (75 ml). Phenylacetylene (1.6 ml) was added to the solution using a syringe. The orange color changed to red rapidly. The reaction was cooled and stirred at room temperature overnight. The fine pinkish solid precipitate was filtered in Schlenk apparatus, washed twice with dried, deoxygenated hexane (20 ml) and dried under vacuum. The sample was dissolved in refluxing dry distilled toluene and allowed to cool slowly. The solid was then refrigerated overnight. The supernatant was separated from the crystals, which were then dried under vacuum at  $60^\circ C$  for 48 hours. The solid gradually changed from deep red to pink as it dried.

The solid sample was then dissolved in refluxing methylene chloride under nitrogen atmosphere. Hexane (15 ml) was added and the solution was slowly cooled to room temperature, then stored in the refrigerator. The precipitate was filtered in the Schlenk apparatus, washed with dry degassed hexane (20 ml), and dried in vacuum at room temperature for 48 hours. The filtrate solution volume was reduced to 30 ml by evaporation under vacuum and a further sample of solid was recovered, washed and dried in the same manner.  $^{31}P$ -NMR showed only a singlet at 27.7 ppm, indicating that the material was pure (Figure 2.3).  $^1H$ -NMR in  $CD_2Cl_2$  showed the aromatic, cyclohexyl and styryl protons in correct proportions. No metal hydride was detected (Figure 2.4).

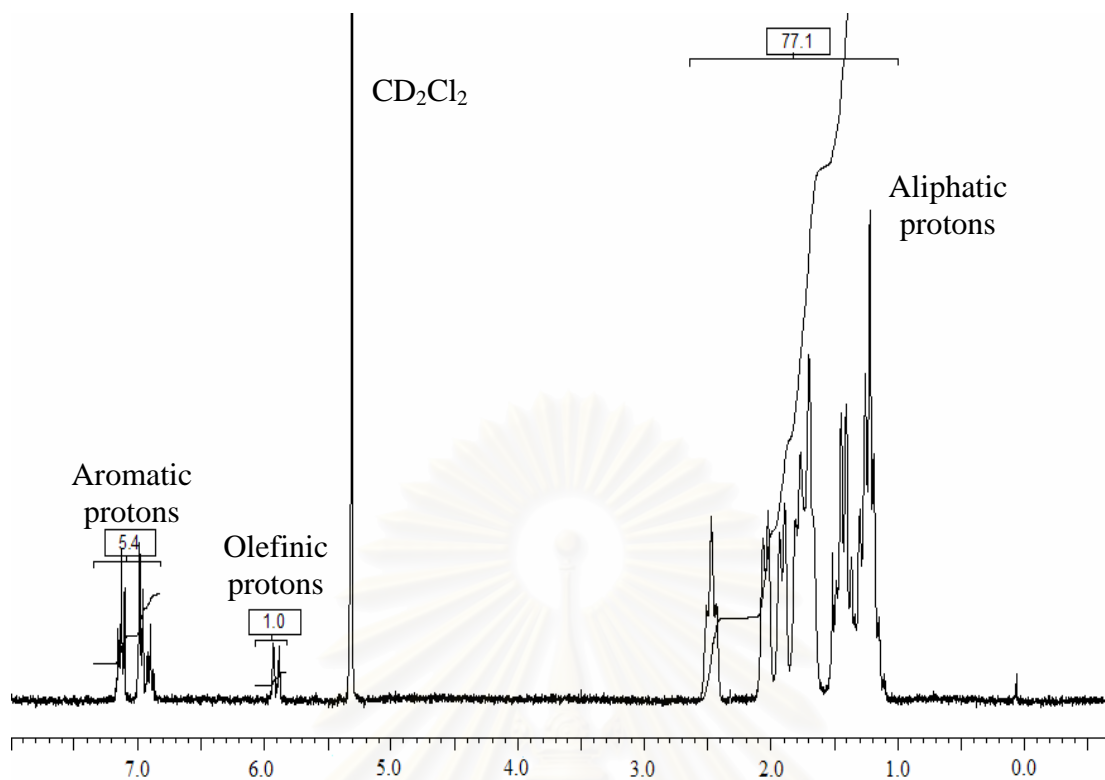


Figure 2.3  $^1\text{H-NMR}$  spectra of  $\text{Ru}(\text{CH}=\text{CHPh})\text{Cl}(\text{CO})(\text{PCy}_3)_2$ .

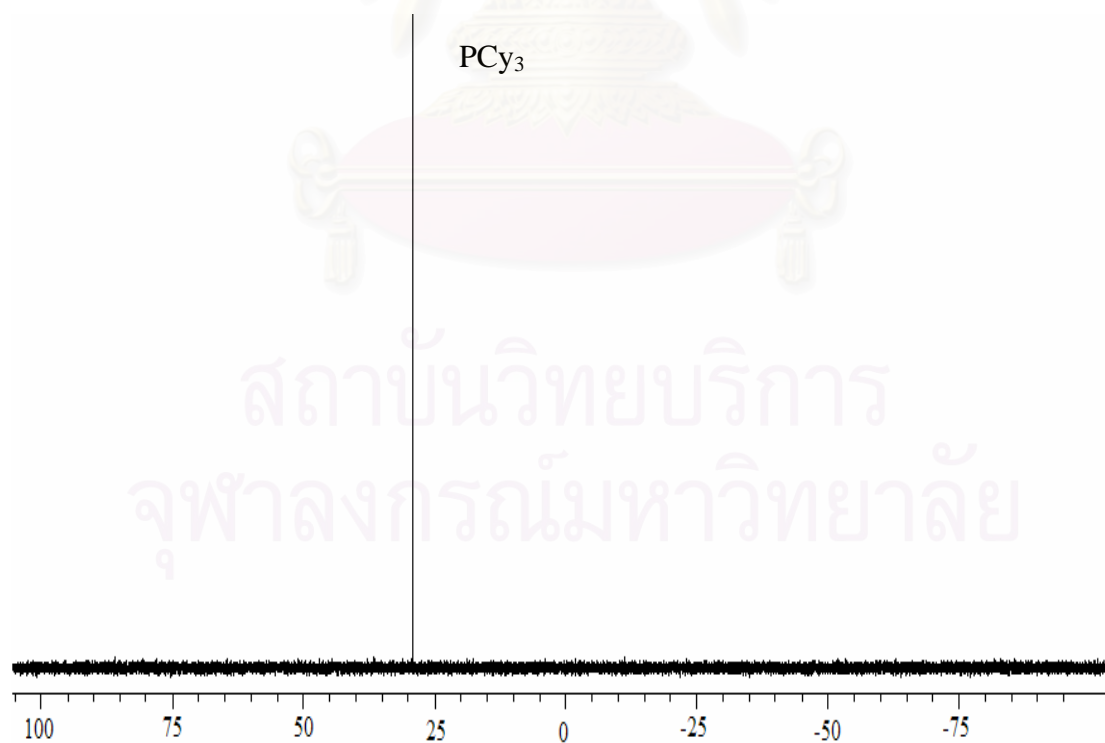


Figure 2.4  $^{31}\text{P-NMR}$  spectra of  $\text{Ru}(\text{CH}=\text{CHPh})\text{Cl}(\text{CO})(\text{PCy}_3)_2$ .

## 2.3 Parr Batch Reactor System

Batch type pressure reactors are commonly used for reactions that involve gas consumption such as hydrogenation, hydroformylation, oxidation, carbonylation, and polymerizations involving gaseous monomers. In fact, such batch reactor can be employed to investigate the kinetics due to consumption of gas as a function of time.

### 2.3.1 Description of Parr Batch Reactor System

The 300-mL mini reactor used in this study was purchased from Parr Instrument Company. A moveable reactor vessel, which is made of Type 316 stainless steel, can be sealed with a flat PTFE flat gasket held in a recess in the vessel and the magnetic drive head. The split ring closure used with this gasket has six caps, which must be tightened when pressuring. The PTFE flat gasket is inert to most chemicals and it will provide good seals under repeated opening and closing if the operating temperature does not exceed 350°C. The flat PTFE flat gasket can be used at operating temperature as high as 350°C and pressure up to 3000 psig (20.79 MPa).

The reactor was attached with a 3.5 inches-size pressure gauge (0-2000psi/140 bar) and ports such as gas inlet, dip tube for liquid sampling gas outlet, thermocouple well. Since it was desired to achieve the desired reaction temperature before the catalyst was added into the solution, a catalyst addition device was used. The gas inlet valve is an angle valve with an attached fitting which provides a socket for attaching a flexible pressure hose connected to the gas supply. The gas inlet port was connected to a dip tube, which extends to a point near the bottom of the reactor vessel. A liquid sampling port was also attached to the same fitting as the gas inlet port and connected to the same dip tube. During sampling, the gas inlet must be closed to withdraw the liquid through the liquid sampling valve. The third valve on the bomb head was a gas outlet valve connected to a side opening on the gage adapter fitting. Gas released from the reactor system will be drawn from the top of the reactor. A safety pressure rated rupture disc is attached to the reactor head to release the bomb pressure before it reaches a dangerous level. A type J thermocouple was set in a stainless steel sheath installed in the bomb head. The catalyst addition device was made of an alloy in a small cylinder shape with a lid sealed with a PTFE o-ring. The

catalyst addition device was installed inside the bomb at the same position as gas release fitting for degassing the catalyst.

The reactor was easily opened by removing it from the support stand for charging, product recovery and cleaning due to the flexible moving stirrer drive design. The Parr reactor was equipped with high temperature fabric heating mantles housed in sturdy aluminum shells. With design of this mantle, it can provide uniform heat distribution to the wall and bottom of the vessel. To prevent burn out, the heating mantle should always be attached fully to the vessel. The operating temperature in reactor was controlled by PID temperature controller which was set in the controller box. An input parameter for the temperature controller can be obtained from the thermocouple. The stirring speed drive system was connected to 1/8 hp-variable speed motor which was also set via the controller box. The controller monitors the stirring speed in units of revolutions per minute (rpm).

### **2.3.2 Bomb Assembly Procedure**

Before closing the bomb, it should be verified that the gasket is in good condition. The reactor head is replaced on the vessel and closed with two rings on the right position. Next, each of the six cap screws was tighten carefully. The bomb was let to stand for about five minutes after initial tightening; then tighten the cap screws again to compensate for the adjustment of the TFE gasket in the reactor. This can prevent the leaking of gas under loading pressure. The retaining ring (drop band) was placed around the outer part of the reactor by tightening the thumbscrew. The bomb is set in the support plate that is attached with the support stand. The head of thumbscrew on the drop band is held in the slot in the metal bracket attached to the support stand. This will prevent the rotation of the bomb when stirring. Finally, the heater was raised into a position

To open the bomb, gas is released when the gas valve is opened to discharge any internal pressure; then the six cap screws in the splitting ring sections were loosened. The cone pointed screw in the outer band was loosened and the band was lowered to rest on the table. The rings and the head attached with fittings were removed from cylinder.

### 2.3.3 Hydroformylation Reaction in a Parr Reactor

A 300-ml Parr reactor was used for high-pressure reactions. The reactor was connected to the gas supply cylinder by using the pressure hose connected to gas inlet valve. Before pressuring the reactor, all valves have to be closed except the gas inlet valve. In addition, the gas in the cylinder must be maintained at a higher pressure used than the pressure in the reactor. Otherwise, liquid will be forced out of the reactor and into the gas tank when the gas inlet valve is opened. A certain amount of purified polymer was dissolved in 100-mL solvent. Catalyst was weighed in a glass bucket, and the bucket was put in the catalyst addition device. The polymer solution was degassed by pressurizing with synthesis gas to about 24 bar, and then vented out, at a temperature below 14°C and stirrer speed of 200 rpm. This degassing of the solution was repeated three times. Subsequently, the reaction system was pressurized to slightly below the desired pressure with synthesis gas. The reactor was heated up to desired temperature and the stirrer speed was increased to 600 rpm. When the system was stable and had reached liquid/vapor thermal equilibrium, the catalyst addition device was connected to the gas supply cylinder, and then pressurized to slightly higher than the system pressure. This caused the catalyst to be dropped into the solution and the reaction was initiated. To determine the incorporation of functional groups within the polymer and to investigate conversion and the rate of the hydroformylation reaction, the polymer solution was sampled at intervals during the reaction and analyzed by  $^1\text{H}$  NMR spectroscopy.

### 2.3.4 Experimental Design

To determine the significant factors for the hydroformylation of polybutadiene,  $2^k$  factorial design was used to design the experiment. This method is widely used for screening the factors for the system. The chosen factors for the hydroformylation reaction were temperature, pressure, polymer concentration and catalyst concentration ( $k=4$ ). In this experimental design method, there are two levels “low” (-1), and “high” (+1) level. Each reaction condition is summarized in Table 2.2. Temperature, pressure, polymer concentration, and catalyst concentration are represented as A, B, C, and D, respectively. The response would be considered as the quantitative value of the degree of hydroformylation over a specified period of time.

The hydroformylation reaction was performed with observation of the final conversion after 24 h of reaction. The determination was obtained from the consideration of treatment combination in standard order following the factorial design procedure.

**Table 2.2** The summarized condition for hydroformylation of polybutadiene in  $2^4$  factorial design: temperature (A), pressure (B), polymer concentration (C)\*, and catalyst concentration (D).

Expt.	Factor					Factor level	
	A	B	C	D		Low (-)	High (+)
(1)	-	-	-	-	A ( $^{\circ}\text{C}$ )	40	80
a	+	-	-	-	B (bar)	13.8	68.9
b	-	+	-	-	C (mM)	222	370
ab	+	+	-	-	D ( $\mu\text{M}$ )	109	326
c	-	-	+	-			
ac	-	-	+	-			
bc	-	+	+	-			
abc	+	+	+	-			
d	-	-	-	+			
ad	+	-	-	+			
bd	-	+	-	+			
abd	+	+	-	+			
cd	-	-	+	+			
acd	+	-	+	+			
bcd	-	+	+	+			
abcd	+	+	+	+			

\*Polymer concentration is defined as the weight of polybutadiene divided by molecular weight of repeating unit.



### 2.3.5 Kinetic Study

The determination of the important parameters from the  $2^4$  factorial experimental design were obtained to decide on the nature of the univariate kinetic study. For the kinetic study, the degree of hydroformylation was detected by sampling the polymer solution every hour during the reaction. The polymer solutions were characterized to determine %hydroformylation. The reaction was carried out with the conversion being followed with time for a 10-h period of time.

## 2.4 Computer Controlled Batch Reactor System (Gas Uptake Apparatus)

The investigation of the gas-liquid kinetic study in the Parr reactor involved sampling the reaction mixture at specific time intervals and analyzing the samples using analytical techniques such as I.R. or N.M.R spectroscopy. Considerable errors may occur due to disturbance by sampling some solution out and limitation of amount solution to analysis. More reliable kinetic studies of the gas-consuming catalytic reactions were carried out in a computer controlled batch reactor using a system that can be maintained at constant pressure. It can be operated with minimum pressure fluctuations in the batch reactor. This system is an alternative and convenient way to observe the kinetic data by monitoring the gas consumption.

### 2.4.1 Description of Gas Uptake Apparatus

The gas uptake apparatus is used for measuring the gas consumption of the reaction as a function of time. The system used was based on the design of Mohammadi and Rempel (1987). It can be used to keep the pressure constant and record continuously the consumption or production of gases in a batch-type reactor. Further, the gas uptake apparatus was modified by Martin, McManus, and Rempel (1997) for operation at high pressure.

The reactor vessel was a  $\frac{1}{2}$  L Autoclave Engineers 'Zipperclave', with a magnetic drive agitator and a  $\frac{1}{3}$  hp brushless motor. The reactor vessel was fitted with gas feed port, gas out port, thermowell, and catalyst addition device. The vessel was heated by using a two-separated clamp on ceramic band heaters. Heating control used for the autoclave was PID digital self-tuning temperature controller with an oil

cooling system. A type K thermocouple in a thermowell was used to measure the temperature in the system. The temperature was kept constant within  $\pm 1^\circ\text{C}$ . The overall pressure system in the gas uptake apparatus consists of two separated systems: (i) a constant-pressure reactor system and (ii) a gas monitoring system. To understand this system, a schematic flow diagram for the overall system is provided in Figure 2.5.

(i) Constant – pressure system

All piping components were constructed of 316 stainless steel (1/4 inch). PT-1 and PT-2 were Validyne variable reluctance differential pressure transducers. A drop of pressure in the reactor due to the gas consumption during reaction is detected by the differential pressure transducer (PT-1). PT-1 was used to detect the pressure in the reactor and generated the signal in the form of analog voltage. The measured signal was converted to the digital signal and sent to the direct controller consisting of an IBM personal computer (PC) and a Lab-master interface. Then, it was processed by a control algorithm in the PC and converted back to analog signals. The manipulated signals from the hold are fed back to an orifice control valve (CV-1). CV-1 was a Kammer pneumatically actuated valve with integral positioner. It allowed the necessary amount of gas into the reactor and the pressure was readjusted accordingly. With this system, the error of the pressure in the vessel can be employed in  $\pm 0.02$  bar.

(ii) A gas monitoring system

Another system was used to detect the amount of gas consumption from the reaction. Due to consumption of gas in the constant-pressure reactor system, the results in the opening of CV-1 by the feedback loop mentioned above. Consequently, the reference pressure in the gasholder, which was a 150-ml steel sample cylinder, decreases. This drop of pressure was detected via the PT-2, which was also involved the Validyne variable reluctance differential pressure transducer. This result was converted into digital signal as same as for the constant-pressure system. The signal was sent to the direct digital controller with subsequent translation into moles of gas consumed. The provided data was detected online by following with monitoring and stored on a floppy disk for further analysis.

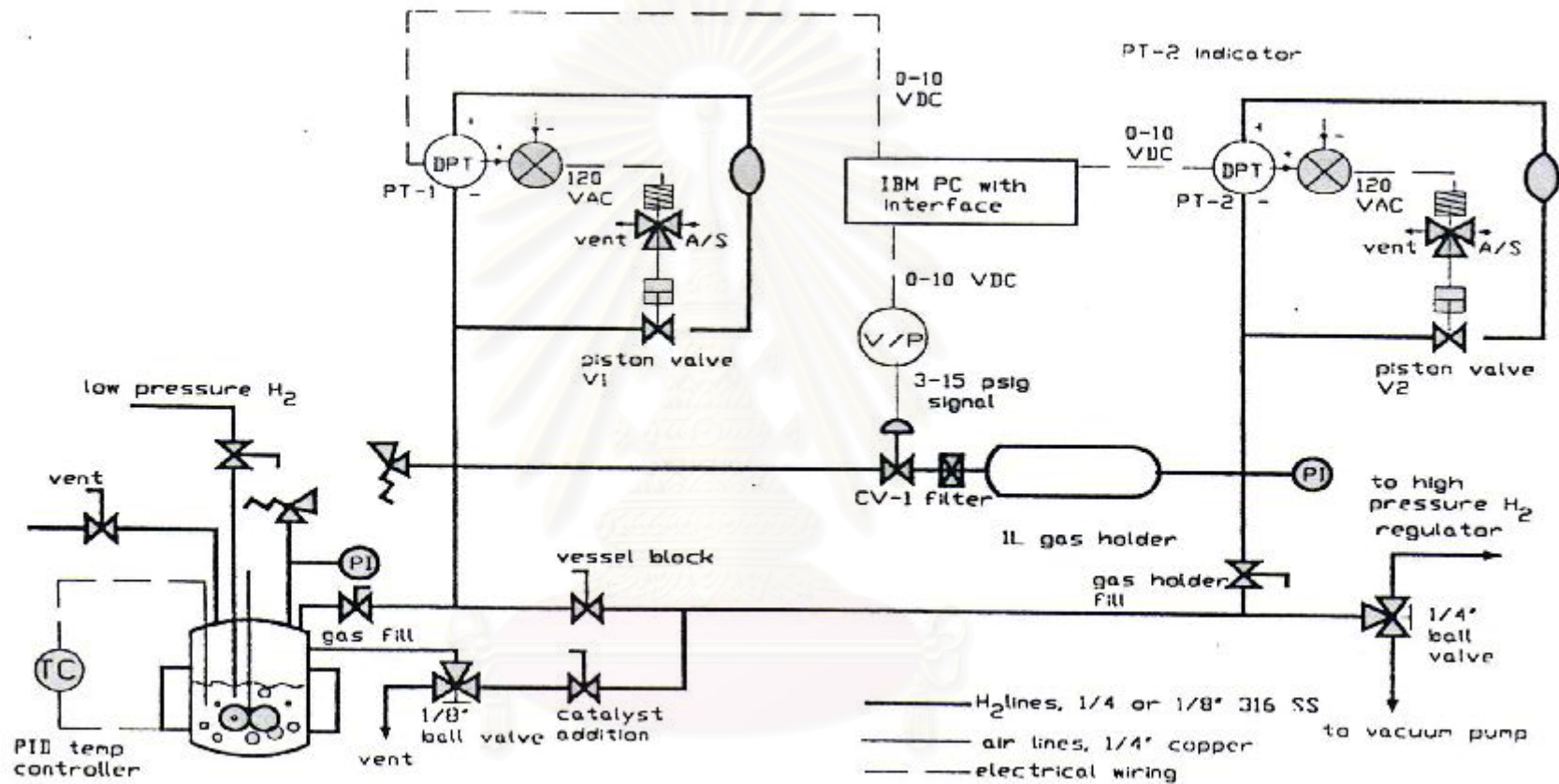


**Figure 2.5** Flow diagram of computer controlled batch reactor system (gas uptake apparatus)

(Mohammadi, 1987).

### 2.4.2 Assembly the Reactor for Gas Uptake Apparatus

Before starting assembly of the gas uptake apparatus, all tubing was blown dry and was followed by checking for leaks. If any leaks were found, the problem would be fixed before starting the experiment. Pressure in the gasholder was required in order to keep the reaction in the pressure range of 1100-1400 psi to make sure that there was enough gas for the reaction. If the pressure gauge attached to the gasholder was less than 1100 psi, the gas fill valve on the autoclave would be closed. The gasholder was simply refilled when the pressure reached 1400 psi by opening the needle valve on the regulator. The catalyst addition device was gently opened to purge the line. The catalyst addition device was replaced and the catalyst addition device was closed. The polymer solution or chemicals for operation was added into the vessel. An o-ring that is designed to be self-sealing was put in the groove on the vessel head. The vessel were replaced and lifted to fit with the vessel head by using a lab jack. The autoclave was assembled using a gentle twisting motion to ensure that the engagement pin on the heads of autoclave lines up with the notch in the autoclave body. The zipper spring was locked in the place and the reaction was started.

### 2.4.3 Hydroformylation in Gas Uptake Apparatus

The polymer solution was obtained by dissolving a certain amount of polymer in 150-mL of the reaction solvent in a 300-mL batch reactor. Catalyst was weighed into a thin glass bucket that was placed into the catalyst addition device fitted in the port of reactor head. Then, the catalyst addition device was closed. The reactor was subsequently assembled. To purge the autoclave headspace, three cycles of charging the reactor with N<sub>2</sub> to 140 psi and venting was carried out with no agitation. The venting of gas was done slowly to prevent a production of vacuum to suck the lid of catalyst addition device open and lead to an early drop of the catalyst. The reactor was chilled by immersing in an ice-water bath to reduce the vapor pressure of the reaction solvent. At a temperature below 10<sup>o</sup>C, the reactor pressure was vented and recharged with N<sub>2</sub> gas at 200 psi and the agitator was started at speed of 200 rpm. To deoxygenate the polymer solution, N<sub>2</sub> gas was purged continuously for ca. 20 min. with an agitator speed of 1200 rpm. After venting the reactor pressure, the reactor was pressurized with synthesis gas and vented out three times to saturate the polymer

solution with only synthesis gas. The system was pressurized to approximately 80% of the desired pressure. The ceramic band heater was installed and the reactor was heated up to set point of temperature. When the chosen conditions had been attained, the autoclave fill valve was opened and the system was left and allowed to be stabilized for ca. 45 min with the temperature and pressure at the set point. The computer was started and the data was input. To start the reaction, the PT-1 control was adjusted above 9.10 V. The PT-1 valve was switched on and PT-2 valve was rezeroed at the run position. The equalization valve of the gas uptake loop was turned on. Pressure of about 100 psi was applied to drop the catalyst bucket into the polymer solution. The catalyst was dispersed in the polymer solution using an agitation rate of 1200 rpm. Then, the 'B' on the keyboard was pressed. When the system was activated, the program was waited for one logging interval before starting the record the time, reaction temperature and amount of synthesis gas consumed.

To stop the reaction, the 'S' key was pressed to stop the computer program and the data file was saved. The rezero valve was switch on by using the manual switches and the equalization valve was switched off. The reactor was then cooled to 50°C by using the cooling unit before venting off the pressure slowly. The temperature controller was disabled; plus, the ice-water bath was used to cool the wall and polymer solution of the autoclave. When the temperature was below 10°C, N<sub>2</sub> gas was pressurized and continuously purged the synthesis gas in the polymer solution for 20 min. After venting all the gas out, the autoclave was disassembled.

#### **2.4.4 Kinetic Studies and Univariate Experiment**

All hydroformylation reactions were carried out over the temperature range of 40-90°C and pressure range of 13.8-55.1 bar. During the reaction, the kinetic was examined by following the gas consumption by using the gas uptake apparatus.

## 2.5 Characterization

Aside from examining the kinetics of the reaction as well as the extent of reaction with the gas uptake apparatus, spectroscopic analysis was used to determine the degree of hydroformylation and the parameters of gas uptake program was calibrated. Samples of the reaction solution were analyzed using two methods: FT-IR,  $^1\text{H}$ -NMR, and  $^{13}\text{C}$ -NMR spectroscopic analysis.

### 2.5.1 Fourier Transform – Infrared Spectroscopic Analysis

All infrared (FT-IR) spectra were obtained using a Bio-Rad FTS 3000X spectrometer. The infrared sample was prepared by casting the polymer solution on sodium chloride disks, which were then kept in the fume hood to evaporate the solvent.

### 2.5.2 $^1\text{H}$ and $^{13}\text{C}$ Nuclear Magnetic Resonance Spectroscopic Analysis

$^1\text{H}$ -NMR and  $^{13}\text{C}$ -NMR spectra of polymer samples were obtained with a Bruker 300 MHz spectrometer. Using  $^1\text{H}$  NMR spectroscopy, the quantitative analysis of the hydroformylated and hydroxymethylated PBD was achieved.  $^{13}\text{C}$  NMR spectra can provide a great wealth of structural information, whereas  $^1\text{H}$  NMR spectra is not always possible to identify the structure. A comparison between the sum of the aldehyde protons, unsaturated protons, and paraffinic protons integration was used to calculate the degree of hydroformylation. The sample solution was collected in a Schlenk tube and then evaporated to dryness under vacuum. The rubber was then dissolved in degassed  $\text{CDCl}_3$  to prepare a sample for NMR analysis. However, it was necessary to retain some small amount of solvent in the NMR sample due to the instability of polyaldehyde when the solvent is completely removed.

## **2.6 Thermal Analysis and Film Properties**

### **2.6.1 Thermogravimetric Analysis (TGA)**

A Perkin Elmer TG/DTA Pyris Diamond was used to determine the degradation properties of hydroformylated products. The temperature was increased under nitrogen atmosphere from 50°C to 800°C at a constant heating rate of 10°C/min. The nitrogen gas flow rate was 50 ml/min. The onset of the degradation, the weight loss due to degradation and the residue remaining at 800°C were evaluated. The initial decomposition temperature ( $T_{id}$ ) and the maximum decomposition temperature ( $T_{max}$ ) were determined.

### **2.6.2 Differential Scanning Calorimetry (DSC)**

Differential scanning calorimetry analysis was carried out on a Mettler Toledo DSC 822. About 20-mg of the hydroformylated PBD sample was first cooled to –150°C with liquid nitrogen and then heated under nitrogen flow at the heating rate of 10°C/min to 70°C.  $Al_2O_3$  was used as the reference sample. The middle of incline was taken to be the glass-transition temperature ( $T_g$ ).

### **2.6.3 Swelling Measurement and Resistance to Solvent**

Hydroformylated polybutadiene was formed as a film as to provide a membrane. Swelling is one of the film properties of a membrane which is determined by measuring the absorption of specific solutions such as solution of ethanol, methanol, or water, etc. Furthermore, the film property is useful in ascertaining the membranes resistance to common solvents such as monochlorobenzene, tetrahydrofuran, etc.

## 2.7 Determination of Degree of hydroformylation and hydroxymethylation

In order to calculate the degree of hydroformylation, the  $^1\text{H}$  NMR spectra of hydroformylated polybutadiene was taken. Integration of the spectra was used to determine the amount of characteristic protons of each structure in the polymer. The %hydroformylation was calculated using equation as follows (Bhattacharjee, 1992):

$$\% \text{ Hydroformylation} = \frac{D}{\frac{1}{2}(C - \frac{B}{2}) + \frac{B}{2} + D + \frac{1}{8}(A - \frac{B}{2} - 2C - 7D)} \quad (2.1)$$

$$\% \text{ Hydroxymet hylation} = \frac{\frac{E}{2}}{\frac{1}{2}(C - \frac{B}{2}) + \frac{B}{2} + D + \frac{1}{8}(A - \frac{B}{2} - 2C - 7D - \frac{7}{2}E) + \frac{E}{2}} \quad (2.2)$$

where

- A = the integral area of aliphatic protons signal
- B = the integral area of olefinic protons signal due to 1,2-PBD
- C = the integral area of olefinic protons signal due to 1,2-PBD and 1,4-PBD
- D = the integral area of aldehydic protons signals
- E = the intergral area of methylene adjacent to hydroxyl groups signal

Examples of %hydroformylation and %hydroxymethylation calculation are described in Appendix II.



## CHAPTER III

### HYDROFORMYLATION OF HIGH MOLECULAR WEIGHT *CIS*-1,4-POLYBUTADIENE IN A PARR BATCH REACTOR

Most studies reported for the hydroformylation of diene polymers, i.e. polybutadiene (PBD) and poly(styrene-butadiene) (SBR) have been carried out in the presence of rhodium catalysts. However, the earliest study showed that the hydroformylation of 1,4-polybutadiene and high-styrene SBR could be achieved at high pressure and temperature using a cobalt catalyst (Ramp, 1966). There was considerable gel formation during this process. The first report of the use of  $\text{HRh}(\text{CO})(\text{PPh}_3)_3$  for the hydroformylation of a polypentenamer was by Sanui et al (1974), and the reaction was carried out at moderate reaction conditions with no gel formation. Later, Tremont et al. (1990) studied the hydroformylation of low molecular weight 1,2- and 1,4-polybutadiene in the presence of  $\text{HRh}(\text{CO})(\text{PPh}_3)_3$  with excess triphenyl phosphine. Scott and Rempel (1992) investigated the kinetics of the hydroformylation of SBR using the same catalyst. Furthermore, they postulated a plausible reaction mechanism and presented an understanding of the catalyst species in solution.

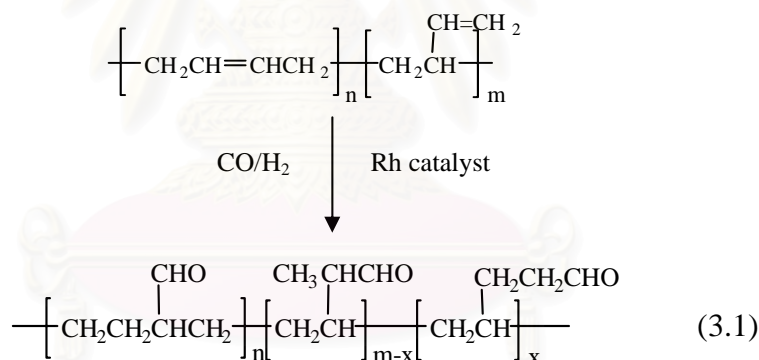
As mentioned above, previous investigations have reported on the use of low molecular weight polymers having  $M_w$  less than 200,000 for hydroformylation with results of moderate conversion. Recently, Chen et al. (1997) studied the hydroformylation of higher molecular weight styrene-butadiene copolymers ( $M_w \sim 200,000$ ) under more severe reaction conditions in the presence of various rhodium catalysts and conversions of higher than 50% were achieved.

The main purpose of this work is to prepare and characterize the hydroformylation products of high molecular weight *cis*-1,4-polybutadiene. Due to its structure, *cis*-1,4-polybutadiene can serve as a primary material for the study of this process to help provide a base for further investigation of other polydienes such as synthetic *cis*-1,4-polyisoprene and natural rubber. The determination of significant parameters for the hydroformylation of *cis*-1,4-PBD was achieved by using  $2^4$  experimental design. This work was also aimed at a study of the detailed kinetics of hydroformylation of *cis*-1,4-polybutadiene to obtain further understanding of the

reaction at high conversion and the postulation of a reaction mechanism. The hydroformylation of PBD (98% *cis* content,  $M_w$  2,000,000-3,000,000) was carried out in the presence of  $\text{HRh}(\text{CO})(\text{PPh}_3)_3$ , in monochlorobenzene (MCB) using a 1:1 mixture of CO and  $\text{H}_2$ . The experimental design and kinetic studies were performed in a Parr batch reactor.

### 3.1 Product Identification for Hydroformylated PBD

Polybutadiene used in this experiment consists of 98 wt% *cis* content (1,4-polybutadiene) and 2 wt% vinyl (1,2-polybutadiene). According to the microstructure of polybutadiene, there are three possible hydroformylated products as shown in Eq. 3.1. The possible products may not be only these products, but also products from side reactions such as chain degradation or hydrogenation of unsaturated polymer or aldehyde.



The infrared spectra of *cis*-1,4-polybutadiene and partially hydroformylated product are shown in Figure 3.1. It is apparent from the spectra that beside a decrease in the intensity of bands at 912, 968, 995 and  $1655 \text{ cm}^{-1}$ , which are attributed to C=C bonds, two new bands appeared at  $1725 \text{ cm}^{-1}$  and  $2700 \text{ cm}^{-1}$ . The band at  $1725 \text{ cm}^{-1}$  is characterized as being due to carbonyl (C=O) stretching vibrations and the band at  $2700 \text{ cm}^{-1}$  is attributed to the C-H stretching vibrations of the aldehyde group. No observation at  $3500 \text{ cm}^{-1}$  due to OH stretching was apparent. This confirmed that there is no appreciable hydrogenation of aldehyde under the reaction conditions employed.

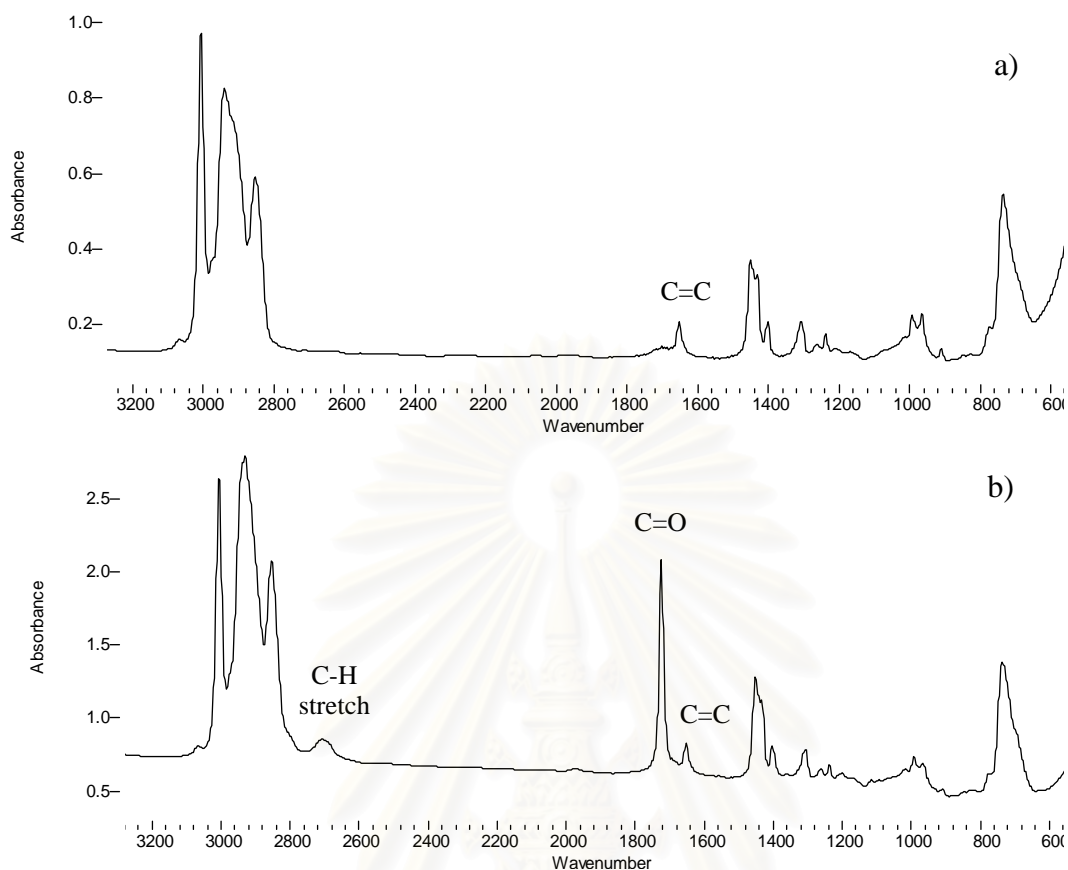


**Figure 3.1** FT-IR spectra of a) *cis*-1,4-polybutadiene b) hydroformylated *cis*-1,4-polybutadiene, [C=C] = 370 mM; [Rh] = 326  $\mu$ M;  $P_{\text{H}_2/\text{CO}}$  = 13.8 bar,  $\text{H}_2:\text{CO}$  = 1:1;  $T = 40^\circ\text{C}$ ; Time = 24 h.

Figure 3.2 shows the  $^1\text{H}$  NMR spectra of *cis*-1,4-polybutadiene and the partially hydroformylated product. The signals in the 1.0-2.0 ppm range are associated with the olefinic protons. The allylic protons occur at about 2.2 ppm, while the olefinic protons due to 1,4-polybutadiene or internal double bond occur at 5.4 ppm and those due to 1,2-polybutadiene or the vinyl double bond occur within the 4.7-5.6 ppm range. The characterization of the aldehyde products is difficult due to the lack of signal splitting. However, this can be distinguished by utilization of some model compounds. Based on the data, peaks attributed to aldehyde groups occur at 9.5 and 9.7 ppm. The peak at 9.5 ppm corresponds to the aldehyde group resulting from the internal or anti-Markovnikov addition. The smaller peak at 9.7 ppm can be assigned to the aldehyde group, which can be the outcome from hydroformylation of 1,2-

polybutadiene as the Markovnikov product (Tremont et al., 1990; Scott and Rempel, 1992; Mohammadi, 1987).

The  $^{13}\text{C}$  NMR spectra of polybutadiene and hydroformylated polybutadiene are shown in Figure 3.3. The peaks in the range of 0-60 ppm correspond to aliphatic carbons, 70-80 ppm correspond to chloroform- $d_1$ , 120-140 ppm correspond to residual olefinic carbons and a single peak at 205 ppm is attributed to the formyl groups.

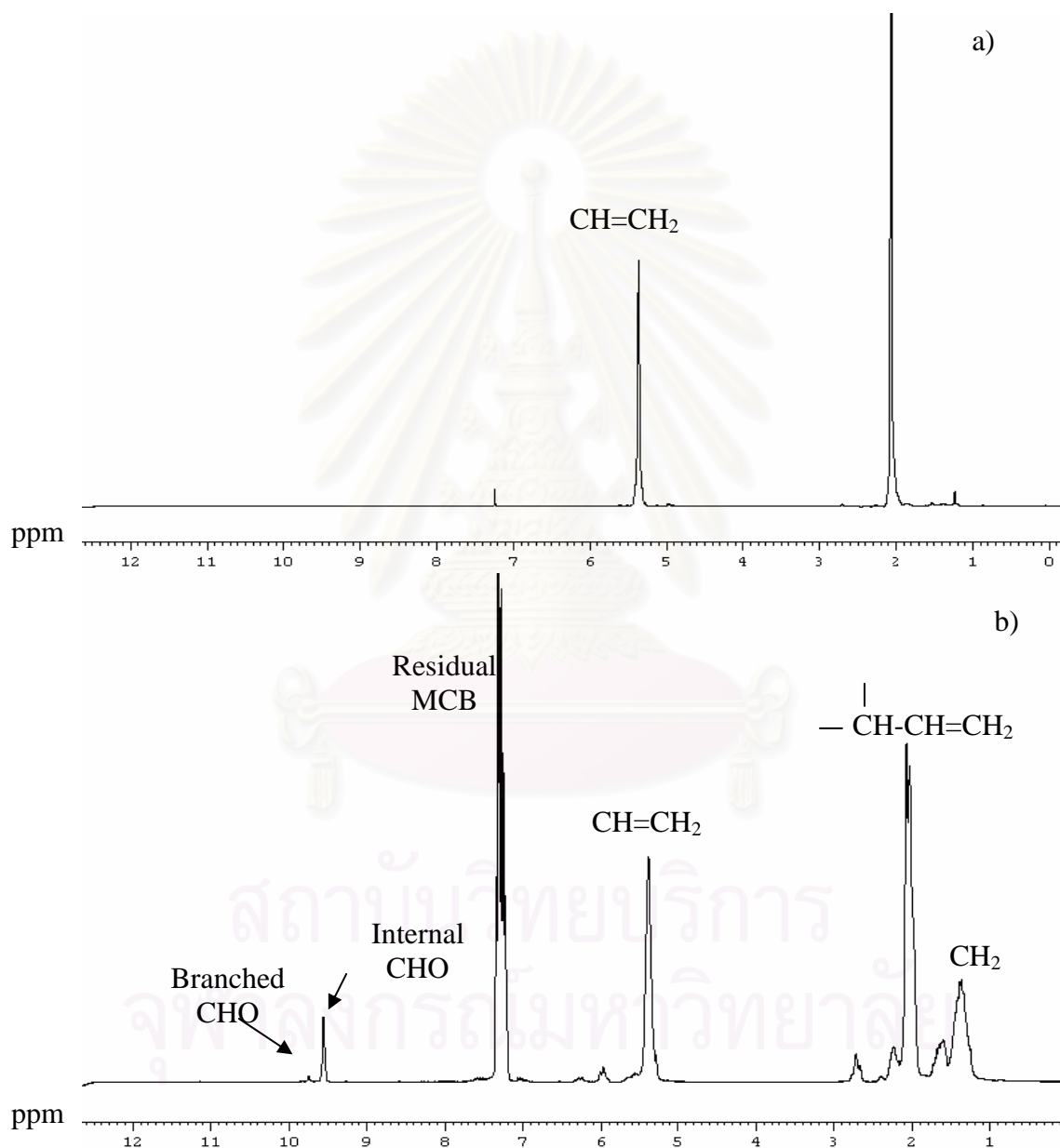


**Figure 3.2**  $^1\text{H}$ -NMR spectra of a) *cis*-1,4-polybutadiene b) *cis*-1,4-hydroformylated polybutadiene,  $[\text{C}=\text{C}] = 370 \text{ mM}$ ;  $[\text{Rh}] = 326 \text{ }\mu\text{M}$ ;  $P_{\text{H}_2/\text{CO}} = 13.8 \text{ bar}$ ;  $\text{H}_2:\text{CO} = 1:1$ ;  $T = 40^\circ\text{C}$ ; Time = 15 h.

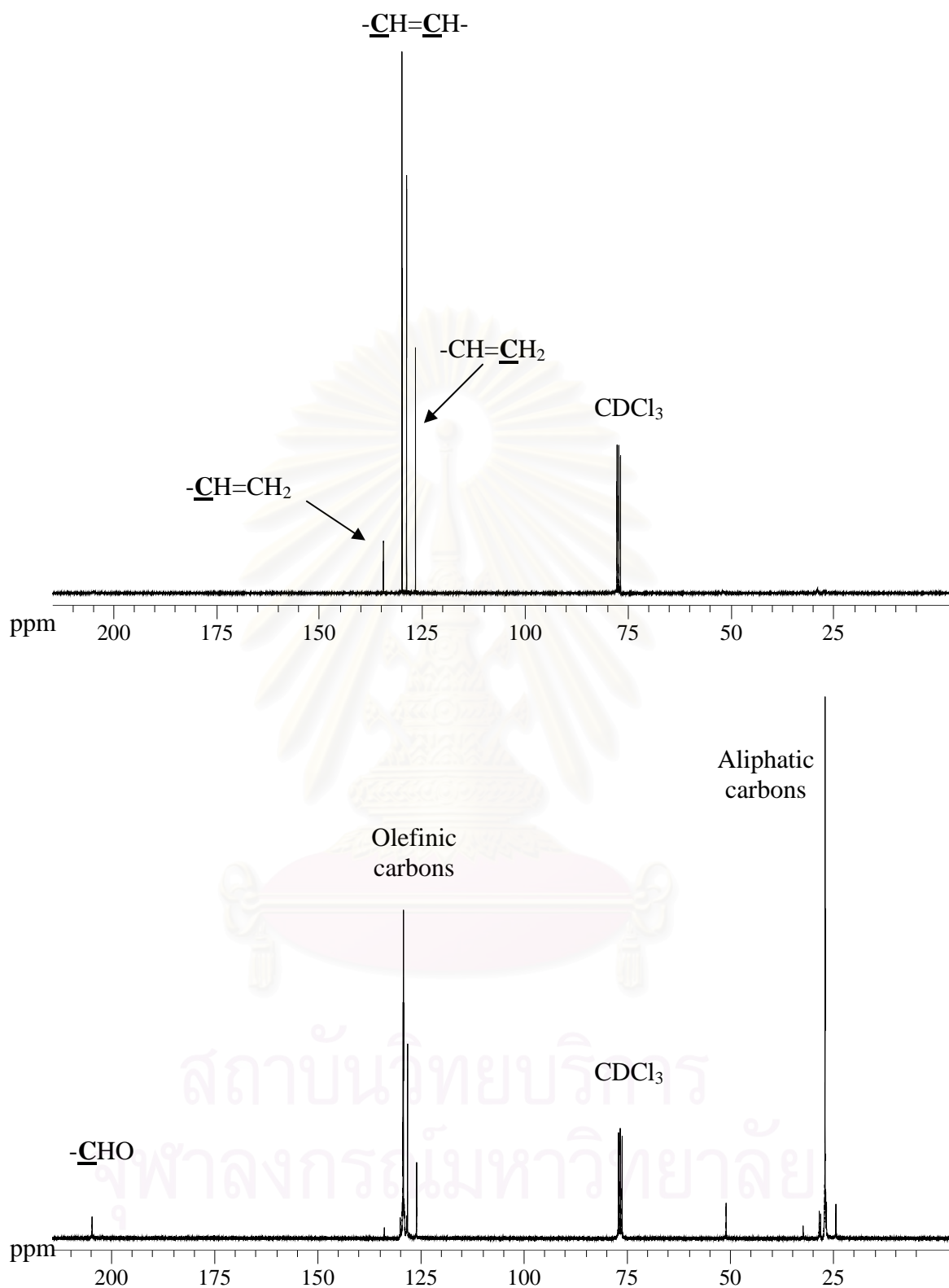


**Figure 3.3**  $^{13}\text{C}$ -NMR spectra of a) *cis*-1,4-polybutadiene b) *cis*-1,4-hydroformylated polybutadiene,  $[\text{C}=\text{C}] = 370 \text{ mM}$ ;  $[\text{Rh}] = 326 \text{ }\mu\text{M}$ ;  $P_{\text{H}_2/\text{CO}} = 13.8 \text{ bar}$ ;  $\text{H}_2:\text{CO} = 1:1$ ;  $T = 40^\circ\text{C}$ ; Time = 15 h.

### 3.2 Hydroformylation Catalyzed by Various Rh Complexes

Many works reported that rhodium complexes are suitable catalysts for hydroformylation reaction. The rhodium complexes chosen in this work were  $\text{HRh}(\text{CO})(\text{PPh}_3)_3$ ,  $\text{Rh}_4(\text{CO})_{12}$ ,  $\text{Rh}_6(\text{CO})_{16}$ ,  $[\text{Rh}(\text{COD})\text{Cl}]_2$ ,  $\text{Rh}(\text{COD})\text{acac}$ , and  $\text{Rh}(\text{COD})\text{acac}/\text{P}(\text{OC}_6\text{H}_4\text{C}(\text{CH}_3)_3)_3$ . All experiment were carried out at the base set of conditions:  $[\text{C}=\text{C}] = 370 \text{ mM}$ ;  $P_{\text{H}_2/\text{CO}} = 41.3 \text{ bar}$ ;  $\text{H}_2:\text{CO} = 1:1$ ;  $T = 80^\circ\text{C}$  in MCB; time = 2 h.

The results for the catalytic hydroformylation of *cis*-1,4-PBD using various Rh complexes are summarized in Table 3.1. Even though all rhodium catalysts in this study was proved to be the efficient catalysts for hydroformylation of small molecules (Chini and Martinengo, 1968; Booth et al., 1968; Kaneda et al., 1981; Jongma et al., 1991). For hydroformylation of PBD, the low degree of hydroformylation was achieved. It was found that  $\text{Rh}_4(\text{CO})_{12}$ ,  $\text{Rh}_6(\text{CO})_{16}$ ,  $[\text{Rh}(\text{COD})\text{Cl}]_2$ , and  $\text{Rh}(\text{COD})\text{acac}$  had low activity (2-11% conversion) for the catalytic hydroformylation of PBD. In addition, the co-catalyst,  $\text{P}(\text{OC}_6\text{H}_4\text{C}(\text{CH}_3)_3)_3$ , was not efficient for PBD hydroformylation. However, one rhodium complex,  $\text{HRh}(\text{CO})(\text{PPh}_3)_3$  was found to be an efficient catalyst for PBD hydroformylation (24.6% conversion). Based on these initial experimental results,  $\text{HRh}(\text{CO})(\text{PPh}_3)_3$  was chosen as the preferred Rh catalyst for a kinetic investigation of PBD hydroformylation.

**Table 3.1** The results of hydroformylation of PBD using Rh (I) complexes.

Catalyst	Mole of Rhodium <sup>a</sup> (mmol)	Co-catalyst <sup>b</sup>	%Hydroformylation
$\text{HRh}(\text{CO})(\text{PPh}_3)_3$	5	none	24.6
$[\text{RhCl}(\text{COD})]_2$	10	none	2.1
$\text{Rh}_4(\text{CO})_{12}$	22	none	11.0
$\text{Rh}_6(\text{CO})_{16}$	35	none	0.5
$\text{Rh}(\text{COD})\text{acac}$	22	none	2.6
$\text{Rh}(\text{COD})\text{acac}$	22	$\text{P}(\text{OC}_6\text{H}_4\text{C}(\text{CH}_3)_3)_3$	0

Conditions:  $[\text{C}=\text{C}] = 370 \text{ mM}$ ;  $P_{\text{H}_2/\text{CO}} = 41.3 \text{ bar}$ ;  $\text{H}_2:\text{CO} = 1:1$ ;  $T = 80^\circ\text{C}$ .

$[\text{C}=\text{C}]$  is defined as the weight of *cis*-1,4-polybutadiene divided by molecular weight of repeating unit.

<sup>a</sup> The mole fraction of rhodium in solution.

<sup>b</sup> 1:1 ratio of catalyst and co-catalyst by mole.

### 3.3 The 2<sup>4</sup> Experimental Design

Factorial experimental design is an effective method to determine how various reaction parameters affect the system. It is very useful in the primary experimental study when there are many factor effects to determine. The interesting parameters in this work are temperature, pressure, polymer concentration and catalyst concentration. For the two-level factorial design, the final conversion of hydroformylation was defined as the response by a change in the level of these factors. The treatment combination in standard order can be written as (1), a, b, c, d, ab, ac, bc, ad, bd, cd, abc, abd, acd, bcd, and abcd (Table 3.2). The experiments were designed to run a single replicate to obtain the response data as the final conversion over 24 h reaction time and the conversion results are also shown in Table 3.2.

**Table 3.2** Results for hydroformylation of polybutadiene in 2<sup>4</sup> factorial design: temperature (A), pressure (B), polymer concentration (C)\*, and catalyst concentration (D).

Expt.	Factor				Conversion at 24 h (%)		Factor level	
	A	B	C	D			Low (-)	High (+)
(1)	-	-	-	-	11.7	A (°C)	40	80
a	+	-	-	-	28.1	B (bar)	13.8	68.9
b	-	+	-	-	17.3	C (mM)	222	370
ab	+	+	-	-	28.8	D (μM)	109	326
c	-	-	+	-	9.8			
ac	-	-	+	-	17.9			
bc	-	+	+	-	4.9			
abc	+	+	+	-	68.0			
d	-	-	-	+	27.1			
ad	+	-	-	+	58.8			
bd	-	+	-	+	12.4			
abd	+	+	-	+	90.0			
cd	-	-	+	+	22.8			
acd	+	-	+	+	46.3			
bcd	-	+	+	+	14.4			
abcd	+	+	+	+	90.9			

\*Polymer concentration is defined as the weight of polybutadiene divided by molecular weight of repeating unit.

The procedure to analyze the data from an unreplicated factorial design is provided through examination of a normal probability plot. The contrast constants for the  $2^4$  design were calculated and the normal probability plot is illustrated in Figure 3.4. From the normal probability plot, all of the effects that lie along the line are negligible, whereas larger effects deviate from the line. Thus, the important effects that emerge from this analysis are the main effect of A, B, and D and the AB and AD interactions as defined in Table 3.2.

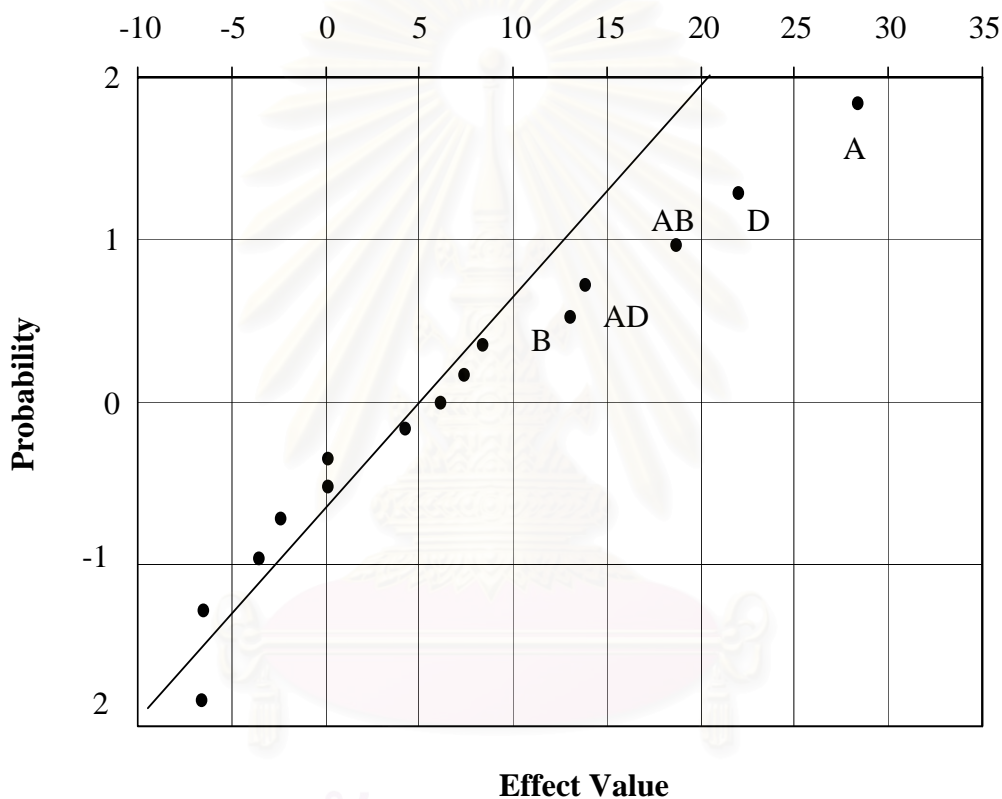


**Figure 3.4** The normal probability plot for the  $2^4$  factorial design for the hydroformylation of polybutadiene.

The main effects of A, B, C, and D are plotted in Figure 3.4. When comparing each main effect; the temperature (A), pressure (B), catalyst concentration (D) positively affect the average conversion of hydroformylation of polybutadiene, but the polymer concentration (C) does not. In order to maximize the conversion, temperature, pressure and catalyst concentration should be at a high level. However, it is also necessary to examine any interactions that are important. Main effects do not have as much meaning when they are also involved in significant interactions.



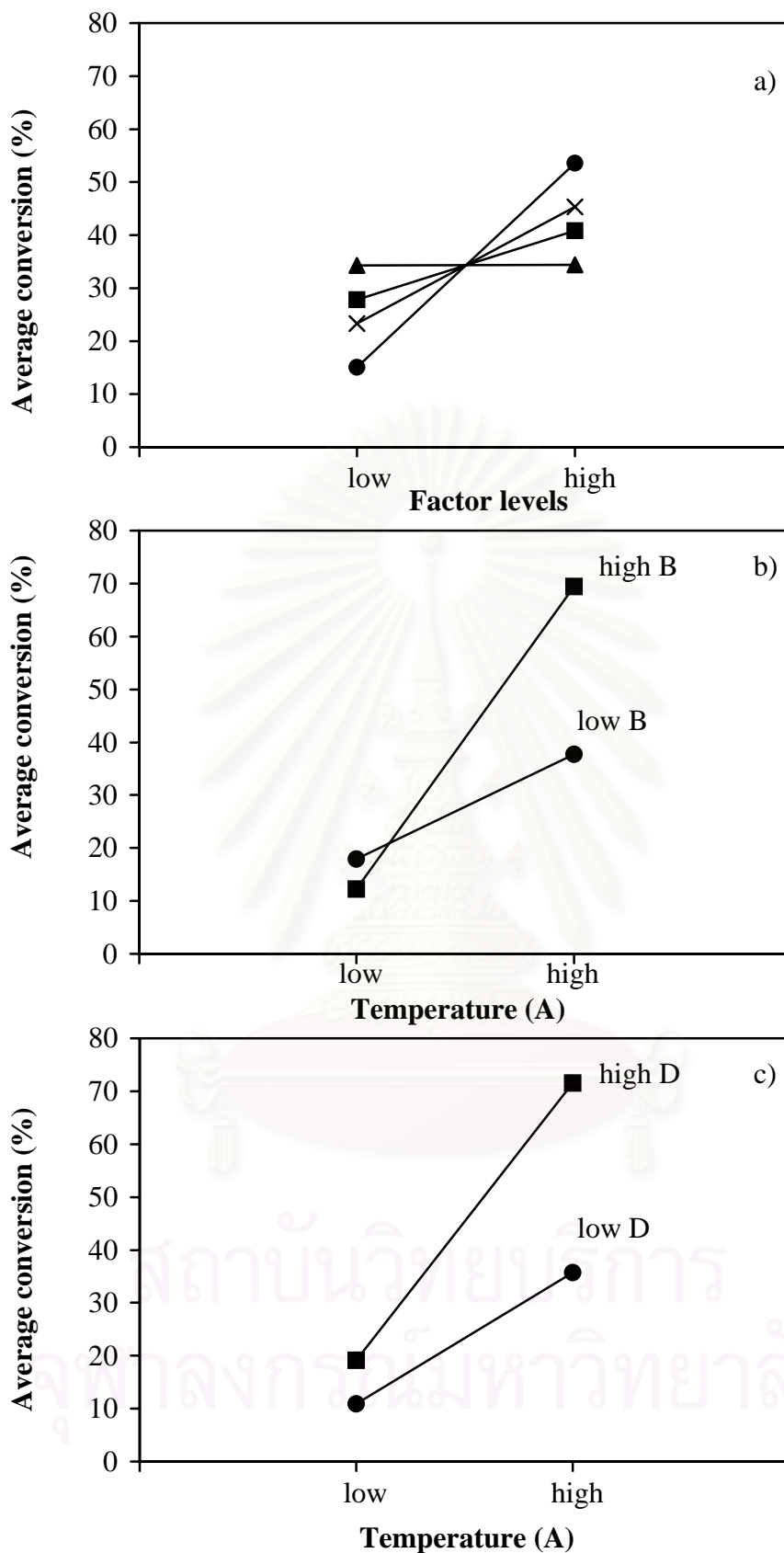


**Figure 3.5** Plots of a) Main effects for hydroformylation of polybutadiene: temperature (●), pressure (■), polymer concentration (▲) and catalyst concentration (×), b) AB interaction and c) AD interaction for hydroformylation of polybutadiene.

Considering all interactions, it is found that BC, BD, AC and CD interactions do not affect each other since the slope value between the two factors are similar. From Figure 3.5, the AB and AD interactions are significant. Considering the AB interaction, the temperature effect is very small when the pressure is at the low level and very large when the pressure is at the high level, therefore the high conversion is obtained at high pressure and high temperature. The AD interaction indicates that catalyst concentration has little effect at low temperature but a large positive effect at high temperature. Therefore, the best conversion for hydroformylation of polybutadiene would appear to be obtained when A, B, and D are at high level.

### 3.4 Kinetics of Hydroformylation by using Parr Batch Reactor

Kinetic results for the hydroformylation of polybutadiene were achieved using  $\text{HRh}(\text{CO})(\text{PPh}_3)_3$  over a 10 h reaction time. In order to obtain the kinetics, the conversion of hydroformylation was observed with time as shown by the representative plot in Figure 3.6. In addition, the conversion of double bond hydrogenation, which is a side reaction, was also obtained from  $^1\text{H}$  NMR spectra. The conversion of hydroformylation follows a first order rate equation. The rate constant ( $k$ ) was derived from the slope of the relation between  $\ln(1-x)$  and reaction time as shown in Figure 3.7 where  $x$  is conversion. According to hydroformylation condition in Figure 3.6 and 3.7, the final conversion at 10 h reaches nearly 80% and the pseudo first order reaction rate constant is  $3.7 \times 10^{-5} \text{ s}^{-1}$ . This can be compared with the results reported by Tremont et al. (1990) that the hydroformylation of *cis*-1,4-polybutadiene with  $M_w \sim 156,800$  using  $\text{HRh}(\text{CO})(\text{PPh}_3)_3$  with excess  $\text{PPh}_3$  at 20 bar and  $87^\circ\text{C}$  to yield the conversion of only 55% in 23 h. The results of hydroformylation of PBD and SBR using the same rhodium catalyst reported by various investigators are also presented in Table 1.2.

From factorial design, the significant parameters for hydroformylation of polybutadiene were temperature, catalyst concentration, and total pressure of synthesis gas. Thus, it is worth to carry out an investigation of the effect of these parameters on the reaction rate constant. Furthermore, the effect of triphenyl phosphine and %CO in synthesis gas were also studied to approach the detailed kinetics. The results of univariate experiments are presented in Table 3.3 and will be subsequently discussed in detail.

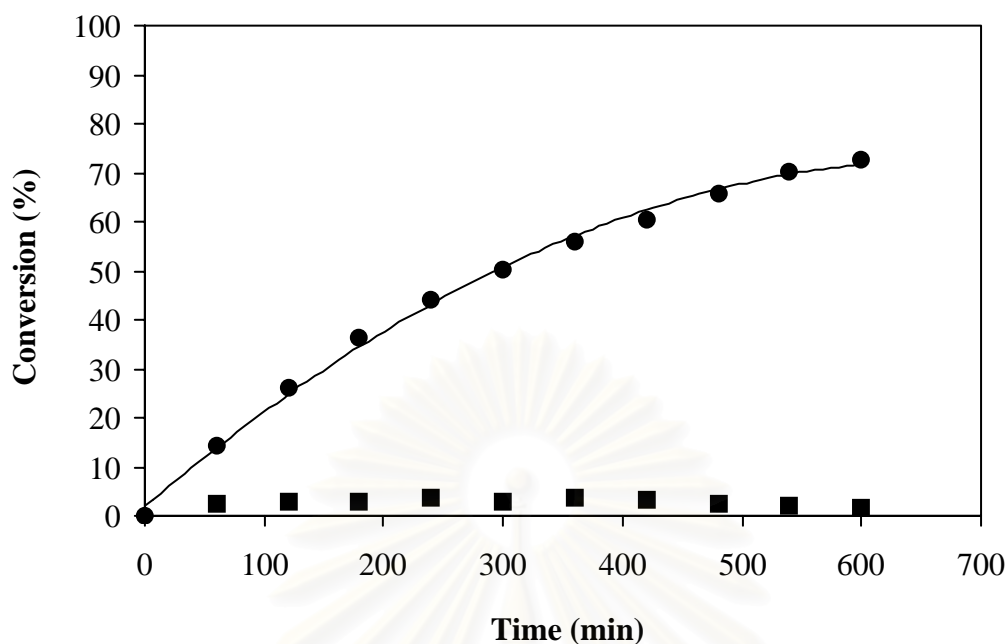


**Figure 3.6** Conversion profile for hydroformylation (●) and hydrogenation (■) of polybutadiene,  $[C=C] = 370$  mM;  $[Rh] = 326$   $\mu$ M;  $P_{H_2/CO} = 68.9$  bar;  $H_2:CO = 1:1$ ;  $T = 70^\circ C$ .

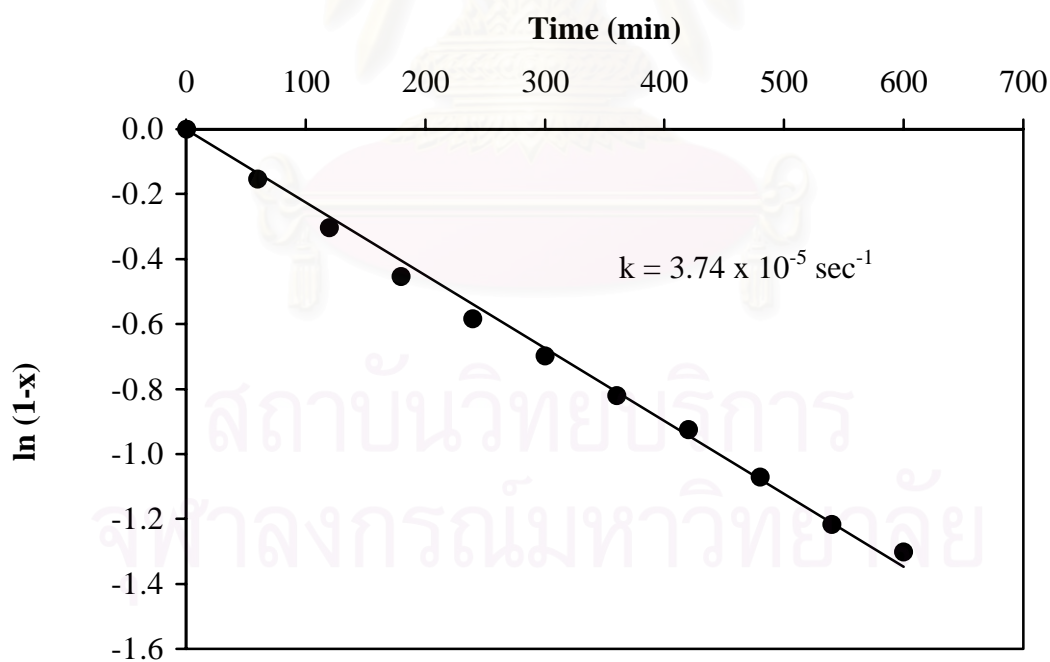


**Figure 3.7** The first order  $\ln(1-x)$  plot for hydroformylation of polybutadiene,  $[C=C] = 370$  mM;  $[Rh] = 326$   $\mu$ M;  $P_{H_2/CO} = 68.9$  bar;  $H_2:CO = 1:1$ ;  $T = 70^\circ C$ .

**Table 3.3 Kinetic results of univariate experiments.**

Expt.	[Rh] <sup>a</sup> ( $\mu\text{M}$ )	Mole ratio of Added $\text{PPh}_3/[\text{Rh}]^a$	$\text{P}_{\text{H}_2/\text{CO}}$ (bar)	%CO in gas mixture	Temp. ( $^\circ\text{C}$ )	Stirring speed (rpm)	$k \times 10^5$ ( $\text{s}^{-1}$ )	Conv. (%) at 10 h
1	327	0	41.3	50	70	400	3.74	42.9 <sup>b</sup>
2	327	0	41.3	50	70	500	4.09	43.6 <sup>b</sup>
3	327	0	41.3	50	70	600	4.26	45.9 <sup>b</sup>
4	327	0	41.3	50	70	700	4.35	47.5 <sup>b</sup>
5	326	0	55.1	50	60	600	2.22	57.4
6	327	0	55.1	50	65	600	3.12	69.3
7	327	0	55.1	50	70	600	4.05	76.0
8	327	0	55.1	50	75	600	5.01	81.1
9	327	0	55.1	50	80	600	5.60	81.4
10	326	0	55.1	50	90	600	6.31	87.2
11	326	0	55.1	50	100	600	5.75	80.4
12	326	0	41.3	25	70	600	5.55	81.8
13	326	0	41.3	42	70	600	4.33	76.4
14	322	0	41.3	50	70	600	3.54	71.4
15	327	0	41.3	67	70	600	2.35	66.3
16	109	0	41.3	50	70	600	1.39	35.7
17	109	0	41.3	25	70	600	1.68	28.0 <sup>b</sup>
18	163	0	41.3	50	70	600	2.00	45.6
19	218	0	41.3	50	70	600	2.85	60.0
20	218	0	41.3	25	70	600	3.05	31.0 <sup>b</sup>
21	272	0	41.3	50	70	600	3.45	68.1
22	326	0	41.3	50	70	600	4.14	80.4
23	326	0	41.3	25	70	600	5.09	51.3 <sup>b</sup>
24	435	0	41.3	50	70	600	4.57	78.3
25	435	0	41.3	25	70	600	6.36	56.0 <sup>b</sup>
26	329	0	13.8	50	70	600	2.03	47.4
27	327	0	13.8	25	70	600	2.55	40.7 <sup>b</sup>
28	326	0	20.7	50	70	600	2.52	52.3
29	327	0	27.6	50	70	600	3.14	64.0
30	327	0	27.6	25	70	600	3.93	49.6 <sup>b</sup>
31	326	0	41.3	50	70	600	4.14	80.4
32	327	0	41.3	25	70	600	5.09	51.3 <sup>b</sup>
33	327	0	55.1	50	70	600	4.05	76.0
34	327	0	55.1	25	70	600	4.57	47.8 <sup>b</sup>
35	326	0	68.9	50	70	600	3.74	72.8
36	326	0	68.9	25	70	600	3.91	35.6 <sup>b</sup>
37	327	10	41.3	50	70	600	3.36	69.7
38	326	25	41.3	50	70	600	2.97	66.4
39	326	75	41.3	50	70	600	1.67	53.1
40	326	100	41.3	50	70	600	1.42	40.7

Polymer concentration for all condition;  $[\text{C}=\text{C}] = 370 \text{ mM}$ .

<sup>a</sup> $[\text{Rh}] = [\text{HRh}(\text{CO})(\text{PPh}_3)_3]$ .

<sup>b</sup>The conversion at 5 h.

### 3.4.1 Effect of Stirring Speed

To approach the kinetic regime, the effect of stirring speed on the rate of hydroformylation was studied over the range of 400 to 700 rpm as shown in Figure 3.8. The reaction was carried out at 70°C and 41.3 bar with a 1:1 synthesis gas mixture. The catalyst concentration was maintained at 326  $\mu\text{M}$  and no  $\text{PPh}_3$  was added. The reaction rate constant increases slightly with increasing stirring speed. For a further increase in agitation above 600 rpm, the reaction rate tends to be independent of stirring speed, thus, the reaction is not affected by mass transfer limitations when experiments are performed at an agitation above 600 rpm

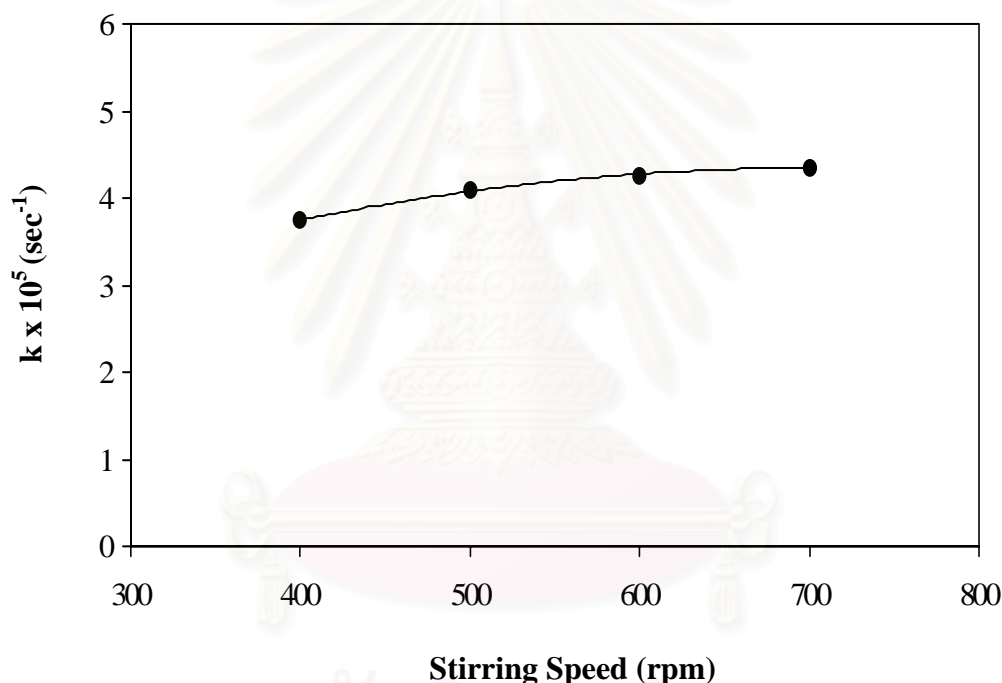


**Figure 3.8** Effect of stirring speed on rate constant,  $[\text{C}=\text{C}] = 370 \text{ mM}$ ;  $[\text{Rh}] = 326 \mu\text{M}$ ;  $P_{\text{H}_2/\text{CO}} = 41.3 \text{ bar}$ ;  $\text{H}_2:\text{CO} = 1:1$ ;  $T = 70^\circ\text{C}$ .

### 3.4.2 Effect of Temperature

The effect of temperature on the rate constant and final conversion is shown in Figure 3.9. The reaction conditions were kept constant as follows:  $[\text{C}=\text{C}] = 370 \text{ mM}$ ,  $[\text{Rh}] = 326 \mu\text{M}$ ,  $[\text{PPh}_3] = 0$ ,  $\text{H}_2:\text{CO} = 1:1$ , and total pressure = 55.1 bar. The rate constant increases with increasing temperature over the range of 60 to 90°C and

decreases when the temperature is above 90°C. A possible reason for this behavior is that the rhodium catalyst may no longer be active due to decomposition at temperature above 90°C in the absence of excess PPh<sub>3</sub>.

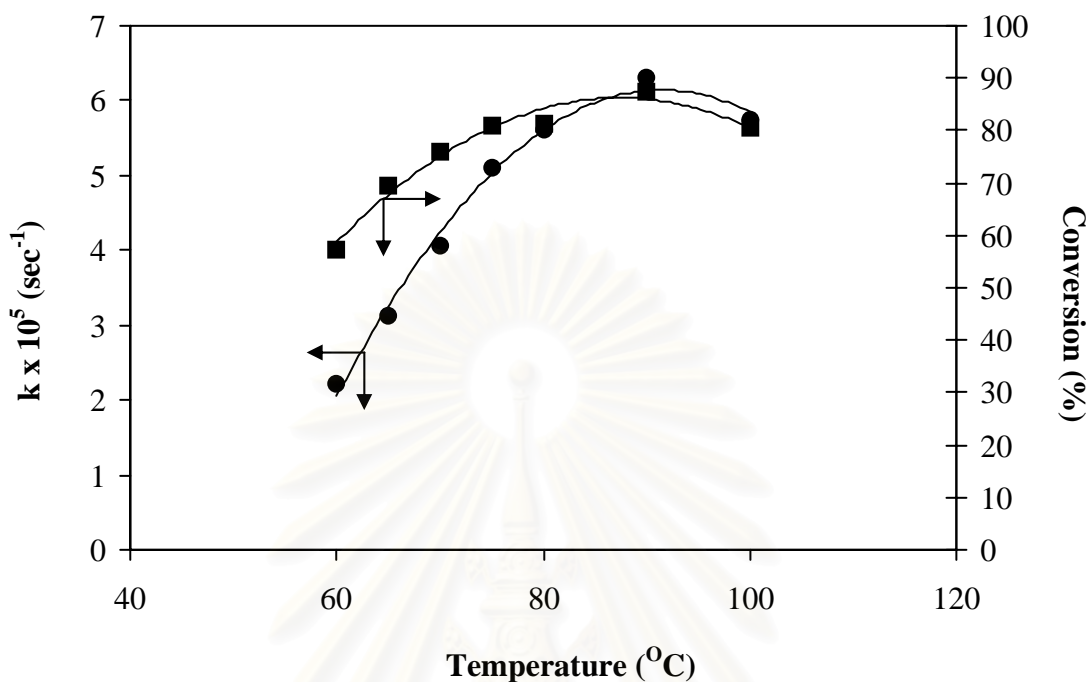


**Figure 3.9** Effect of temperature on rate constant (●) and conversion at 10 h (■),  $[\text{C}=\text{C}] = 370 \text{ mM}$ ;  $[\text{Rh}] = 326 \text{ }\mu\text{M}$ ;  $P_{\text{H}_2/\text{CO}} = 55.1 \text{ bar}$ ;  $\text{H}_2:\text{CO} = 1:1$ .

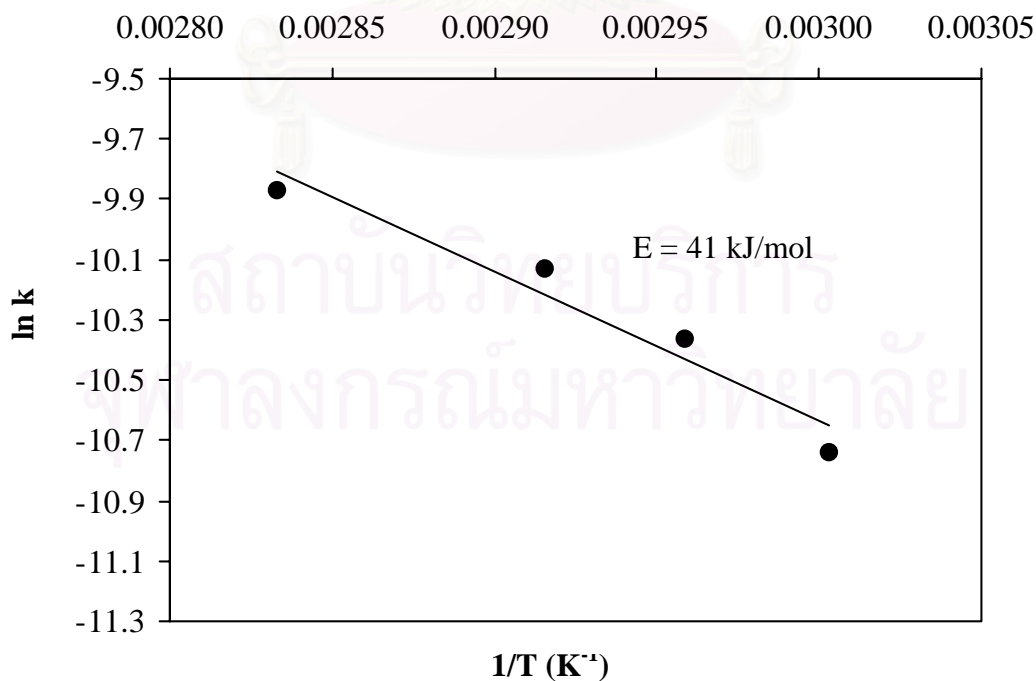


**Figure 3.10** Arrhenius plot for the hydroformylation of polybutadiene:  $[\text{C}=\text{C}] = 370 \text{ mM}$ ;  $[\text{Rh}] = 326 \text{ }\mu\text{M}$ ;  $P_{\text{H}_2/\text{CO}} = 55.1 \text{ bar}$ ;  $\text{H}_2:\text{CO} = 1:1$ .

The apparent activation energy was obtained from the slope of Arrhenius plot as shown in Figure 3.10. Over the temperature range of 60 to 80°C, it is estimated to be 41.0 kJ/mol. For hydroformylation of SBR using  $\text{HRh}(\text{CO})(\text{PPh}_3)_3$ , an activation energy value of 64.3 kJ/mol was reported by Scott and Rempel (1992). Although the observed apparent activation energy of 41.0 kJ/mol is fairly low, it still is indicative of a reaction which is subject to chemical reaction control.

### 3.4.3 Effect of %CO in Synthesis

The effect of %CO in synthesis gas on the reaction rate and final conversion as shown in Figure 3.11 is included in this study to provide some understanding of the mechanism of hydroformylation. The reaction conditions were maintained at 70°C and total pressure of 41.3 bar. Polymer concentration and catalyst concentration were employed at 370 mM and 326  $\mu\text{M}$ , respectively and no triphenyl phosphine was added.

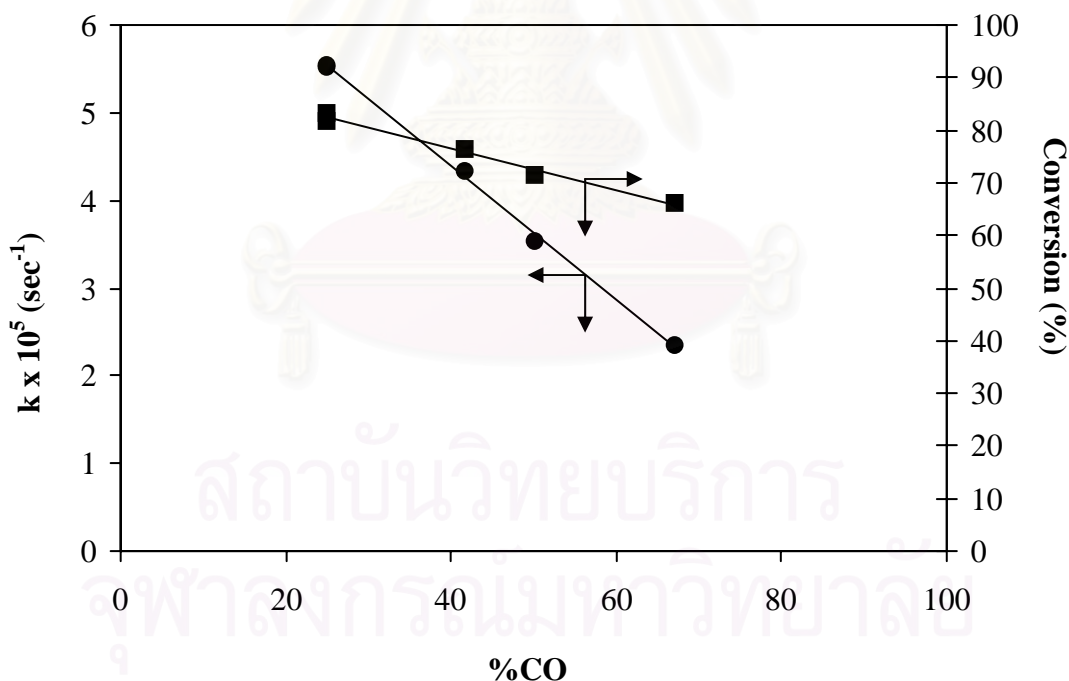
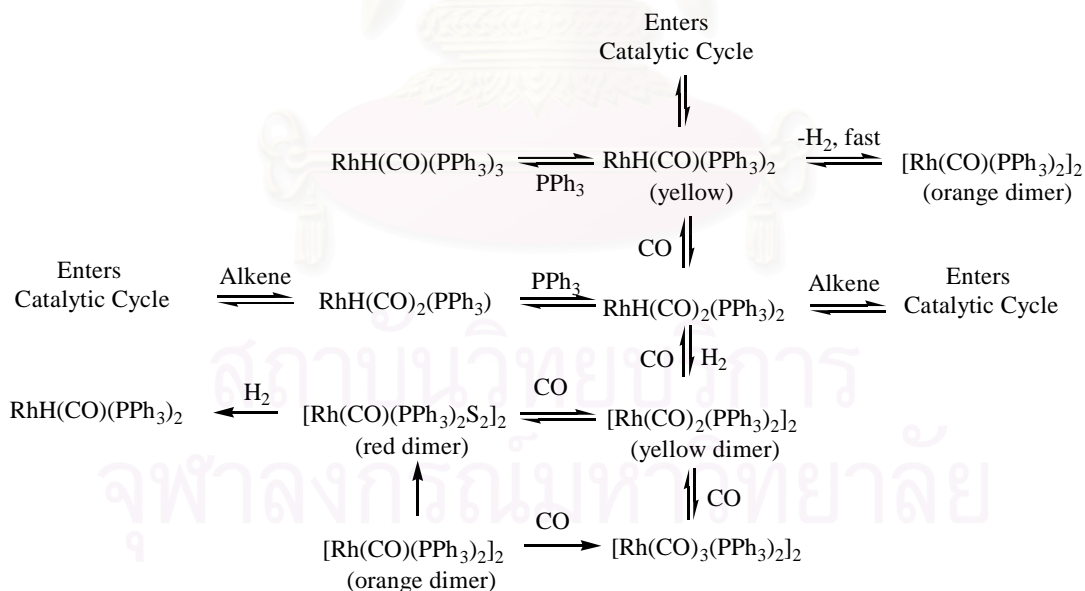


**Figure 3.11** Effect of %CO in synthesis gas on rate constant (●) and conversion at 10 h (■),  $[\text{C}=\text{C}] = 370 \text{ mM}$ ;  $[\text{Rh}] = 326 \mu\text{M}$ ;  $P_{\text{H}_2/\text{CO}} = 41.3 \text{ bar}$ ;  $T = 70^\circ\text{C}$ .

This figure indicates that the reaction rate is inversely proportional to %CO in synthesis gas mixture over the %CO range of 25% to 67% and the highest reaction

rate was achieved at 25% CO in the synthesis gas. This can be explained by examination of the possible species of rhodium that were proposed by Scott and Rempel. In solution, the rhodium catalyst is dissociated to other species as shown in Scheme 3.1 and  $\text{HRh}(\text{CO})(\text{PPh}_3)_2$  is the first species from dissociation between rhodium catalyst and  $\text{PPh}_3$ . They noted that under an atmosphere of hydrogen the formation of  $\text{Rh}(\text{CO})_2(\text{PPh}_3)_2$  is preferred because of its activity toward hydroformylation. On the other hand, under an atmosphere of carbon monoxide formation of inactive species such as  $[\text{Rh}(\text{CO})_2(\text{PPh}_3)_2]_2$  and  $[\text{Rh}(\text{CO})_3(\text{PPh}_3)_2]_2$  occurred. Furthermore, the dicarbonyl species,  $\text{Rh}(\text{COR})(\text{CO})_2(\text{PPh}_3)_2$  that is formed in the catalytic cycle is also an inactive species. This effect was also studied by Scott and Rempel (1990). However, they reported that optimum %CO in synthesis gas mixture for their system was about 30% which gave the highest conversion for hydroformylation of SBR under moderate conditions. From the study of the effect of %CO in synthesis gas in the present study, it is interesting that the reaction rate constant also increases as %CO decreases. Hence, this leads to an examination of the effect of catalyst concentration and total pressure at both 25% and 50% CO in the synthesis gas mixture.



**Scheme 3.1** Possible rhodium species in solution under hydroformylation conditions (S= solvent) (Scott, 1992).



### 3.4.4 Effect of Catalyst Concentration

The effect of catalyst concentration on the rate constant is shown in Figure 3.12. The temperature was kept constant at 70°C, the total pressure at 41.3 bar with a 3:1 or 1:1 synthesis gas mixture; the polymer concentration at 370 mM; and PPh<sub>3</sub> concentration at 0 μM. Over the range of catalyst concentration of 109 to 435 μM, the reaction rate is first order with respect to catalyst concentration up to approximately 350 μM for the 1:1 synthesis gas mixture, at which point the reaction rate tends toward a zero order behavior. Similar observation was made by Scott and Rempel (1990) for the hydroformylation of SBR using HRh(CO)(PPh<sub>3</sub>)<sub>3</sub>. Also included in Figure 3.12 are results for the effect of catalyst concentration for a 3:1 H<sub>2</sub>:CO mixture. The reaction rate constant increases linearly with increasing catalyst concentration. The reaction rate of 3:1 H<sub>2</sub>:CO mixture is much higher than that of 1:1 H<sub>2</sub>:CO mixture at a catalyst concentration above 350 μM since the first order rate dependence of catalyst concentration is maintained for the whole range investigated.

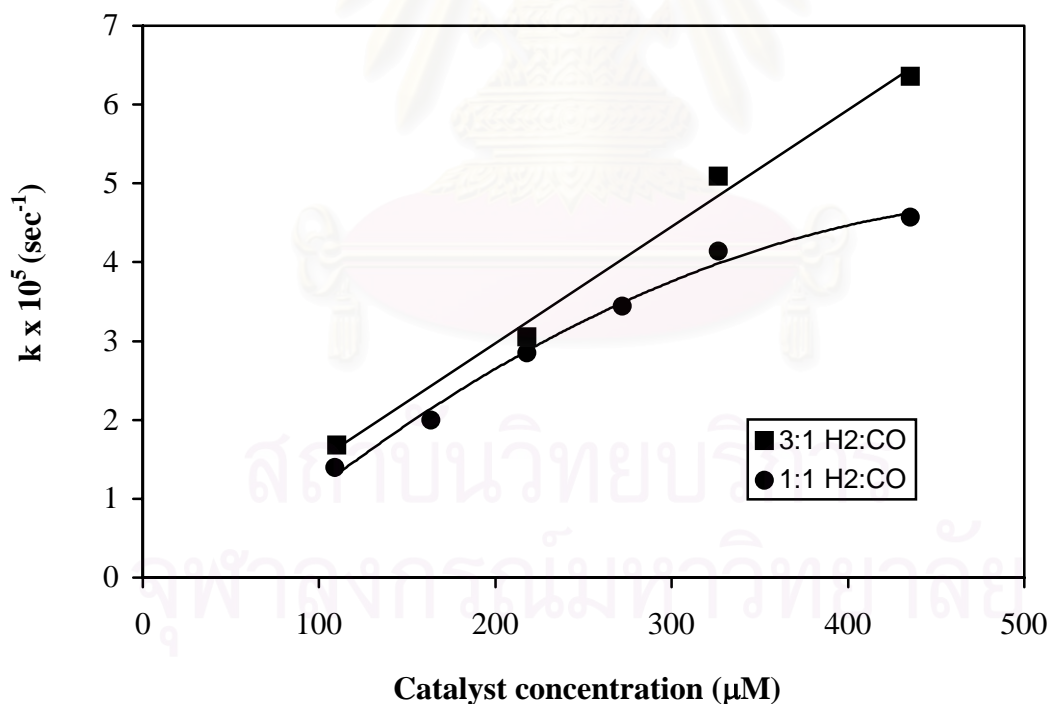


**Figure 3.12** Effect of catalyst concentration on rate constant at H<sub>2</sub>:CO of 1:1 (●) and 3:1 (■), [C=C] = 370 mM; P<sub>H<sub>2</sub>/CO</sub> = 41.3 bar; T = 70°C.

### 3.4.5 Effect of Total Pressure

The change of reaction rate constant with the total pressure of 1:1 synthesis gas ( $\text{H}_2$  and  $\text{CO}$ ) is shown in Figure 3.13. The temperature was maintained at  $70^\circ\text{C}$  with a polymer concentration of  $370\text{ mM}$  and a catalyst concentration of  $326\text{ }\mu\text{M}$  with no added triphenyl phosphine. The total pressure of synthesis gas was varied from  $13.8$  to  $68.9\text{ bar}$  for 3:1 and 1:1  $\text{H}_2:\text{CO}$ . It is apparent from the plot that the reaction rate is first order with respect to total pressure up until about  $41.3\text{ bar}$ . Above this pressure, the reactions rate constant decreases. It is evident that this catalyst is most suitable under moderate pressure. Scott and Rempel (1990) also reported that the reaction rate is first order with respect to total pressure and shifts to zero order at higher pressure for the hydroformylation of SBR using the same rhodium catalyst.

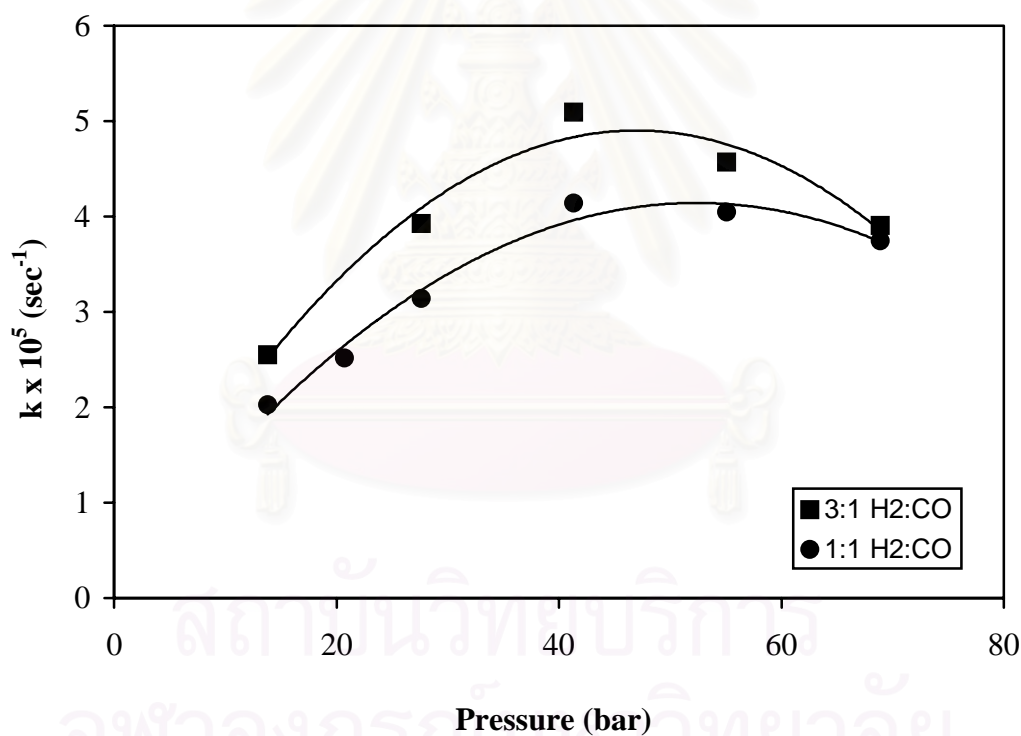


**Figure 3.13** Effect of total pressure on rate constant at  $\text{H}_2:\text{CO}$  of 1:1 ( $\bullet$ ) and 3:1 ( $\blacksquare$ ),  $[\text{C}=\text{C}] = 370\text{ mM}$ ;  $[\text{Rh}] = 326\text{ }\mu\text{M}$ ;  $\text{H}_2:\text{CO} = 1:1$ ;  $T = 70^\circ\text{C}$ .

### 3.4.6 Effect of Added PPh<sub>3</sub>

In Figure 3.14, the change of the rate constant and final conversion with respect to the mole ratio of triphenyl phosphine to rhodium catalyst is shown. The reaction was maintained at 70°C and 41.3 bar, and a 1:1 H<sub>2</sub>/CO mixture was used. The polymer concentration and catalyst concentration were at 370 mM and 326 μM, respectively. The mole ratio of triphenyl phosphine and rhodium catalyst was varied over the range of 0 to 100. The reaction rate appears to be inverse first order with respect to the mole ratio of triphenyl phosphine and rhodium catalyst upto about a mole ratio of 75:1. It should be noted that the triphenyl phosphine has the inhibiting effect of the rhodium catalyst due to retardation of triphenyl phosphine dissociation in the catalytic cycle. This is in keeping with the observation by Scott and Rempel (1990) for hydroformylation of SBR using HRh(CO)(PPh<sub>3</sub>)<sub>3</sub>.

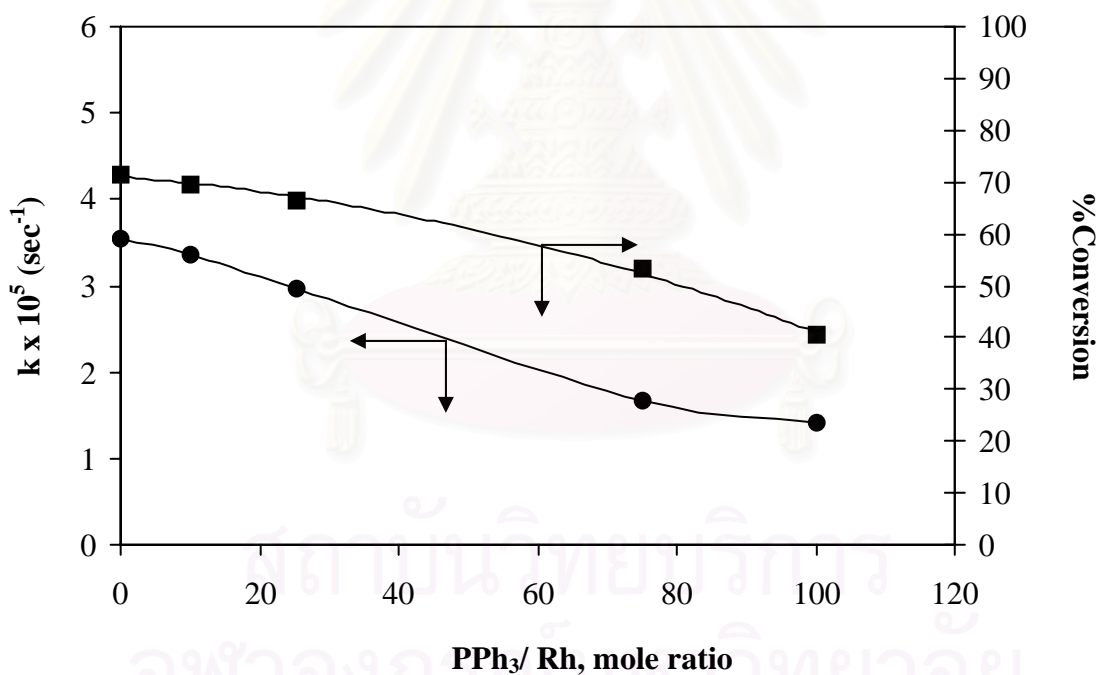
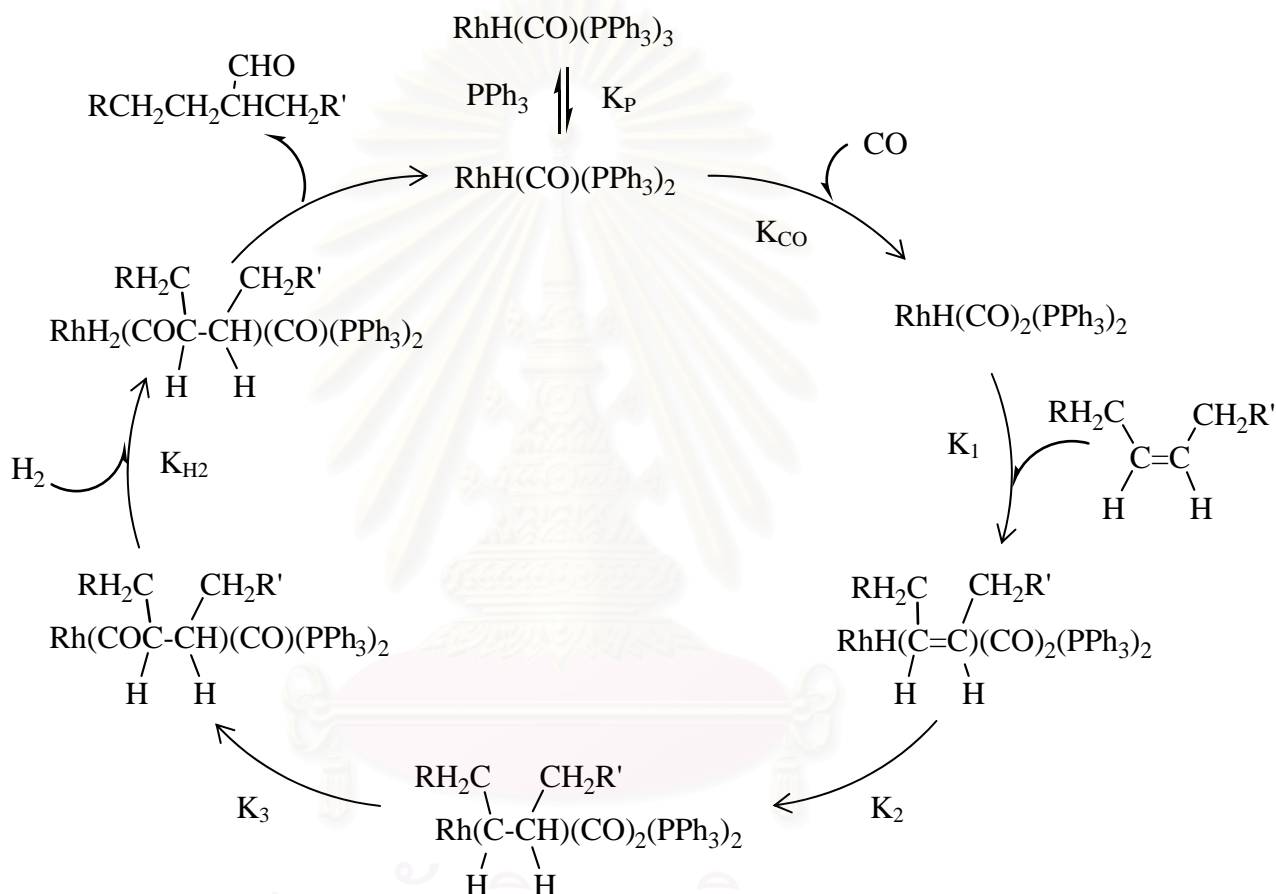


**Figure 3.14** Effect of added triphenyl phosphine on rate constant (●) and conversion at 10 h (■), [C=C] = 370 mM; [Rh] = 326 μM; P<sub>H<sub>2</sub>/CO</sub> = 41.3 bar; H<sub>2</sub>:CO = 1:1; T = 70°C.

### 3.5 Reaction Mechanism and Rate Law

Scott and Rempel (1990) suggested a mechanism for the  $\text{RhH}(\text{CO})(\text{PPh}_3)_3$  catalyzed hydroformylation of SBR that is consistent with the observation of hydride stretch and carbonyl stretch shift by IR spectroscopy. This proposed mechanism can be used for describing the hydroformylation of polybutadiene in this work as shown in Scheme 3.2.

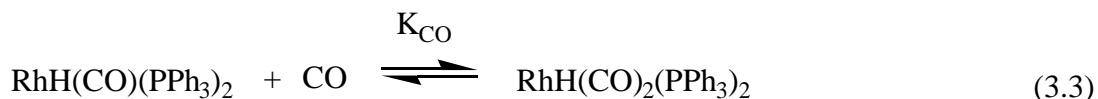


**Scheme 3.2** Mechanism of hydroformylation of polybutadiene using  $\text{HRh}(\text{CO})(\text{PPh}_3)_3$ .

The  $\text{RhH}(\text{CO})(\text{PPh}_3)_3$  is dissociated to form  $\text{RhH}(\text{CO})(\text{PPh}_3)_2$  as the first species in catalytic cycle and this reaction can be reversed as shown in Eq. 3.2.



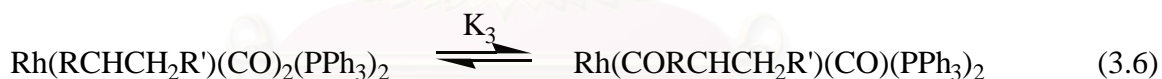
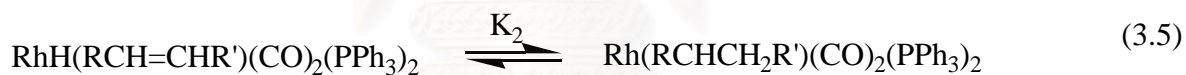
Under the hydroformylation reaction condition, the dicarbonyl complex,  $\text{RhH}(\text{CO})_2(\text{PPh}_3)_2$  can be formed by reacting  $\text{RhH}(\text{CO})(\text{PPh}_3)_2$  with CO according to the following equilibrium:



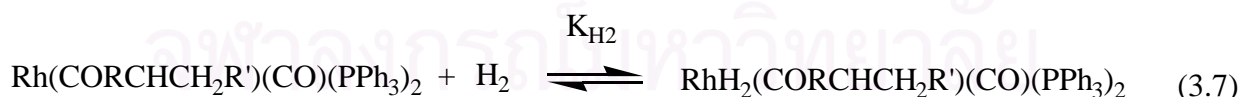
The dicarbonyl complex is interacted with the carbon-carbon double bonds to form the olefin complex as shown in Eq. 3.4.



Subsequently, the complex is reformed by substituting the double bond with  $\text{H}_2$  at the Rh centre to obtain  $\text{Rh}(\text{RCHCH}_2\text{R})(\text{CO})_2(\text{PPh}_3)_2$ , Eq. 3.5. Furthermore, the dicarbonyl species is transformed into a monocarbonyl species and the carbonyl group is inserted into the coordinated olefin molecule on rhodium complex to form an acyl ligand as shown in Eq. 3.6.



The hydrogen molecule is then added to coordinate with  $\text{Rh}(\text{CORCHCH}_2\text{R}')(\text{CO})(\text{PPh}_3)_2$  to give  $\text{RhH}_2(\text{CORCHCH}_2\text{R}')(\text{CO})(\text{PPh}_3)_2$  as shown in Eq. 3.7.



According to the catalytic cycle for hydroformylation reaction, the rate expression can be written as Eq. 3.8:

$$-\frac{d[\text{C}=\text{C}]}{dt} = k_{\text{rds}} [\text{RhH}_2(\text{CORCHCH}_2\text{R}')(\text{CO})(\text{PPh}_3)_2] \quad (3.8)$$

Considering that the system is at equilibrium, a material balance on the rhodium charged to the system is given by Eq. 3.9.

$$\begin{aligned}
 [\text{Rh}]_{\text{T}} = & [\text{RhH}(\text{CO})(\text{PPh}_3)_3] + [\text{RhH}(\text{CO})(\text{PPh}_3)_2] + [\text{RhH}(\text{CO})_2(\text{PPh}_3)_2] + \\
 & [\text{RhH}(\text{RCH}=\text{CHR}')(\text{CO})_2(\text{PPh}_3)_2] + [\text{Rh}(\text{RCHCH}_2\text{R}')(\text{CO})_2(\text{PPh}_3)_2] + \\
 & [\text{Rh}(\text{CORCHCH}_2\text{R}')(\text{CO})(\text{PPh}_3)_2] + [\text{RhH}_2(\text{CORCHCH}_2\text{R}')(\text{CO})(\text{PPh}_3)_2] \quad (3.9)
 \end{aligned}$$

By applying the equilibrium relation for each reaction step, Eq. 3.4–3.9,  $\text{RhH}_2(\text{CORCHCH}_2\text{R}')(\text{CO})(\text{PPh}_3)_2$  can be substituted for in Eq. 3.8. Thus, the rate law for hydroformylation can be obtained as shown in Eq. 3.10.

$$\frac{-d[\text{C}=\text{C}]}{dt} = \frac{[\text{Rh}]_{\text{T}} K_1 K_2 K_3 K_{\text{H}_2} K_{\text{CO}} K_{\text{P}} [\text{H}_2] [\text{CO}] [\text{C}=\text{C}]}{\alpha} \quad (3.10)$$

where

$$\begin{aligned}
 \alpha = & [\text{PPh}_3] + K_{\text{P}}(1 + K_{\text{CO}}[\text{CO}]) + K_1 K_{\text{CO}} K_{\text{P}} [\text{C}=\text{C}](1 + K_2) \\
 & + K_1 K_2 K_3 K_{\text{CO}} K_{\text{P}} [\text{CO}] [\text{C}=\text{C}](1 + K_{\text{H}_2}[\text{H}_2])
 \end{aligned}$$

According to the proposed mechanism, the rate expression is consistent with the observed kinetic data. From the kinetic study, the reaction rate is first order with respect to  $[\text{C}=\text{C}]$  and catalyst concentration, which agrees with Eq. 3.10. From the experiments, the first-order behavior with respect to total pressure was observed over the range of 13.8 to 41.3 bar. This can be explained by Eq. 3.10 if the term of  $K_1 K_2 K_3 K_{\text{CO}} K_{\text{P}} [\text{CO}] [\text{C}=\text{C}](1 + K_{\text{H}_2}[\text{H}_2])$  is small relative to the others in the denominator, the reaction rate is first order with respect to  $[\text{H}_2]$ . Above the total pressure of 41.3 bar, the reaction rate becomes zero order with respect to total pressure as a result of the term,  $K_1 K_2 K_3 K_{\text{CO}} K_{\text{P}} [\text{CO}] [\text{C}=\text{C}](1 + K_{\text{H}_2}[\text{H}_2])$  becoming more predominant, of Eq (3.10). Also, it can be seen that the reaction rate is inversely proportional to  $[\text{PPh}_3]$  which consistent with the results of kinetic studies.

## CHAPTER IV

### HYDROFORMYLATION OF HIGH MOLECULAR WEIGHT *CIS*-1,4-POLYBUTADIENE USING A COMPUTER CONTROLLED BATCH REACTOR SYSTEM

The reactor used for kinetic studies of homogeneous catalytic processes are commonly batch reactor type. Some conventional methods for gas/liquid reaction kinetic studies involve sampling the reaction mixture at specific time intervals and analyzing the samples using analytical techniques such as gas chromatography, infrared, or N.M.R. spectroscopy. However, the major disadvantages associated with this system are the relatively large sampling period and/or difficulty in data collection which makes the study tedious and often subject to considerable error.

A computer controlled batch reactor is an alternative apparatus for investigating catalytic reactions involving gas consumption and provides reliable data. In this system, the computer controlled constant pressure reactor system is designed and fabricated to keep constant pressure in the reactor. Besides it can provide facile reaction control and provide precise analysis for reliable kinetic data. The reaction can be achieved by maintaining a constant pressure with a minimum of pressure fluctuation in the batch reactor. The reaction rate can be followed by detecting the pressure drop in a gas supply reservoir due to the gas consumption in the reactor system. The gas consumption data can be conveniently stored and analyzed by using the computer at specified intervals of time to determine the kinetic data.

The completed computer controlled batch reactor system was successfully used to study the kinetics for hydrogenation of nitrile-butadiene rubber (NBR) (Parent et al., 1998), *cis*-1,4-polyisoprene (CPIP) (Charmondusit et al., 2001; Tangtongkul et al., 2003) and natural rubber (NR) (Hinchiranan et al., 2003). The work on the hydroformylation of PBD by various investigators has been studied in batch reactors; however, the kinetics were not elucidated. In this chapter, an attempt is made to study the hydroformylation of PBD using a computer-controlled batch reactor, gas uptake apparatus. Due to capability of detecting the reaction gas consumption precisely as a

function of time, the detailed kinetics could be achieved. The significant parameters, catalyst and polymer concentration, temperature, pressure, stirring speed, %CO in synthesis gas, addition of triphenylphosphine, and solvent type were investigated. The kinetics of PBD hydroformylation is presented and the mechanism is proposed.

#### 4.1 Kinetics of Hydroformylation of *Cis*-1,4-Polybutadiene using a Gas Uptake Apparatus

To study the kinetics of hydroformylation of *cis*-1,4-polybutadiene catalyzed by  $\text{HRh}(\text{CO})(\text{PPh}_3)_3$ , a gas uptake apparatus was used to detect the reaction gas consumption with reaction time. The reaction was carried out over 2 h and the final product was sampled to determine the degree of conversion by  $^1\text{H}$  NMR analysis (see section 3.2.2). Then, the conversion results were used to calibrate the conversion profile from the gas uptake apparatus. The obtained conversion profile was found to follow a first order profile as shown in Figure 4.1. The figure also shows the relation between  $\ln(1-x)$  and time where  $x$  is conversion and the slope of this plot is the

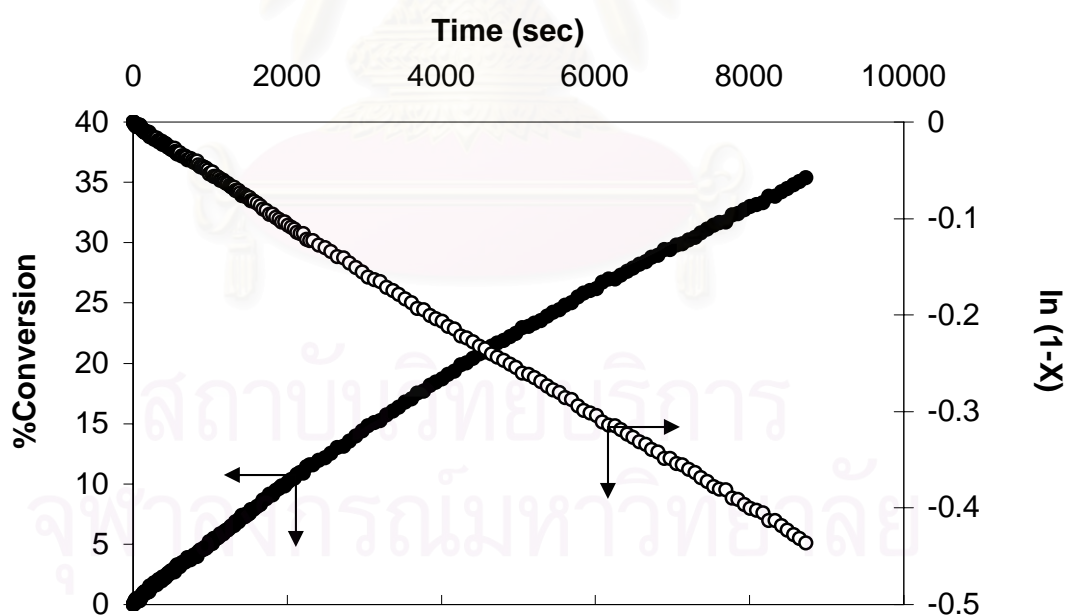


**Figure 4.1** Conversion profile (●) and 1<sup>st</sup> order reaction plot (○) for hydroformylation of PBD using  $\text{HRh}(\text{CO})(\text{PPh}_3)_3$ :  $[\text{C}=\text{C}] = 370 \text{ mM}$ ,  $[\text{Catalyst}] = 327 \text{ }\mu\text{M}$ , Solvent = MCB,  $P = 41.3 \text{ bar}$ , and  $T = 70 \text{ }^\circ\text{C}$ .



experimental reaction rate constant ( $k$ ). The reaction is pseudo first order, a reaction rate constant of  $5.19 \times 10^{-5} \text{ s}^{-1}$  under the following conditions:  $[\text{C}=\text{C}] = 370 \text{ mM}$ ,  $[\text{Catalyst}] = 327 \text{ }\mu\text{M}$ , Solvent = MCB,  $P = 41.3 \text{ bar}$ , and  $T = 70^\circ\text{C}$ .

## 4.2 Hydroformylation Catalyzed by Various Rh Complexes

The rhodium complex,  $\text{HRh}(\text{CO})(\text{PPh}_3)_3$ , is the one of the most efficient homogeneous catalysts for hydroformylation. According to the ease of ligand modification of the catalyst, there are many types of rhodium complexes which have been used in the hydroformylation process.  $\text{HRh}(\text{CO})(\text{PPh}_3)_3$  is commonly used in the industrial process due to the facility of syntheses and good performance at mild condition. However, other rhodium complexes such as  $\text{Rh}_4(\text{CO})_{12}$ ,  $\text{Rh}_6(\text{CO})_{16}$ ,  $[\text{Rh}(\text{COD})\text{Cl}]_2$ ,  $\text{Rh}(\text{COD})\text{acac}$ , and  $\text{Rh}(\text{COD})\text{acac}/\text{P}(\text{OC}_6\text{H}_4\text{C}(\text{CH}_3)_3)_3$  are still widely used as hydroformylation catalysts. Thus, they should be considered to observe whether the ligand effects activity and selectivity. The results for the hydroformylation of PBD using three rhodium complexes are shown in Table 4.1. In addition, the conversion profiles for hydroformylation of *cis*-1,4-PBD using various rhodium complexes in the gas uptake apparatus are illustrated in Figure 4.2.

Commonly the activity of transition metal complexes depends on the stability of ligand and reactivity of active site. Consequently, the types of ligand and their structures may have important effects on the selectivity and activity. In the case of  $\text{Rh}_4(\text{CO})_{12}$ , the steric hindrance in this complex probably causes less activity for hydroformylation of the polymer, especially high molecular weight PBD. In case of  $[\text{Rh}(\text{COD})\text{Cl}]_2$ , the steric hindrance of the complex could also be one reason for lower activity. Another reason may be due to the formation of  $\text{HCl}$ , is resulted from coordination of  $\text{H}_2$  in synthesis gas and  $\text{Cl}$  on rhodium complex, which is an inhibitor for the hydroformylation process. In the  $\text{HRh}(\text{CO})(\text{PPh}_3)_3$  complex,  $\text{PPh}_3$  is a suitable ligand for the rhodium species. The dissociation of  $\text{PPh}_3$  generates the necessary vacant sites to receive the activation of the polymer backbone.

**Table 4.1** Investigation of hydroformylation of *cis*-1,4-PBD using various Rh complexes.

Catalyst	Mole of Rhodium* (mmol)	$k \times 10^5$ ( $s^{-1}$ )	Conv. (%) at 2 h
HRh(CO)(PPh <sub>3</sub> ) <sub>3</sub>	5	9.18	44
Rh <sub>4</sub> (CO) <sub>12</sub>	22	1.43	11
[Rh(COD)Cl] <sub>2</sub>	10	0.35	2

Conditions: [C=C] = 370 mM;  $P_{H_2/CO}$  = 41.3 bar;  $H_2:CO$  = 1:1;  $T$  = 80°C.

[C=C] is defined as the weight of *cis*-1,4-polybutadiene divided by molecular weight of repeating unit.

\* The mole fraction of rhodium in solution.

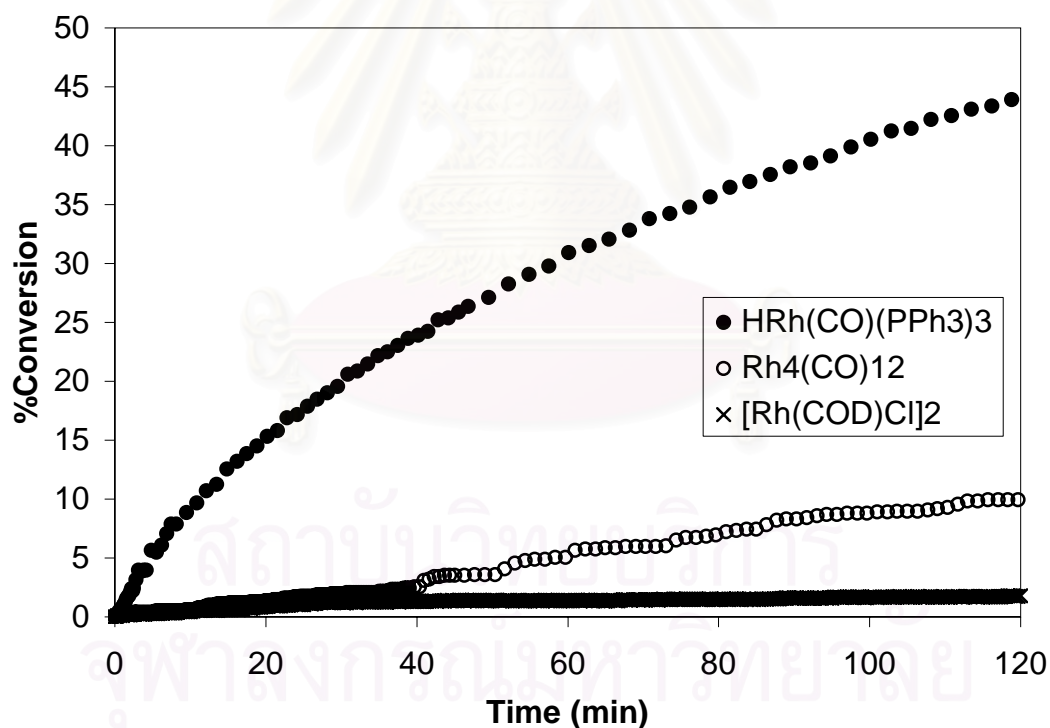


**Figure 4.2** Conversion profile of hydroformylation using various rhodium complexes, [C=C] = 370 mM;  $P_{H_2/CO}$  = 41.3 bar;  $H_2:CO$  = 1:1;  $T$  = 80°C.

### 4.3 Kinetics of Hydroformylation in the presence of $\text{Rh}_4(\text{CO})_{12}$

After the initial study on the hydroformylation of *cis*-1,4-PBD using various rhodium complexes mentioned above, the reaction kinetics of the hydroformylation process was also investigated in the presence of  $\text{Rh}_4(\text{CO})_{12}$ . The parameters such as temperature, total pressure of synthesis gas, and catalyst concentration were studied. The results for this study are presented in Table 4.2. For all experiments, the reaction is pseudo first order with respect to double bond concentration. The reaction rate is relatively slow, ( $k \sim 1\text{-}14 \times 10^{-6} \text{ s}^{-1}$ ) and the conversion at 2 h is low (1-11%).

**Table 4.2** Kinetic results of PBD hydroformylation catalyzed by  $\text{Rh}_4(\text{CO})_{12}$  in gas uptake apparatus.

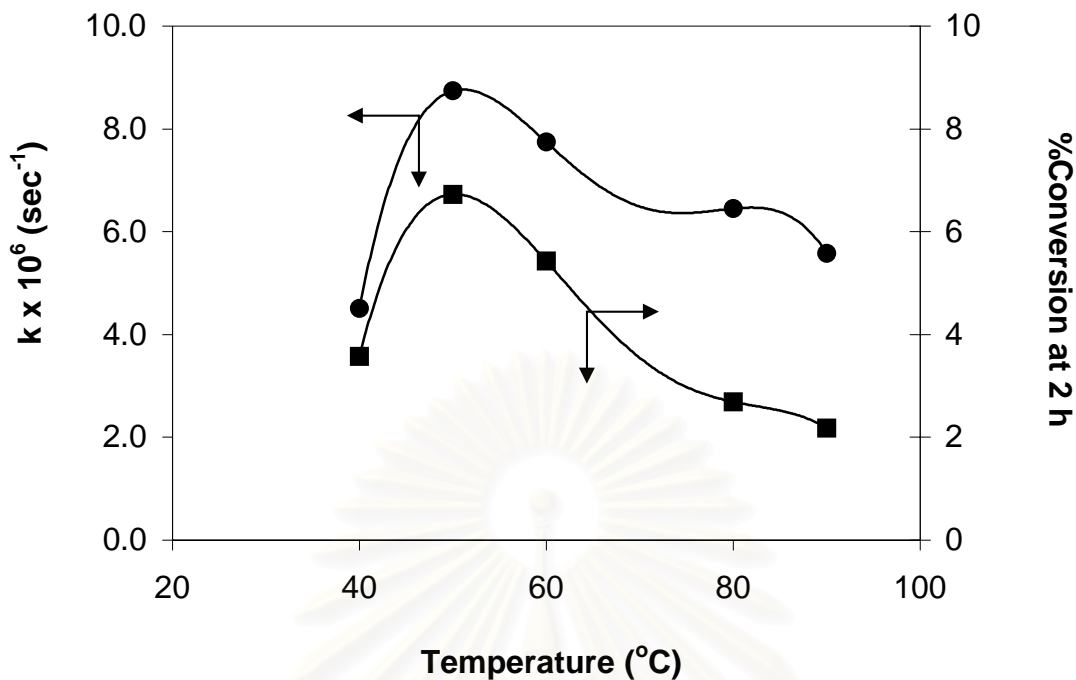
Expt.	[C=C] (mM)	[Rh] <sup>a</sup> ( $\mu\text{M}$ )	$P_{\text{H}_2/\text{CO}}$ (bar)	T ( $^{\circ}\text{C}$ )	$k \times 10^6$ ( $\text{s}^{-1}$ )	Conv. (%) at 2 h
1	370	75	41.3	40	4.51	3.6
2	370	75	41.3	50	8.74	6.7
3	370	75	41.3	60	7.74	5.4
4	375	75	41.3	80	6.45	2.7
5	370	75	41.3	90	5.58	2.2
6	370	75	13.8	50	1.00	0.8
7	370	75	27.6	50	3.84	3.0
8	370	75	55.1	50	10.07	7.9
9	370	179	41.3	50	10.78	8.2
10	370	269	41.3	50	12.27	9.5
11	370	358	41.3	50	14.32	11.0

All reaction was carried out under following reaction condition: mole of rhodium = 5 mM, stirring speed = 1200 rpm, solvent = MCB.

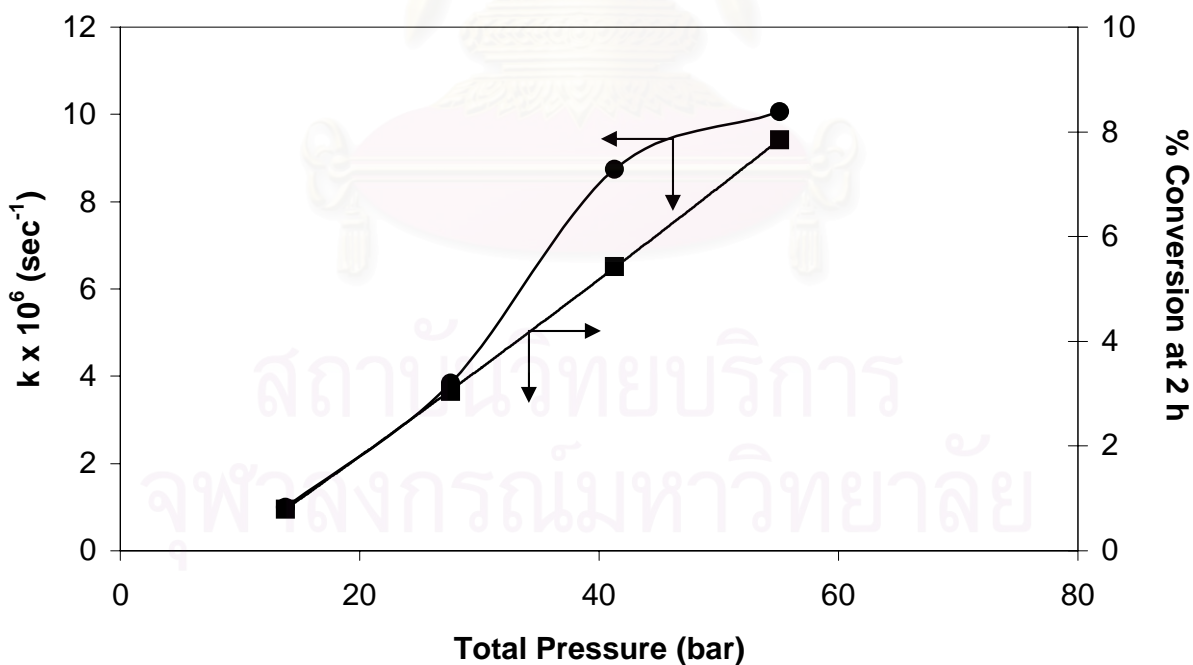
### a) Effect of Temperature and Total Pressure

Figure 4.3 shows the effect of temperature on reaction rate constant and % hydroformylation at 2 h. When investigating the effect of temperature, a total pressure of 41.3 bar and a synthesis gas mixture of 1:1 H<sub>2</sub>:CO was used. The polymer concentration and catalyst concentration were kept constant at 370 mM and 75 μM, respectively. For the temperature range of 40 to 90°C, the rate constant and conversion tend to increase with increasing temperature and reach a maximum at 50°C, then decrease. The decrease in reaction rate constant at temperature above 50°C may be attributed to the decomposition of catalyst. For PBD hydroformylation using HRh(CO)(PPh<sub>3</sub>)<sub>3</sub> as the catalyst, the reaction rate constant reached a maximum at 80°C, and then decreased (Section 3.3.2).

The change of reaction rate constant with the total pressure for a 1:1 synthesis gas (H<sub>2</sub>:CO) is shown in Figure 4.4. The temperature was maintained at 50°C, with a polymer concentration of 370 mM and catalyst concentration of 75 μM with no added triphenyl phosphine. The total pressure of synthesis gas was varied from 13.8 to 55.1 bar. From the plot shown in Figure 4.4, it appears that the reaction rate is probably first order with respect to total pressure, and shifts to zero order at higher pressure. The conversion obtained under these conditions was between about 1 and 8 % hydroformylation at 2 h. To achieve higher conversion, the reaction required longer reaction time. For HRh(CO)(PPh<sub>3</sub>)<sub>3</sub>, the PBD hydroformylation also shows a first order reaction with respect to total pressure over the range of 13.8 and 41.3 bar (Section 3.3.5).



**Figure 4.3** Effect of temperature on rate constant (●) and conversion at 2 h (■) in the presence of  $\text{Rh}_4(\text{CO})_{12}$ ,  $[\text{C}=\text{C}] = 370 \text{ mM}$ ;  $[\text{Rh}] = 75 \text{ }\mu\text{M}$ ;  $P_{\text{H}_2/\text{CO}} = 41.3 \text{ bar}$ ;  $\text{H}_2:\text{CO} = 1:1$ .



**Figure 4.4** Effect of total pressure on rate constant (●) and conversion at 2 h (■) in the presence of  $\text{Rh}_4(\text{CO})_{12}$ ,  $[\text{C}=\text{C}] = 370 \text{ mM}$ ;  $[\text{Rh}] = 75 \text{ }\mu\text{M}$ ;  $\text{H}_2:\text{CO} = 1:1$ ;  $T = 50^\circ\text{C}$ .

### b) Effect of Catalyst Concentration

The effect of catalyst concentration on reaction rate constant and %conversion at 2 h is illustrated in Figure 4.5. The reaction was maintained at 50°C at a total pressure at 41.3 bar with a synthesis gas mixture of 1:1 H<sub>2</sub>:CO. The polymer concentration was kept constant at 370 mM. To investigate the effect of catalyst concentration, PPh<sub>3</sub> was not added. Over the catalyst concentration range of 75 to 358 μM, there is a linear increase of rate constant with respect to catalyst concentration. Extrapolation of this plot to zero catalyst concentration would however provide positive intercept. This is not possible as no hydroformylation takes place in the absence of catalyst. Consequently, further work is needed to understand this peculiar behavior, work at lower catalyst concentration is necessary.

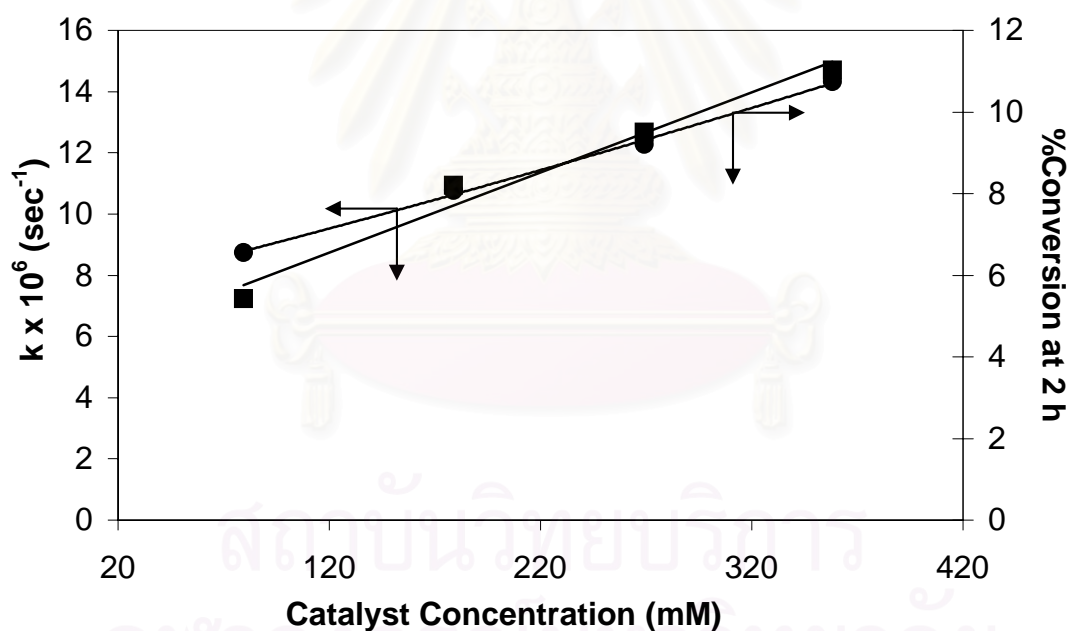


**Figure 4.5** Effect of catalyst concentration on rate constant (●) and conversion at 2 h (■) in the presence of Rh<sub>4</sub>(CO)<sub>12</sub>, [C=C] = 370 mM; P<sub>H<sub>2</sub>/CO</sub> = 41.3 bar; H<sub>2</sub>:CO = 1:1; H<sub>2</sub>:CO = 1:1; T = 50°C.

#### 4.4 Kinetics of the Hydroformylation of *Cis*-1,4-Polybutadiene in the presence of $\text{HRh}(\text{CO})(\text{PPh}_3)_3$

According to the initial study of *cis*-1,4-polybutadiene (PBD) hydroformylation using various rhodium complexes,  $\text{HRh}(\text{CO})(\text{PPh}_3)_3$  had higher activity than  $\text{Rh}_4(\text{CO})_{12}$  and  $[\text{Rh}(\text{COD})\text{Cl}]_2$ . Therefore, the kinetics of PBD hydroformylation using  $\text{HRh}(\text{CO})(\text{PPh}_3)_3$  was studied in detail using the gas uptake apparatus. The process parameters are temperature, total pressure of synthesis gas, catalyst concentration, polymer concentration, triphenylphosphine addition, and solvent type. The summary of all kinetics results is shown in Table 4.3.

##### 4.4.1 Effect of Stirring Speed

Due to the capability of the agitator in the gas uptake apparatus, the stirring speed was varied over the range of 800 to 1400 rpm. The reaction rate constant and %conversion at 2 h are shown in Figure 4.6a. The reaction was carried out at 70°C and a total pressure of 41.3 bar with a 1:1 ( $\text{H}_2$ :CO) synthesis gas mixture. The catalyst concentration was maintained at 326  $\mu\text{M}$  and no  $\text{PPh}_3$  was added. The reaction rate is independent on stirring speed above 800 rpm. Thus, reaction rate is not affected by mass transfer limitations when experiments are performed at an agitation above 800 rpm.

Compared with results from the study carried out in the Parr reactor as presented in Figure 4.6b, the reaction rate at 800 rpm obtained from gas uptake apparatus was somewhat higher (~20%) than that of Parr reactor at 700 rpm. This can be explained in that the efficiency of the agitator affected the mass transfer in the gas uptake apparatus showing superiority in mixing over that in the Parr reactor due to the configuration of the impeller. Moreover, this superiority may be caused in that the L/D ratio of Parr reactor is much lower than that of autoclave used in the gas uptake apparatus. Thus, another benefit of the gas uptake is that it provides superior of mixing.

**Table 4.3** Kinetic results of univariate experiments in the presence of  $\text{HRh}(\text{CO})(\text{PPh}_3)_3$ .

Expt.	Stirring speed (rpm)	[C=C] (mM)	[Rh] <sup>a</sup> (μM)	Mole ratio of Added $\text{PPh}_3/[\text{Rh}]^a$	$\text{P}_{\text{H}_2/\text{CO}}$ (bar)	%CO in gas mixture	Temp. (°C)	$k \times 10^5$ (s <sup>-1</sup> )	Conv. (%) at 2 h
1	803	370	326	0	41.3	50	70	5.31	32.1
2	1005	370	326	0	41.3	50	70	5.75	32.4
3	1200	370	326	0	41.3	50	70	5.91	32.7
4	1412	370	326	0	41.3	50	70	5.90	32.1
5	1200	100	326	0	41.3	50	70	5.57	31.8
6	1200	201	326	0	41.3	50	70	5.70	32.1
7	1200	250	326	0	41.3	50	70	5.72	32.2
8	1200	300	326	0	41.3	50	70	5.82	32.5
9	1200	325	326	0	41.3	50	70	5.91	32.8
10	1200	370	50	0	41.3	50	70	1.22	9.1
11	1200	370	100	0	41.3	50	70	2.65	15.5
12	1200	370	150	0	41.3	50	70	4.07	21.9
13	1200	370	200	0	41.3	50	70	4.84	25.0
14	1200	370	257	0	41.3	50	70	5.42	30.6
15	1200	370	325	0	41.3	50	70	5.91	32.1
16	1200	370	400	0	41.3	50	70	6.14	35.4
17	1200	370	326	1	41.3	50	70	4.85	31.8
18	1200	370	326	20	41.3	50	70	3.13	21.4
19	1200	370	326	40	41.3	50	70	2.23	15.7
20	1200	370	326	60	41.3	50	70	1.70	12.6
21	1200	370	326	0	55.1	50	60	2.69	18.0
22	1200	370	326	0	55.1	50	65	3.86	24.7
23	1200	370	326	0	55.1	50	70	5.78	31.2
24	1200	370	326	0	55.1	50	75	8.36	45.2
25	1200	370	326	0	55.1	50	80	9.89	48.8
26	1200	370	326	0	13.8	50	70	4.21	27.0
27	1200	370	326	0	20.7	50	70	4.80	30.2
28	1200	370	326	0	27.6	50	70	5.26	30.8
29	1200	370	326	0	35.1	50	70	5.49	31.9
30	1200	370	326	0	55.1	50	70	5.78	32.3
31	1200	370	326	0	41.3	8	70	9.42	46.1
32	1200	370	326	0	41.3	25	70	8.03	36.0
33	1200	370	326	0	41.3	42	70	6.65	32.1
34	1200	370	326	0	41.3	92	70	0.96	7.5

All reaction was carried out in monochlorobenzene

<sup>a</sup>[Rh] =  $[\text{HRh}(\text{CO})(\text{PPh}_3)_3]$



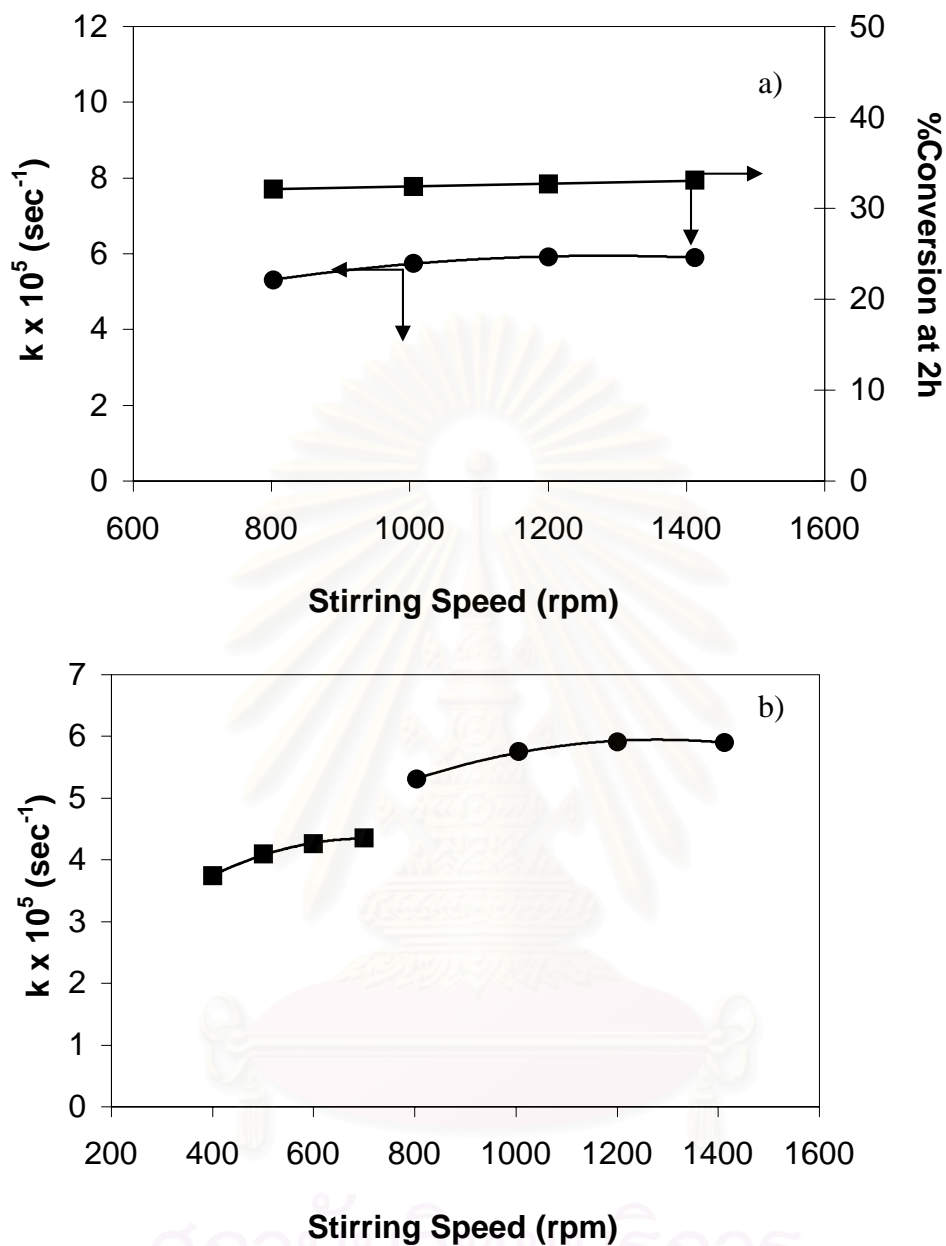


**Figure 4.6**

a) Effect of stirring speed on rate constant (●) and conversion at 2 h (■) by using gas uptake apparatus,  $[C=C] = 370 \text{ mM}$ ;  $[Rh] = 326 \text{ }\mu\text{M}$ ;  $P_{H_2/CO} = 41.3 \text{ bar}$ ;  $H_2:CO = 1:1$ ;  $T = 70^\circ\text{C}$ .

b) Effect of stirring speed on reaction rate in gas uptake apparatus (●) and Parr reactor (■),  $[C=C] = 370 \text{ mM}$ ;  $[Rh] = 326 \text{ }\mu\text{M}$ ;  $P_{H_2/CO} = 41.3 \text{ bar}$ ;  $H_2:CO = 1:1$ ;  $T = 70^\circ\text{C}$ .

#### 4.4.2 Effect of Polymer Concentration

The effect of polymer concentration on the reaction rate constant and %conversion at 2 h are shown in Figure 4.7. The temperature was kept constant at 70°C, and the total synthesis gas pressure (1:1 H<sub>2</sub>:CO) was 41.3 bar. The catalyst concentration was maintained at 326 μM and there was no PPh<sub>3</sub> addition. The reaction rate constant is apparently independent of the polymer concentration. Considering the reaction mechanism previously proposed in Scheme 3.2 and the derived rate law for hydroformylation of PBD in Eq. 3.10, the reaction rate is first order with respect to [C=C] concentration, so the rate constant is independent of the polymer concentration as shown by the kinetic results since the reaction was observed at a total pressure of 41.3 bar which is in the zero order range of total pressure.

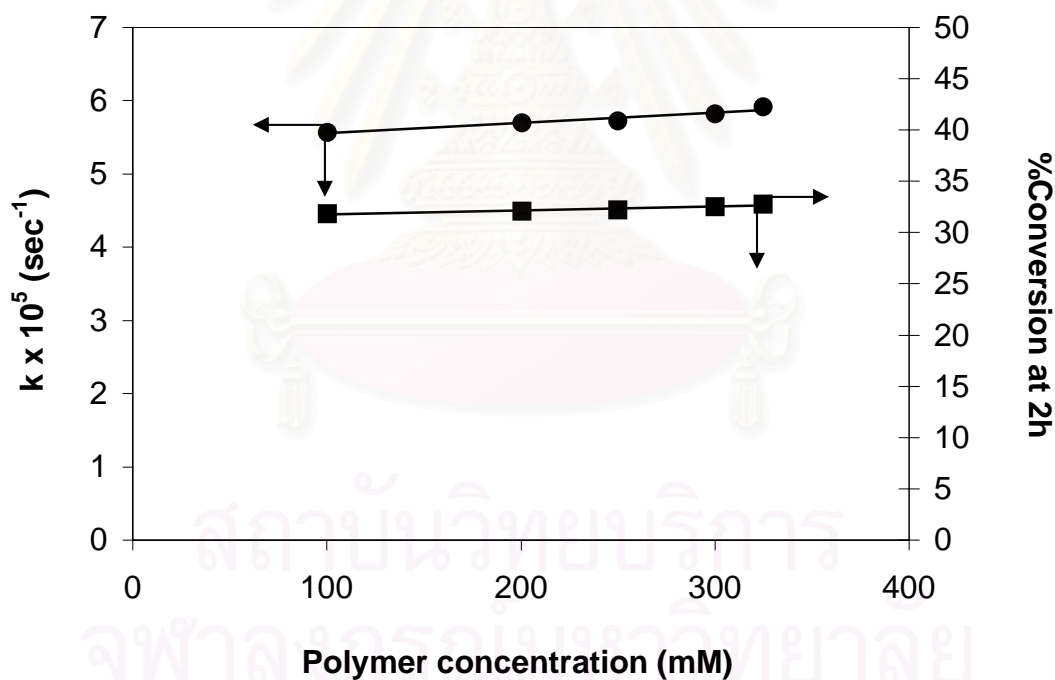


**Figure 4.7** Effect of polymer concentration on rate constant (●) and %conversion at 2 h (■), [Rh] = 326 μM; no added PPh<sub>3</sub>; P<sub>H<sub>2</sub>/CO</sub> = 41.3 bar; H<sub>2</sub>:CO = 1:1; T = 70°C.

#### 4.4.3 Effect of Temperature

The effect of temperature on the rate constant and %conversion at 2 h are shown in Figure 4.8. The reaction was carried out over the temperature range of 60-80°C with a 1:1 synthesis gas mixture of 55.1 bar. The polymer concentration of 370 mM, and the catalyst concentration of 326  $\mu\text{M}$  was used and there was no added  $\text{PPh}_3$ . The rate constant is proportional to temperature. The calculated reaction rate constant followed the Arrhenius equation, the apparent activation energy ( $E$ ) was obtained from the slope of Arrhenius plot as shown in Figure 4.9a. It is estimated to be 66 kJ/mole over the temperature range of 60 to 80°C. In the case of using the Parr reactor for the hydroformylation of PBD (see Section 3.3.2), the value of  $E$  was 41 kJ/mol which suggested that the reaction was primarily under chemical reaction control for hydroformylation process. Nevertheless, this relatively low  $E$  values suggests that the hydroformylation process in the Parr reactor may still be influenced on some extent of mass transfer control as was apparent from the effect of stirring speed results presented in Section 4.4.1. According to Eyring equation (Eq 4.1), the apparent activation enthalpy and entropy were estimated by plotting the relation between  $R \ln(kh/k_B T)$  with respect to  $1/T$  (Figure 4.9b) for the gas uptake results. The slope of the graph is represented as apparent activation enthalpy, 63.2 kJ/mole and intercept as apparent activation entropy, 0.13 kJ/(mole.K).

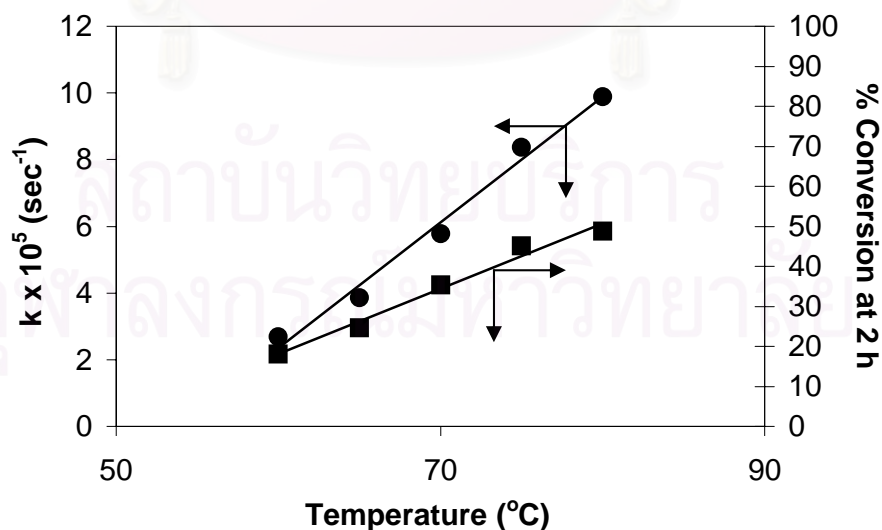


**Figure 4.8** Effect of temperature on rate constant (●) and conversion at 10 h (■),  $[\text{C}=\text{C}] = 370 \text{ mM}$ ;  $[\text{Rh}] = 326 \text{ }\mu\text{M}$ ; no added  $\text{PPh}_3$ ;  $P_{\text{H}_2/\text{CO}} = 41.3 \text{ bar}$ ;  $\text{H}_2:\text{CO} = 1:1$ .

$$k = \frac{k_B T}{h} e^{-\frac{\Delta H^\ddagger}{RT}} e^{\frac{\Delta S^\ddagger}{R}} \quad (4.1)$$

where  $k_B$  = Boltzmann's constant =  $0.381 \times 10^{-23} \text{ J K}^{-1}$   
 $h$  = Plank constant =  $6.626 \times 10^{-34} \text{ J s}$

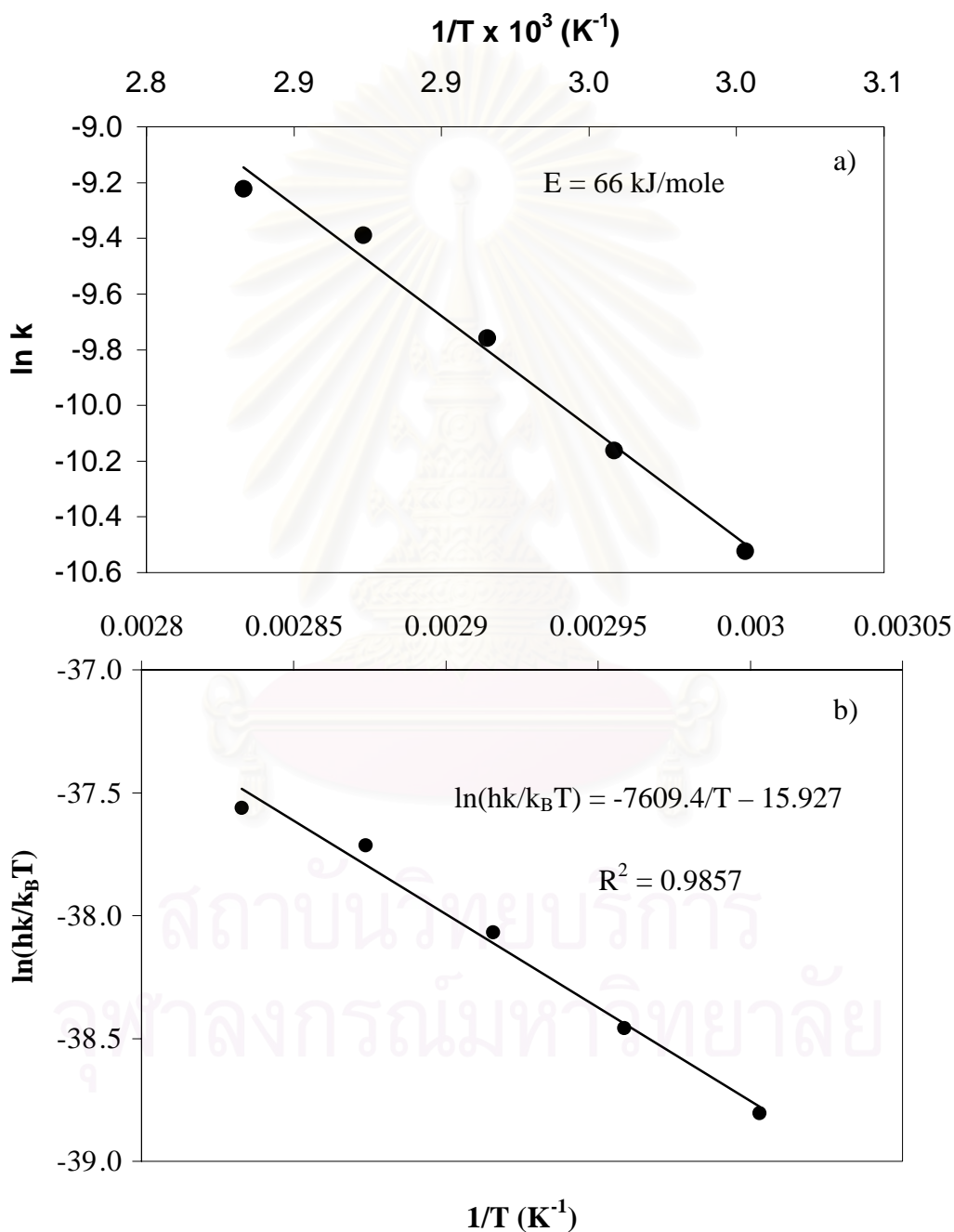


**Figure 4.9** a) Arrhenius plot for the hydroformylation of polybutadiene.  
 b) Eyring plot for PBD hydroformylation,  $[\text{C}=\text{C}] = 370 \text{ mM}$ ;  $[\text{Rh}] = 326 \text{ }\mu\text{M}$ ; no added  $\text{PPh}_3$ ;  $\text{P}_{\text{H}_2/\text{CO}} = 41.3 \text{ bar}$ ;  $\text{H}_2:\text{CO} = 1:1$ .

#### 4.4.4 Effect of Total Pressure of Synthesis Gas

The change of reaction rate constant with the total pressure of 1:1 synthesis gas ( $\text{H}_2:\text{CO}$ ) is shown in Figure 4.10. The temperature was maintained at  $70^\circ\text{C}$  with polymer concentration of 370 mM and catalyst concentration of  $326\ \mu\text{M}$  without added triphenyl phosphine. The total pressure of synthesis gas was varied from 13.8 to 55.1 bar. It is apparent from the plot that the reaction rate is probably first order with respect to total pressure up to about 30 bar, and then shifts to zero order behavior when the pressure is increased further. However, the  $k$  vs. total pressure results obtained in the Parr reactor shows that a zero order relation only starts to be observed above 41.3 bar. Thus, a zero order relation from the gas uptake apparatus was found at the lower pressure than that from Parr reactor. This also can be explained in that superior mixing in the autoclave of the gas uptake apparatus can overcome the mass transfer limitation.

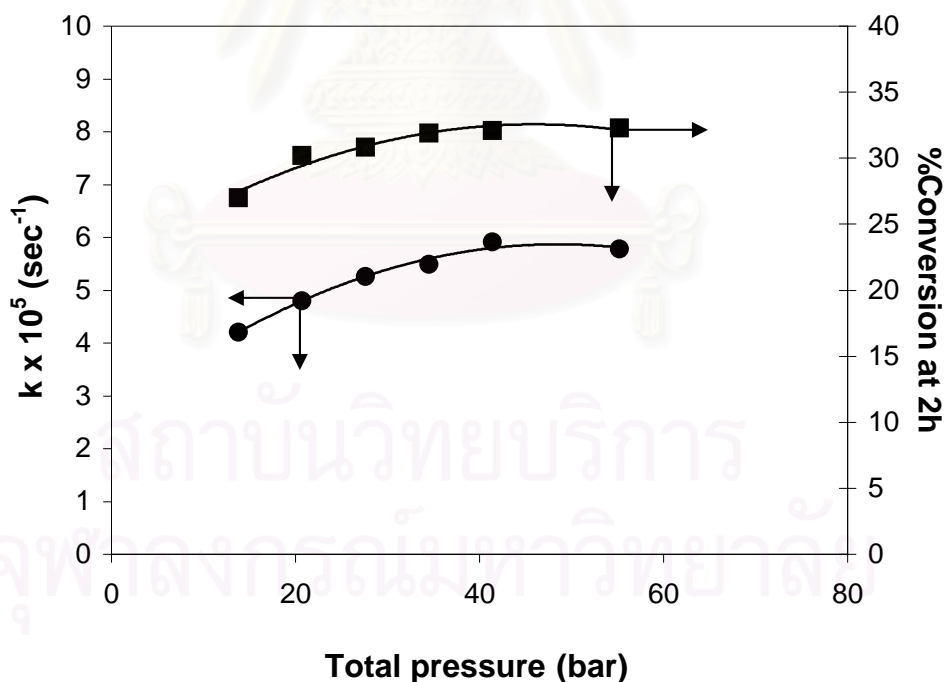


**Figure 4.10** Effect of total pressure on rate constant (●) and conversion at 2 h (■),  $[\text{C}=\text{C}] = 370\ \text{mM}$ ;  $[\text{Rh}] = 326\ \mu\text{M}$ ; no added  $\text{PPh}_3$ ;  $\text{H}_2:\text{CO} = 1:1$ ;  $T = 70^\circ\text{C}$ .

#### 4.4.5 Effect of %CO in synthesis gas

The effect of %CO in synthesis gas on the reaction rate and final conversion at 2 h is shown in Figure 4.11. The reaction conditions were maintained at 70°C and a total pressure of 41.3 bar. Polymer and catalyst concentration were employed at 370 mM and 326  $\mu\text{M}$ , respectively and no triphenyl phosphine was added. The reaction shows an inverse first order behavior with increasing %CO in synthesis gas. This can be attributed to the formation of inactive Rh species as discussed in Section 3.3.3

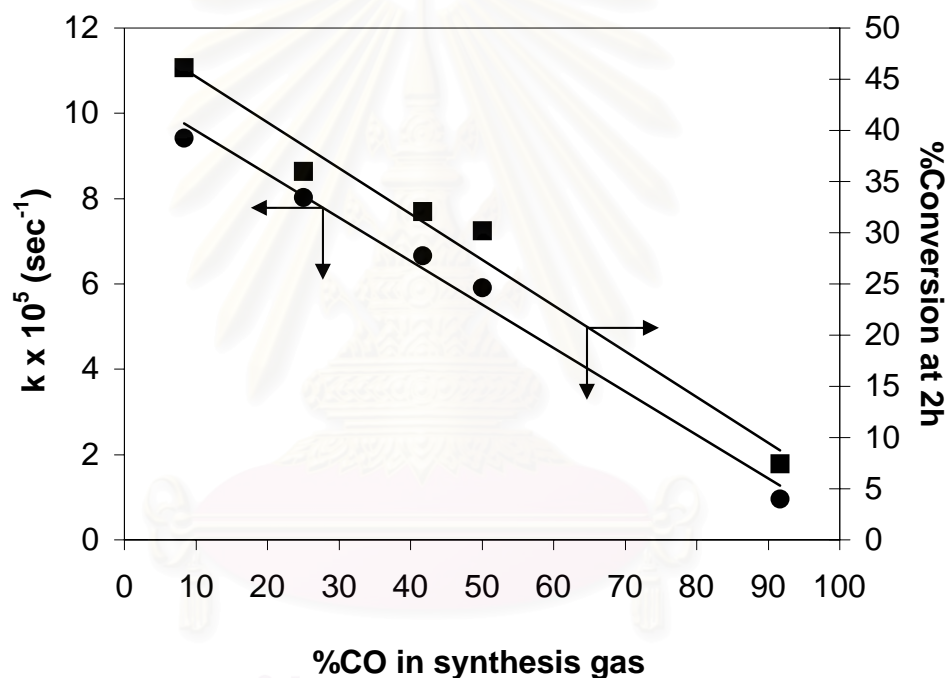


**Figure 4.11** Effect of %CO in synthesis on rate constant (●) and conversion at 2 h (■),  $[\text{C}=\text{C}] = 370 \text{ mM}$ ;  $[\text{Rh}] = 326 \mu\text{M}$ ; no added  $\text{PPh}_3$ ;  $P = 41.3 \text{ bar}$ ;  $T = 70^\circ\text{C}$ .

#### 4.4.6 Effect of Catalyst Concentration

Figure 4.12 shows a plot of the change in the reaction rate constant and % conversion at 2 h with respect to catalyst concentration. The temperature was maintained at 70°C. The total pressure was 41.3 bar, with a synthesis gas mixture of 1:1 (H<sub>2</sub>:CO). The polymer concentration was kept constant at 370 mM. To investigate the effect of catalyst concentration, PPh<sub>3</sub> was not added. The effect of catalyst concentration was studied from 50 to 400 μM. The resultant plot was first order with respect to catalyst concentration upto about 150 μM and then shifted toward a zero order behavior with further increase in catalyst concentration.

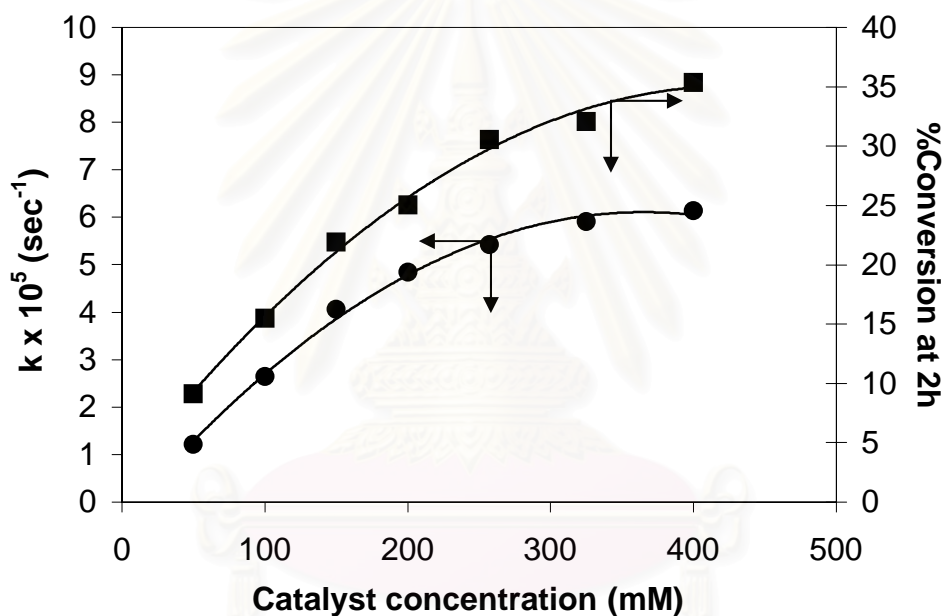


**Figure 4.12** Effect of catalyst concentration on rate constant (●) and conversion at 2 h (■), [C=C] = 370 mM; no added PPh<sub>3</sub>; P<sub>H<sub>2</sub>/CO</sub> = 41.3 bar; H<sub>2</sub>:CO = 1:1; T = 70°C.

#### 4.4.7 Effect of PPh<sub>3</sub> addition

Figure 4.13 shows the effect of PPh<sub>3</sub> addition on the reaction rate constant and %conversion at 2 h. There was evidence that high temperature may cause the deactivation of catalyst. Consequently, the addition of ligand could stabilize the catalyst. For HRh(CO)(PPh<sub>3</sub>)<sub>3</sub>, various mole ratio of PPh<sub>3</sub>/Rh were studied. The temperature was kept constant at 90°C and the total pressure of a 1:1 CO:H<sub>2</sub> synthesis gas mixture was hold at 41.3 bar. It can be seen from the Figure 4.13 that the reaction rate constant decreases with increasing PPh<sub>3</sub>/Rh. Hence, added PPh<sub>3</sub> is an inhibitor for hydroformylation of PBD. This can be explained due to the retardation of PPh<sub>3</sub> in the catalytic cycle as discussed in Section 3.3.6 and 3.4.

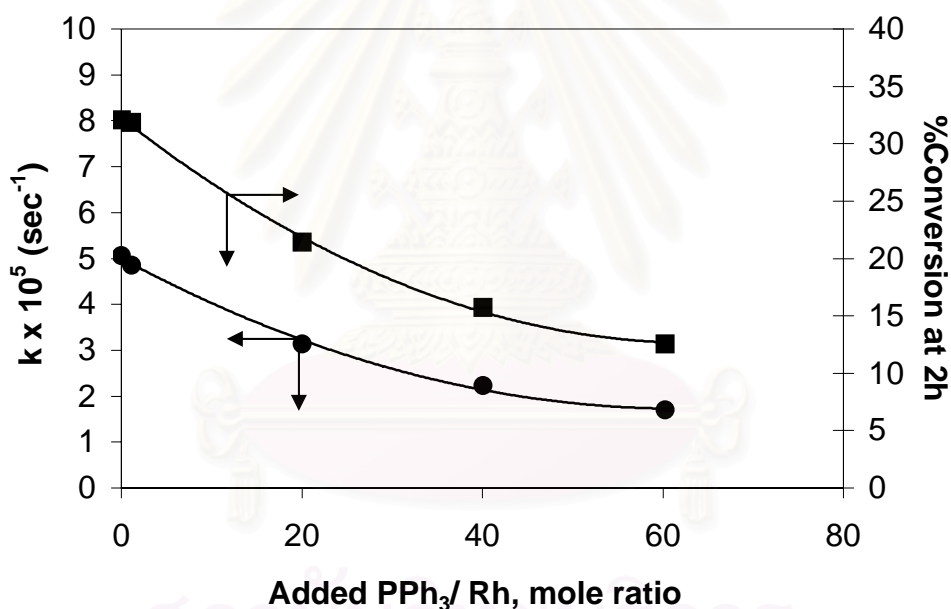


**Figure 4.13** Effect of PPh<sub>3</sub> addition on rate constant (●) and conversion at 2 h (■), [C=C] = 370 mM; [Rh] = 326 μM; P<sub>H<sub>2</sub>/CO</sub> = 41.3 bar; H<sub>2</sub>:CO = 1:1; T = 70°C.



#### 4.4.8 Effect of Solvent Type

To investigate the effect of solvent on the hydroformylation reaction, three solvents, namely monochlorobenzene, benzene, and toluene were examined. The reaction was carried out at a temperature of 70°C and total pressure of 41.3 bar (CO:H<sub>2</sub> = 1:1). A polymer concentration of 370 mM, catalyst concentration of 326 μM, with no added PPh<sub>3</sub> was used. The conversion profiles obtained via the gas uptake apparatus for each solvent are given in Figure 4.14. Benzene and monochlorobenzene gave similar and higher conversion profiles than toluene. Therefore, benzene and monochlorobenzene appear to be better at promoting the dissociation of the triphenylphosphine ligand from the HRh(CO)(PPh<sub>3</sub>)<sub>3</sub> complex (see Section 3.4) than toluene. In addition, from Table 4.4 it was found that the rate constant and % conversion at 2 h increased with increasing solvating power of the solvent in the order: monochlorobenzene > benzene > toluene.

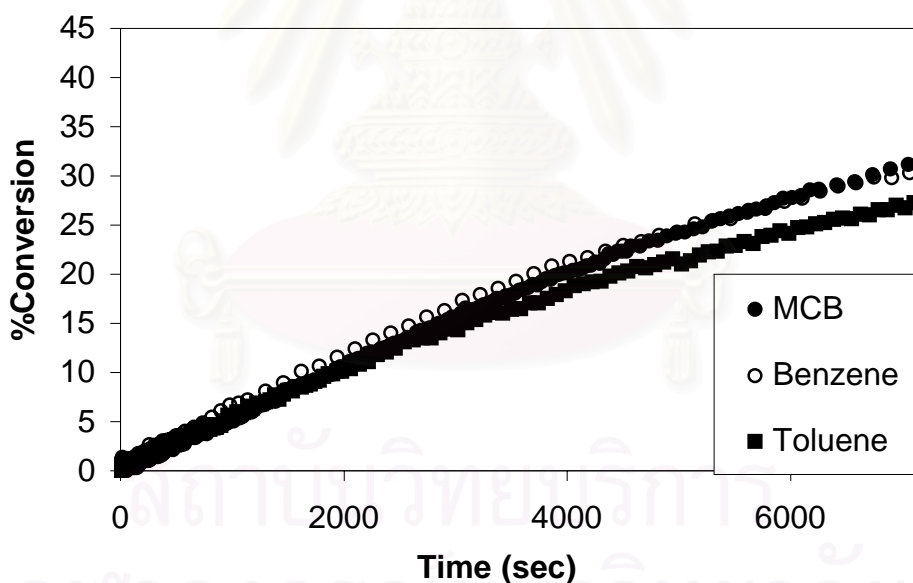


**Figure 4.14** Effect of solvent types in synthesis on rate constant; monochlorobenzene (●), benzene (○), and toluene (■), [C=C] = 370 mM ; [Rh] = 326 μM; no added PPh<sub>3</sub>; P = 41.3 bar; H<sub>2</sub>:CO = 1:1; T = 70°C.

**Table 4.4** Effect of Solvent on the PBD Hydroformylation

Solvent	$k \times 10^5 \text{ (sec}^{-1}\text{)}$	Conversion (%) at 2 h
Monochloro benzene	5.91	32.1
Benzene	5.53	31.2
Toluene	3.08	27.3

Condition:  $[\text{C}=\text{C}] = 370 \text{ mM}$ ;  $[\text{Rh}] = 326 \text{ }\mu\text{M}$ ;  $P_{\text{H}_2/\text{CO}} = 41.3 \text{ bar}$ ;  $\text{H}_2:\text{CO} = 1:1$ ;  $T = 70^\circ\text{C}$ .

### 6.5 Reaction Mechanism and Rate Law

In monochlorobenzene,  $\text{HRh}(\text{CO})(\text{PPh}_3)_3$  is an efficient catalyst for the hydroformylation of PBD. The mechanism of PBD hydroformylation was proposed in section 3.4. An experimental rate law based on kinetic results shows first order with respect to catalyst concentration, carbon carbon double bond concentration, total pressure and an inverse first order with respect to  $\text{PPh}_3$  concentration. The kinetic results obtained in gas uptake apparatus are quite consistent with that in Parr batch reactor (Ch. 3), even though the Parr reactor suffers from some mass transfer limitations, as reflected from a comparison of the effect of stirring and effect of temperature studies for the two reactors. For PBD hydroformylation catalyzed by  $\text{Rh}_4(\text{CO})_{12}$ , the mechanism is not proposed due to the limited numbers of experimental data, and low conversion obtained.

According to the proposed mechanism, the rate law of PBD hydroformylation is given as follows:

$$\frac{-d[\text{C}=\text{C}]}{dt} = \frac{[\text{Rh}]_T K_1 K_2 K_3 K_{\text{H}_2} K_{\text{CO}} K_P [\text{H}_2][\text{CO}][\text{C}=\text{C}]}{\alpha} \quad (3.10)$$

where

$$\alpha = [\text{PPh}_3] + K_P(1+K_{\text{CO}}[\text{CO}]) + K_1 K_{\text{CO}} K_P [\text{C}=\text{C}](1+K_2) + K_1 K_2 K_3 K_{\text{CO}} K_P [\text{CO}][\text{C}=\text{C}](1+K_{\text{H}_2}[\text{H}_2])$$

Assuming  $K_{H,H_2}$  and  $K_{H,CO}$  is the Henry's Law constant for the solubility of hydrogen and carbonmonoxide in monochlorobenzene, respectively. The equilibrium relations substituted with  $K_H$  were rearranged.

$$k = \frac{K_1 K_2 K_3 K_{H_2} K_{CO} K_P K_{H,H_2} K_{H,CO} [Rh]_T [H_2] [CO] [C = C]}{A} \quad (\text{AIII-B})$$

where

$$A = [PPh_3] + K_P + K_P K_{CO} K_{H,CO} P_{CO} + (K_1 K_{CO} K_P + K_1 K_2 K_{CO} K_P) [C = C] + K_1 K_2 K_3 K_{CO} K_P K_{CO} K_{H,CO} P_{CO} [C = C] + K_1 K_2 K_3 K_{CO} K_{H_2} K_P K_{H,CO} K_{H,H_2} P_{CO} P_{H_2} [C = C]$$

The functional relationship between the observed first order reaction constant,  $k$  and the studied factors can be written as Eq. 4.1 (see Appendix III).

$$k = \frac{K_A [Rh]_T P_{H_2} P_{CO} [C = C]}{[PPh_3] + K_B + K_C P_{CO} + K_D [C = C] + K_E P_{CO} [C = C] + K_F P_{CO} P_{H_2} [C = C]} \quad (4.1)$$

where

$$\begin{aligned} K_A &= K_1 K_2 K_3 K_{H_2} K_{CO} K_P K_{H,H_2} K_{H,CO} \\ K_B &= K_P \\ K_C &= K_P K_{CO} K_{H,CO} \\ K_D &= K_1 K_{CO} K_P + K_1 K_2 K_{CO} K_P \\ K_E &= K_1 K_2 K_3 K_{CO} K_P K_{H,CO} \\ K_F &= K_1 K_2 K_3 K_{CO} K_{H_2} K_P K_{H,H_2} K_{H,CO} \end{aligned}$$

In order to test the validity of the model given by Eq. 4.1 with the observed kinetic data, the non-linear least square method for parameter estimation was employed. Regression estimates for the parameter are provided in Table 4.3 along with their associated error estimates. The results of an analysis of variance (ANOVA) summarized in Table 4.4 shows the significance of the model. The residue plot as illustrated in Figure 4.15 shows fairly random scattering of errors, thus confirms that none of systematic error present. Actual model predictions of conversion profile relative to the data from gas uptake are plotted in Figure 4.16.

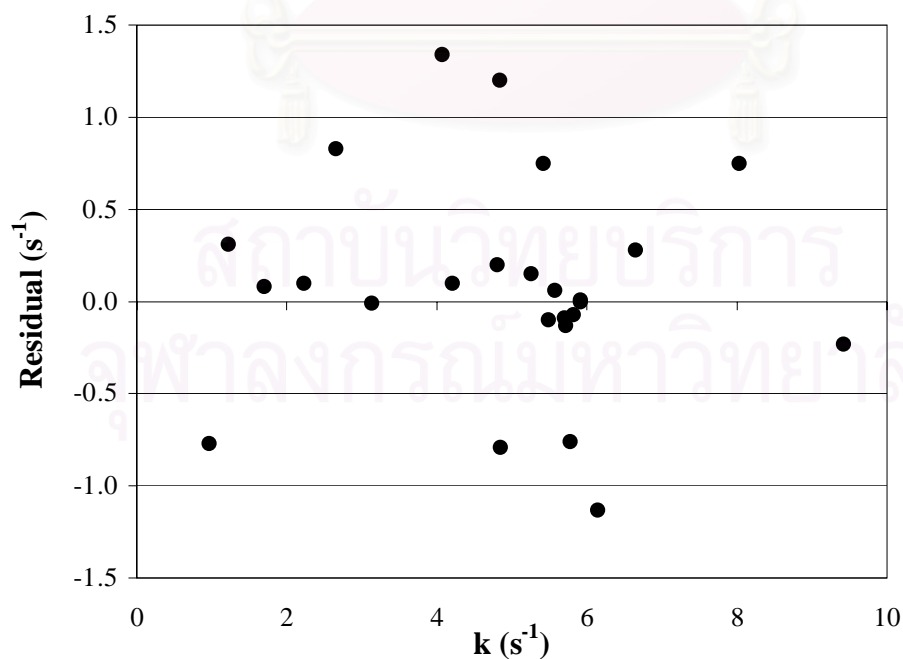
**Table 4.5** Model parameter estimates

Parameter	Asymptotic 95%			
	Asymptotic		Confidence Interval	
	Estimate	Std. Error	Lower	Upper
K <sub>A</sub>	8.50E-04	2.45E-04	3.37E-04	1.36E-03
K <sub>B</sub>	1.22E+01	2.81E+07	-5.87E+07	5.87E+07
K <sub>C</sub>	-5.80E-01	1.36E+06	-2.84E+06	2.84E+06
K <sub>D</sub>	-3.43E-02	7.58E+04	-1.59E+05	1.59E+05
K <sub>E</sub>	2.04E-03	3.67E+03	-7.69E+03	7.69E+03
K <sub>F</sub>	2.70E-05	8.51E-06	9.15E-06	4.48E-05

**Table 4.6** Model analysis of variance results

Source	DF	Sum of Squares	Mean Square
Regression	6	678.55	113.09
Residual	19	8.51	0.45
Uncorrected Total	25	687.06	
(Corrected Total)	24	96.77	

R squared = 1 - Residual SS / Corrected SS = 0.91206

**Figure 4.15** Residual plot from non-linear regression

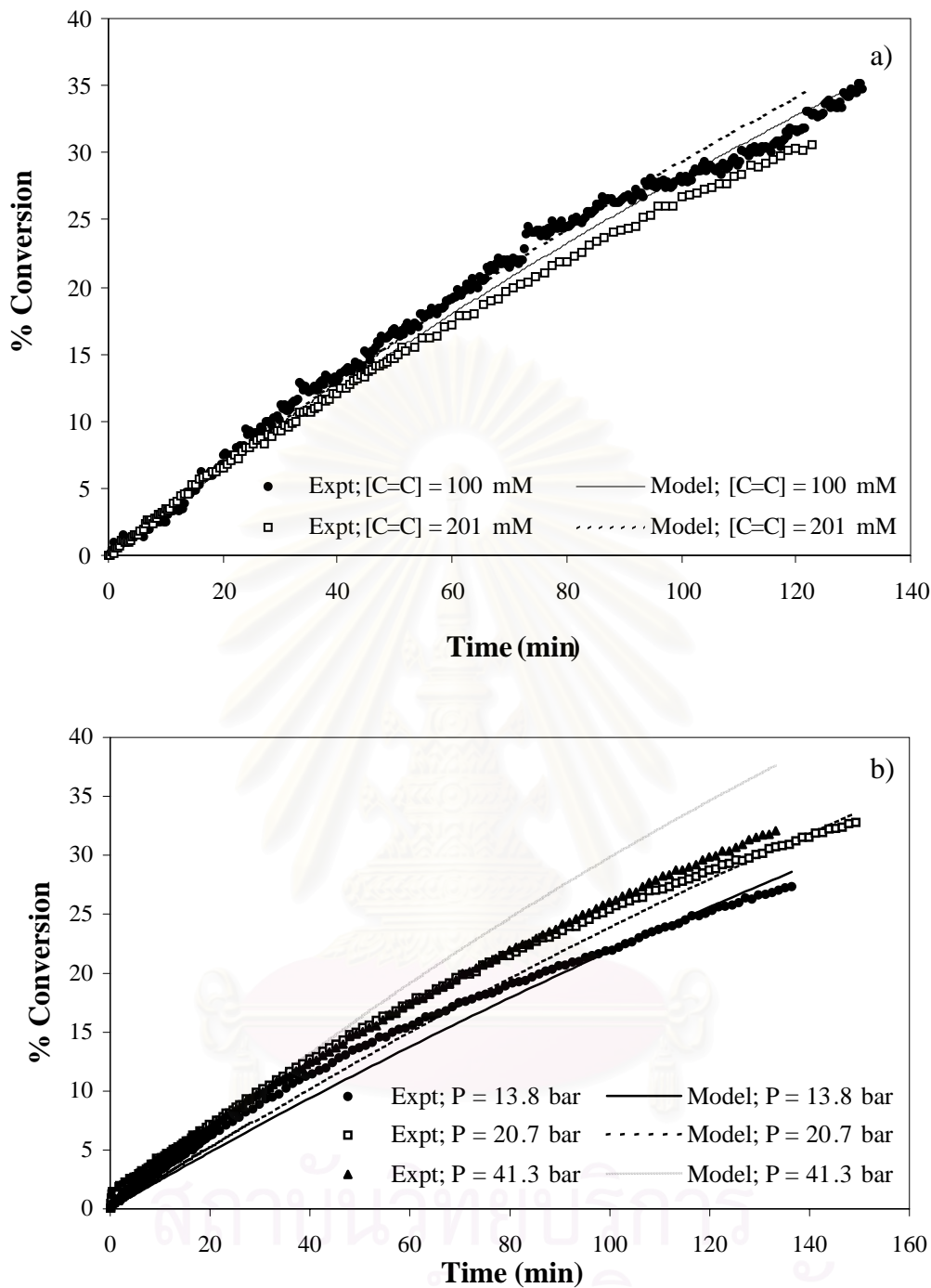


**Figure 4.16** Comparison of the conversion profiles of experiment with model prediction.

- (a) Conversion profile at various polymer concentration,  $[Rh] = 326 \mu\text{M}$ ; no added  $\text{PPh}_3$ ;  $P_{\text{H}_2/\text{CO}} = 41.3 \text{ bar}$ ;  $\text{H}_2:\text{CO} = 1:1$ ;  $T = 70^\circ\text{C}$ .
- (b) Conversion profile at various pressure,  $[\text{C}=\text{C}] = 370 \text{ mM}$ ;  $[Rh] = 326 \mu\text{M}$ ; no added  $\text{PPh}_3$ ;  $\text{H}_2:\text{CO} = 1:1$ ;  $T = 70^\circ\text{C}$ .

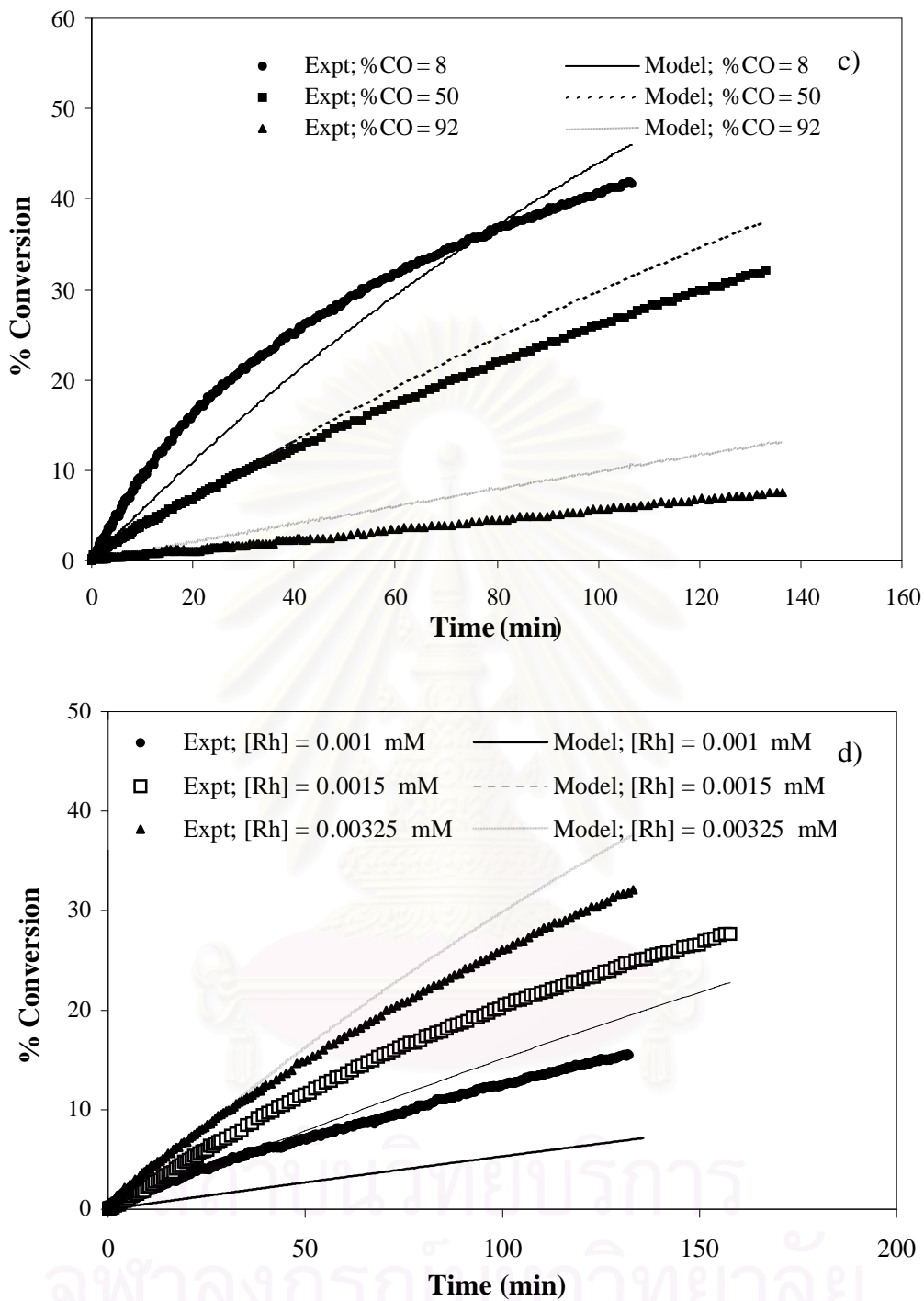


**Figure 4.16 (continued)**

- (c) Conversion profile at various %CO of synthesis gas,  $[C=C] = 370 \text{ mM}$ ;  $[Rh] = 326 \mu\text{M}$ ; no added  $\text{PPh}_3$ ;  $P = 41.3 \text{ bar}$ ;  $T = 70^\circ\text{C}$ .
- (c) Conversion profile at various catalyst concentration,  $[C=C] = 370 \text{ mM}$ ; no added  $\text{PPh}_3$ ;  $P_{\text{H}_2/\text{CO}} = 41.3 \text{ bar}$ ;  $\text{H}_2:\text{CO} = 1:1$ ;  $T = 70^\circ\text{C}$ .

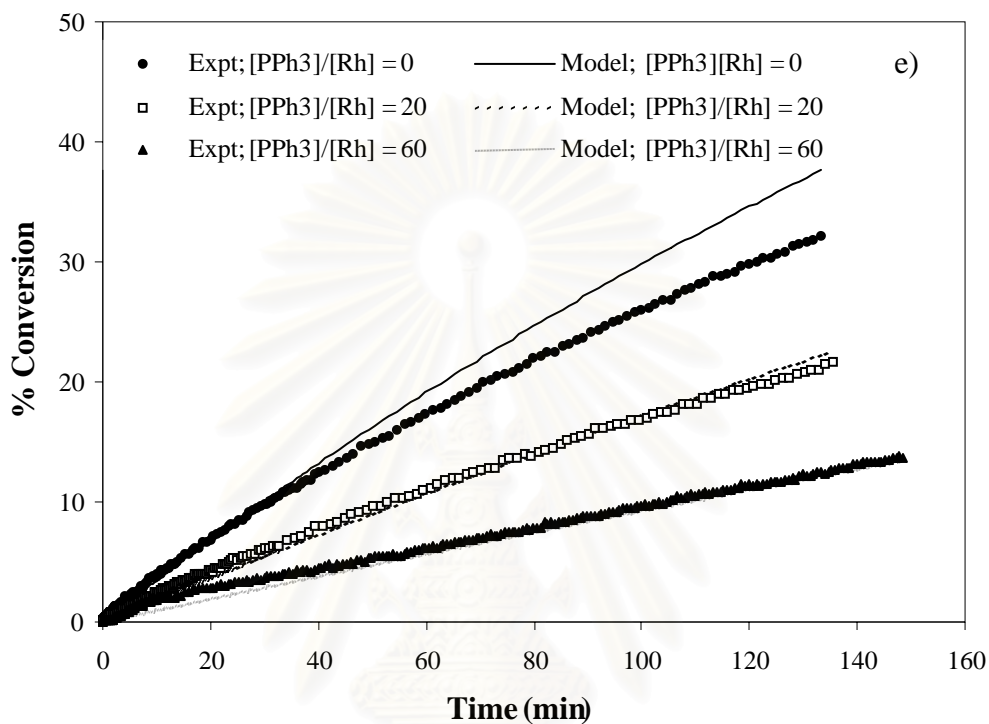


**Figure 4.16 (continued)**

(e) Conversion profile at various PPh<sub>3</sub>/Rh by mole, [C=C] = 370 mM; [Rh] = 326 μM; P<sub>H<sub>2</sub>/CO</sub> = 41.3 bar; H<sub>2</sub>:CO = 1:1; T = 70°C.

สถาบันวิทยบริการ  
จุฬาลงกรณ์มหาวิทยาลัย

## CHAPTER V

### HYDROXYMETHYLATION OF HIGH MOLECULAR WEIGHT *CIS*-1,4-POLYBUTADIENE

The addition of formyl groups by hydroformylation of the carbon-carbon double bonds in the backbone of polymers, PBD leads to be the incorporation of an extremely reactive group onto the polymer. The reactivity of formyl group offers potential for a variety of subsequent reactions to produce many useful products (Sanui et al., 1974; Ogata et al., 1976; Azuma et al., 1980; McGrath et al., 1995). One of common subsequent modification reaction for hydroformylated product is hydrogenation leading to overall hydroxymethylation. This secondary modification, hydrogenation, can change the formyl groups on the polymers to hydroxyl methyl group.

Hydroxymethylation of PBD can be carried out by a two-step process of controlled hydroformylation and subsequent hydrogenation. There are two systems for the hydrogenation step: a non-catalytic system and a catalytic system. In the case of non-catalytic systems, hydrogenation is achieved by reduction using a variety of reducing agents, e.g., sodium tetrahydroborate or trimethyloxyborohydride (Sanui et al., 1974; Ogata et al., 1976; Azuma et al., 1980; McGrath et al., 1995). Using a reducing agent, reduction of the aldehyde generates the polymeric alcohol without further reaction of the remaining double bonds. These unique hydrophobic polyols were reported in that they could be used as intermediates to produce other polymer systems. As an example, polyurethanes have been prepared from these polyols by reacting them with diisocyanates (Tremont et al., 1990; Mill et al., 1990; McGrath et al., 1995). This product can also be made from modified nylon 6 block copolymers (Tremont et al., 1990; Mill et al., 1990). Most previous studies reported that the solubility of hydroxymethylated polymers decreased with increasing conversion due to crosslinking with formyl group.

Catalytic hydrogenation, an alternative route for producing polyols from polyaldehyde, has been reported mostly in the presence of ruthenium complexes (Mohammadi, 1987; Sibtain and Rempel, 1991). Using these catalysts, all residual carbon-carbon double bonds in hydroformylated PBD were hydrogenated completely,

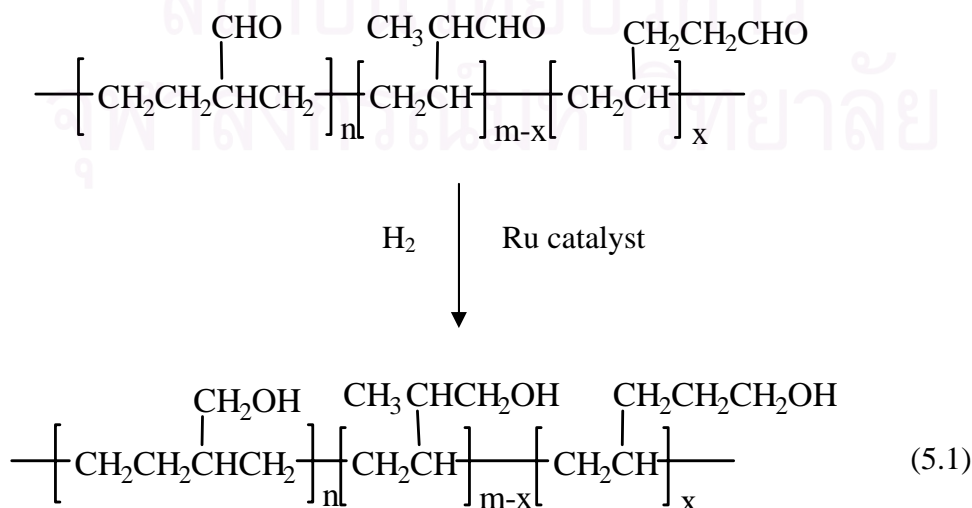


with hydrogenation of formyl groups to hydroxyl methyl groups. Sibtain and Rempel (1991) claimed that the problem of crosslinking was overcome by utilizing homogeneous transition metal complex catalyzed hydrogenation of the hydroformylated polymer. Due to the completion of hydrogenation of the remaining carbon-carbon double bonds in polymers, the product polymer is easily soluble in various hydrocarbon solvents. Despite the relatively severe reaction conditions required for complete hydrogenation, no crosslinking or main chain degradation occurred.

The hydroformylation of PBD was carried out in presence of  $\text{HRh}(\text{CO})(\text{PPh}_3)_3$  in MCB using a 1:1 mixture of  $\text{CO}$  and  $\text{H}_2$ . In this chapter, an attempt is made to study the hydroxymethylation of hydroformylated PBD catalyzed by  $\text{RuCl}(\text{CO})(\text{CH}=\text{Cl}(\text{Ph}))(\text{PCy}_3)_2$  in a Parr batch reactor. This catalyst was reported to be efficient for hydrogenation of NBR (Parent et al., 1998), CPIP, and NR. (Tangtongkul et al., 2003). The effect of formyl loading on hydroxymethylation was also investigated.

### 5.1 Product Identification for Hydroxymethylated PBD

As described in section 3.1, polybutadiene used in this experiment consists of 98 wt% *cis* content (1,4-polybutadiene) and 2 wt% vinyl (1,2-polybutadiene). When considering the microstructure of PBD, there are three possible hydroformylated products as shown in Eq. 3.1. These products were subsequently hydrogenated to form the products as shown in Eq. 5.1.



According to the  $^1\text{H-NMR}$  spectra of hydroformylated PBD as shown in Figure 3.2, two peaks attributed to aldehyde groups are at 9.5 and 9.7 ppm. The peak at 9.5 ppm and smaller peak at 9.7 ppm correspond to the aldehyde group from 1,4-PBD and 1,2-PBD, respectively. The hydroformylated PBD from 1,4-PBD is an internal polyaldehyde and that from 1,2 PBD is a terminal-branched polyaldehyde. Consequently, the possible hydroxymethylated PBD could be derived from the aldehyde group from 1,4-PBD and 1,2-PBD.

The infrared spectrum of a 10% hydroformylated PBD sample is shown in Figure 5.1a. It can be seen from this spectrum that beside bands at 910, 965, 996, and  $1640\text{ cm}^{-1}$ , which are due to C=C bond, two new bands at  $1727$  and  $2700\text{ cm}^{-1}$  appeared (see Table 5.1). The band at  $1727\text{ cm}^{-1}$  is attributed to C=O stretching vibrations of the aldehyde group and at  $2700\text{ cm}^{-1}$  is attributed to the C-H stretching vibrations of the aldehyde functional group.

The infrared spectrum of a hydroxymethylated PBD sample is illustrated in Figure 5.1b. A broad band at  $3310\text{ cm}^{-1}$ , which is the characteristic of -OH stretching vibrations, can be seen. The band at  $1100\text{ cm}^{-1}$  is attributed to the  $\nu(\text{C-OH})$ . Comparing with the spectrum of hydroformylated PBD, it can be observed that bands at  $1727$  and  $2700\text{ cm}^{-1}$  decreased. Furthermore, some of the characteristic bands for carbon-carbon unsaturation, i.e. at  $1640$ ,  $910$ ,  $970$ , and  $992\text{ cm}^{-1}$ , also decreased. This suggests that  $\text{RuCl}(\text{CO})(\text{CH}=\text{Cl}(\text{Ph}))(\text{PCy}_3)_2$  is an active catalyst for the quantitative hydrogenation of -CHO and C=C functional groups under the given reaction condition.

**Table 5.1** IR absorption of functional groups in polybutadiene, hydroformylated, and hydroxymethylated polybutadiene

Unit	Wavenumber, $\text{cm}^{-1}$
C-H of C=C	967
C-OH	1100
C=C stretch	1655
C=O stretch	1727
C-H stretch due to CHO	2700
OH stretch	3310

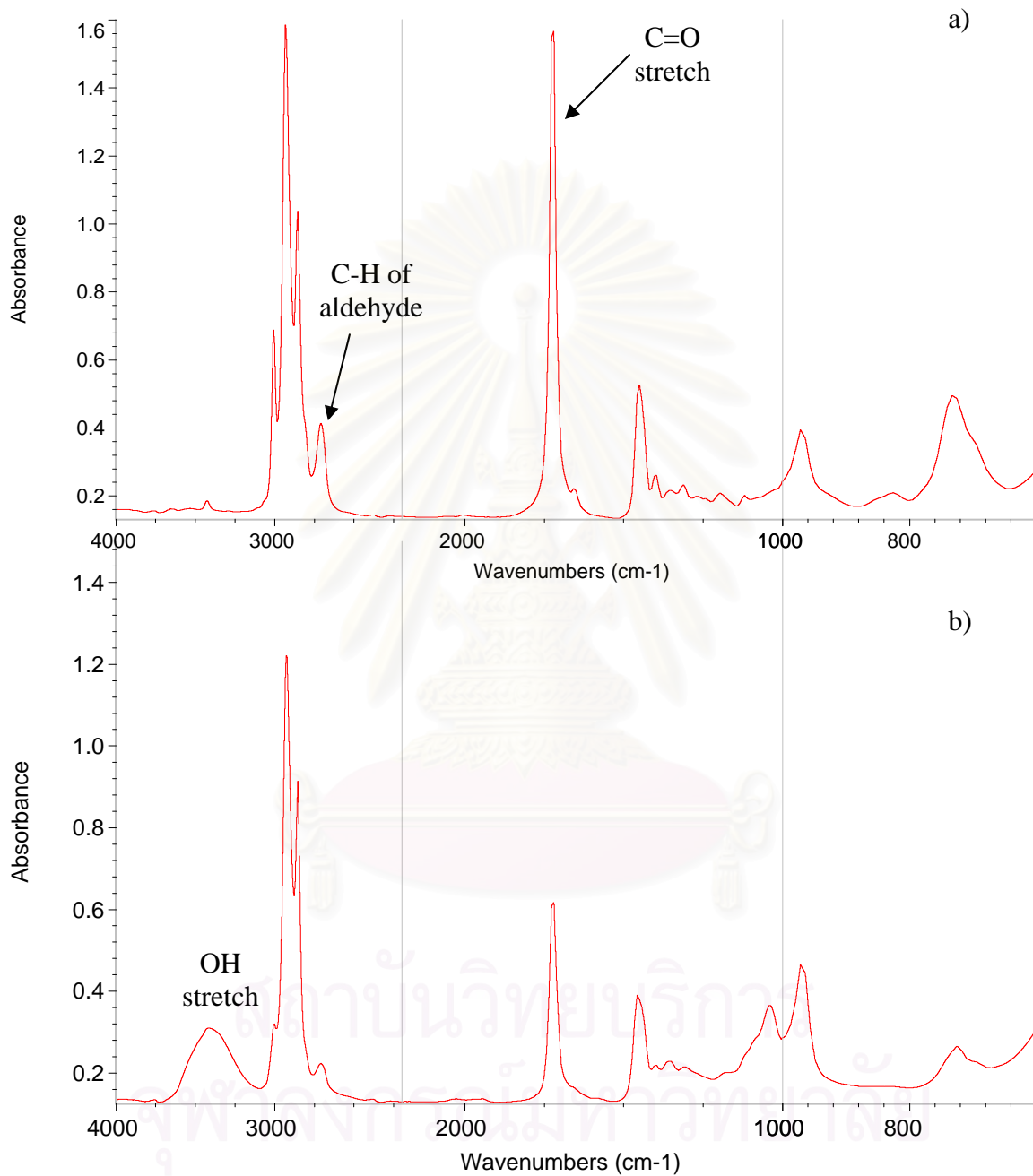


**Figure 5.1** FT-IR spectra of a) 10 % hydroformylated *cis*-1,4-polybutadiene b) hydroxymethylated *cis*-1,4-polybutadiene, [C=C] = 247 mM; [Ru] = 161  $\mu$ M;  $P_{H_2}$  = 41.3 bar; T = 150°C; Solvent = MCB; Time = 4 h.

The  $^1\text{H}$  NMR spectrum of a 10% hydroformylated PBD sample is shown in Figure 2a. From this spectrum, the peak at 9.5 ppm, which is characteristic of the formyl group, confirms the presence of  $-\text{CHO}$  group. The peaks in the range of 5.0 to 5.5 ppm are due to the olefinic protons of the residual  $\text{C}=\text{C}$  (see Table 5.2).

The  $^1\text{H}$  NMR spectrum of dissolved hydroxymethylated PBD in  $\text{CDCl}_3$  is shown in Figure 5.2b. A triplet at 3.54 ppm, which is due to the methylene protons adjacent to the hydroxyl group, can be observed. After the hydrogenation of hydroformylated PBD, the characteristic peak for the aldehyde protons, i.e. at 9.5 and 9.7 ppm have disappeared completely. The peaks in the range of 5.0 to 5.5 ppm, which are due to olefinic protons, also decreased significantly. This confirms a quantitative hydrogenation of  $-\text{CHO}$  functional groups and some extent for  $\text{C}=\text{C}$  double bonds.

**Table 5.2** Peak assignment of  $^1\text{H}$  NMR spectrum of hydroformylated (Figure 5.2a) and hydroxymethylated (Figure 5.2b) polybutadiene.

Unit	Type of proton	$\delta$ , ppm
1,4	$=\text{CH}-$	5.5
	$-\text{CH}_2-$	1.8-2.4
1,2	$-\text{CH}=\text{}$	5.15-5.9
	$=\text{CH}_2$	4.85-5.15
	$-\text{CH}-$	1.8-2.4
	$-\text{CH}_2-$	1.2-1.75
CHO	Internal aldehyde	9.5
	Terminal aldehyde	9.7
$\text{CH}_2\text{OH}$	Methyl group adjacent to hydroxy group	3.54

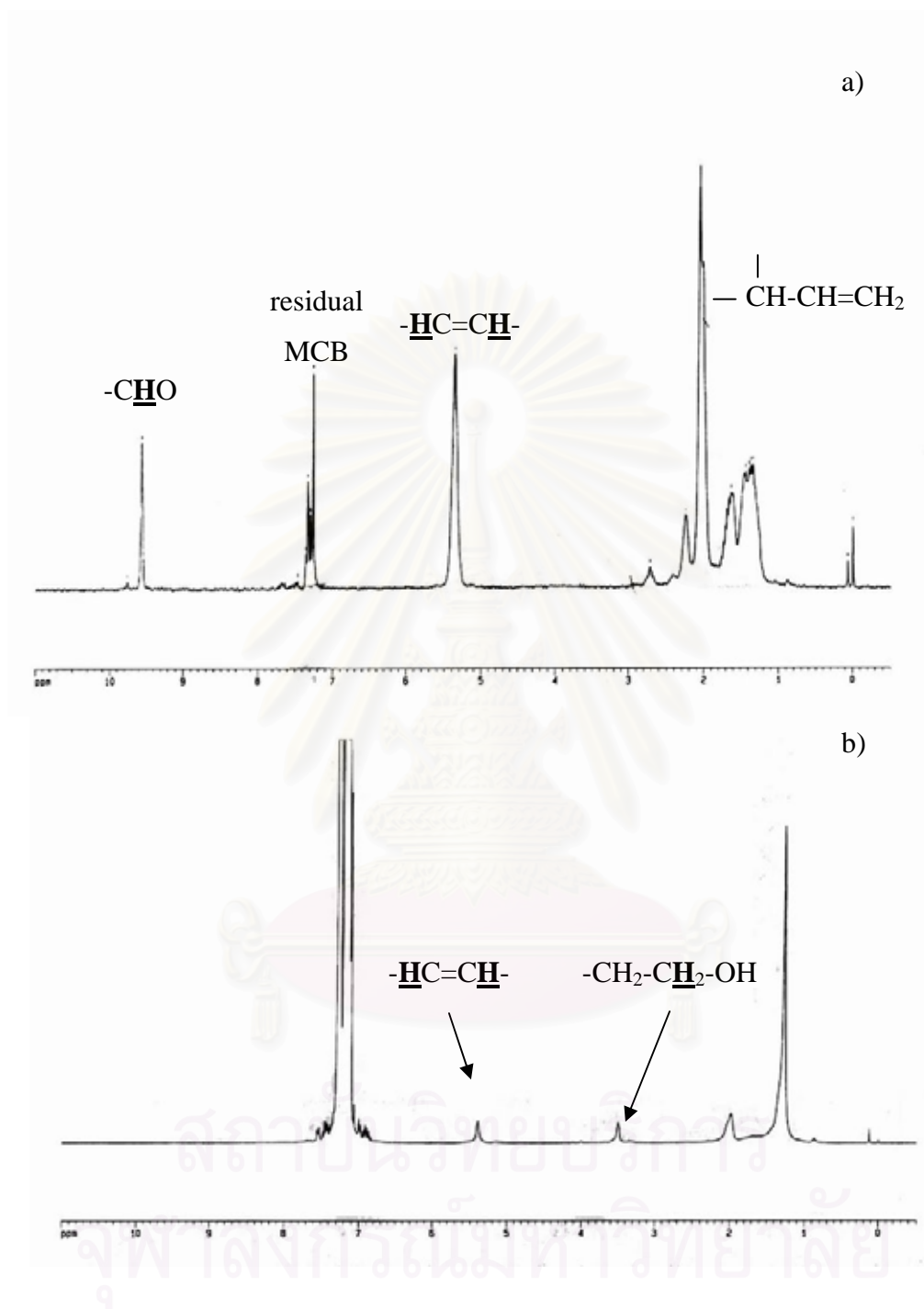


**Figure 5.2**  $^1\text{H-NMR}$  spectra of a) 10 % hydroformylated *cis*-1,4-polybutadiene b) hydroxymethylated *cis*-1,4-polybutadiene,  $[\text{C}=\text{C}] = 247 \text{ mM}$ ;  $[\text{Ru}] = 161 \text{ }\mu\text{M}$ ;  $P_{\text{H}_2} = 41.3 \text{ bar}$ ;  $T = 150^\circ\text{C}$ ; Solvent = MCB; Time = 4 h.

## 5.2 Hydroxymethylation of High Molecular Weight of Cis-1,4-Polybutadiene

It was mentioned in Section 2.5.2 that the partially hydroformylated PBD (1-80%) was soluble in the solvent (MCB) as long as the polymer was not separated by complete removal of solvent or precipitating with ethanol. However, only 1-40% hydroformylated PBD solution with less than 40% formyl loading obtained directly from the hydroformylation step could be used for subsequent hydrogenation. The reason was that crosslinking of the hydroxyl group increased with increasing initial formyl group loading from the hydroformylation step. In addition, the hydroxymethylated PBD could be precipitated from the solvent when the reaction time of hydroxymethylation was long.

The hydrogenation of the formyl functional groups in the hydroformylated PBD was carried out in the presence of  $\text{Ru}(\text{CH}=\text{CHPh})\text{Cl}(\text{CO})(\text{PCy}_3)_2$  at a temperature of  $150^\circ\text{C}$  and a hydrogen pressure of 41.3 bar for 2 h. These conditions as well as the polymer and catalyst concentration chosen were appropriate for the hydrogenation of CPIP and natural rubber in which 95% hydrogenation was achieved (Tangthongkul, 2004). Thus,  $-\text{CHO}$  as well as  $\text{C}=\text{C}$  functional groups were quantitatively hydrogenated to  $-\text{CH}_2(\text{OH})$  and  $\text{C}-\text{C}$  respectively. The results on hydroxymethylation of high MW cis-1,4-PBD are presented in Table 5.3. The appearance of hydroformylated film and hydroxymethylated product are shown in Appendix IV.

**Table 5.3** Results of hydroformylation and hydroxymethylation of high molecular weight *cis*-1,4-polybutadiene.

Expt.	Step : Hydroformylation <sup>a</sup>			Step 2: Hydroxymethylation <sup>b</sup>	
	[Rh] ( $\mu\text{M}$ )	Time (h)	%CHO	%OH	%Hydrogenation
1	109	1	1.9	9.5	84.5
2	109	2	6.2	13.2	86.2
3	325	1	16.4	14.0	75.4
4	327	1	18.7	32.6	40.8
5	327	2	28.9	13.1	67.2
6	327	4	39.1	13.8	72.4
7	327	6	48.0	Gel	Gel

<sup>a</sup>Hydroformylation reaction: [polymer] = 370 mM, P = 600 psi, T =  $70^\circ\text{C}$ , Solvent = MCB

<sup>b</sup>Hydroxymethylation reaction: [polymer] = 264 mM, [Ru] = 161  $\mu$ M, P = 600 psi, T = 150°C, Solvent = MCB, Time = 2h.

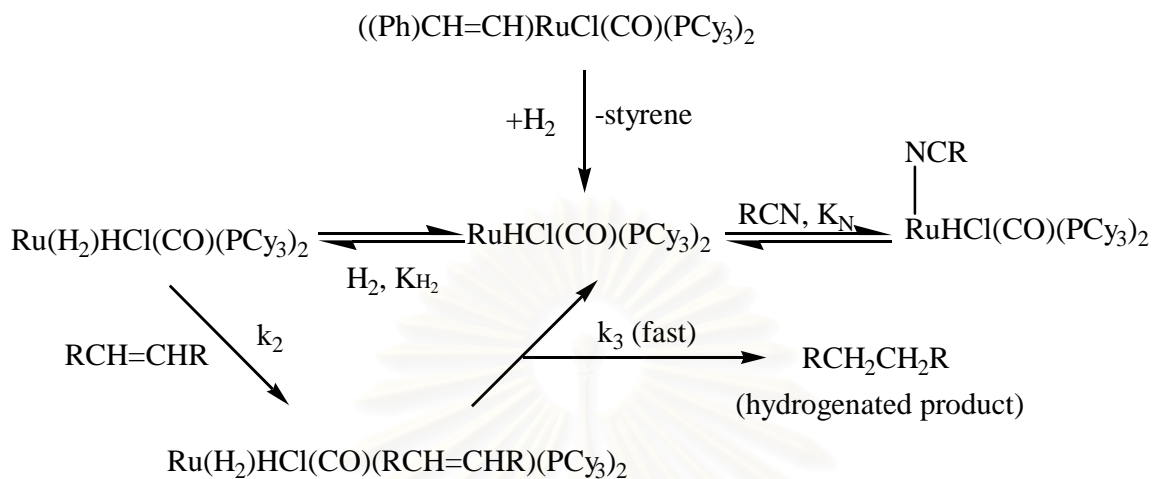
Since one mole of  $-\text{CHO}$  forms one mole of the  $-\text{OH}$  functional group, the OH content in the polymer chains was determined from the known  $-\text{CHO}$  functional group content. At low (1-16.4%) and medium (28.9-39.1) formyl loading, the experiments showed the same methyl hydroxyl group loading ( $-\text{CH}_2\text{OH}$ ) with approximately 13.8-14% and hydrogenation of PBD about 72.4-75.4%. In addition, the residual  $\text{C}=\text{C}$  double bonds of PBD was about 10%. However, the calculated conversion results for hydroxymethylation were not consistent the comparing with conversion results for hydroformylation. This may be caused by partial solubility of the hydroxymethylated product in the NMR solvent,  $\text{CDCl}_3$ . Moreover, above 40% CHO of hydroformylated PBD, there was gel formation due to the increase in the hydrophilic nature of the  $-\text{OH}$  group in the hydroxymethylated PBD.

### 5.3 Mechanism of Hydroxymethylation and Hydrogenation

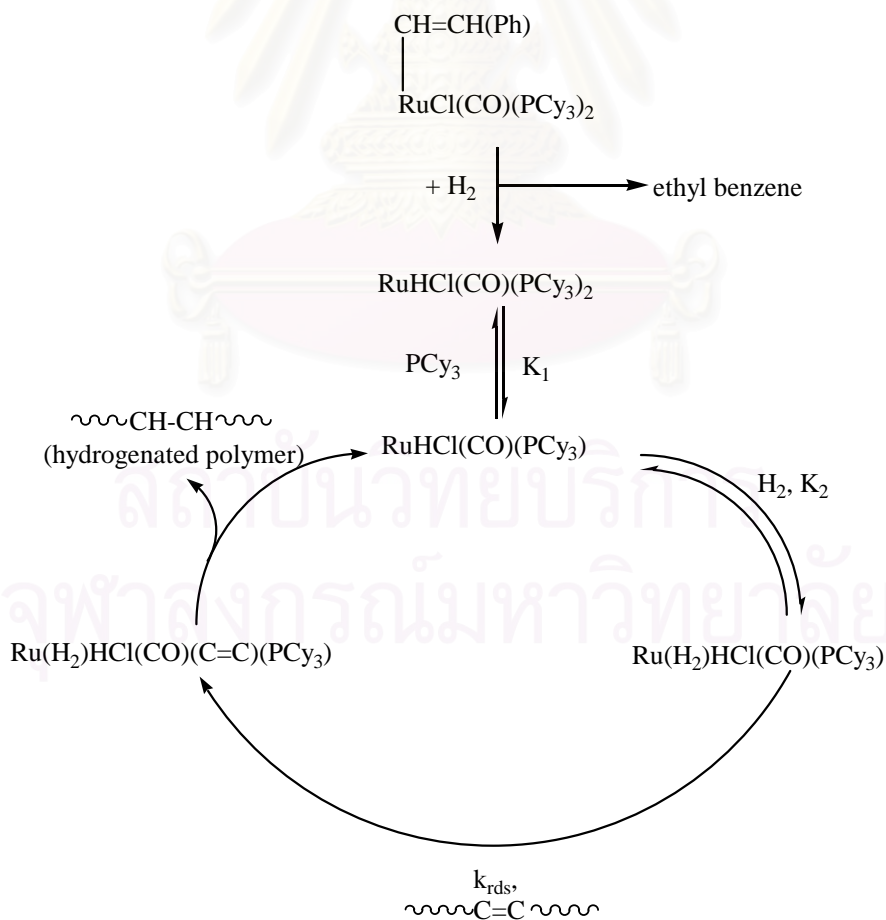
The postulated mechanism for the hydroformylation of polybutadiene in this work is shown in Scheme 3.2 (Scott et al., 1992). The obtained hydroformylated PBD was directly subjected to subsequent hydrogenation reaction, hydroxymethylation. The effective catalyst for hydrogenation of polyaldehyde in this work is ruthenium complexes,  $\text{Ru}(\text{CH}=\text{CHPh})\text{Cl}(\text{CO})(\text{PCy}_3)_2$ . Although there have been some reports for its mechanism of hydrogenation, the mechanism for hydroxymethylation has not been proposed.

To approach the mechanism of hydroxymethylation using  $\text{Ru}(\text{CH}=\text{CHPh})\text{Cl}(\text{CO})(\text{PCy}_3)_2$ , the mechanism for hydrogenation of other polydiene was reviewed. Martin et al. (1997) studied the kinetics of NBR hydrogenation catalyzed by  $\text{Ru}(\text{X})\text{Cl}(\text{CO})\text{L}_2$  where X = H or  $\beta$ -styryl ( $\text{CH}=\text{CH}(\text{Ph})$ ) and L was a bulky phosphine such as tricyclohexyl or triisopropyl-phosphine. The proposed mechanism of NBR hydrogenation could be expressed as shown in Scheme 5.1. Although Ru complexes are the efficient catalysts for hydrogenation, their activity is slower than that of analogous Rh complexes; therefore, it is necessary to operate the reaction under higher temperature and pressure. Moreover, Ru catalysts can promote gel formation in NBR hydrogenation due to the reduction of the  $-\text{CN}$  group to secondary amines (Parent, 2001).

Later, the study of hydrogenation of CPIP was also reported in the presence of  $\text{Ru}(\text{CH}=\text{CHPh})\text{Cl}(\text{CO})(\text{PCy}_3)_2$  (Tangtongkul et al., 2003). The proposed mechanism was presented similarly in the work of Martin et al. (1997) as shown in Scheme 5.2.



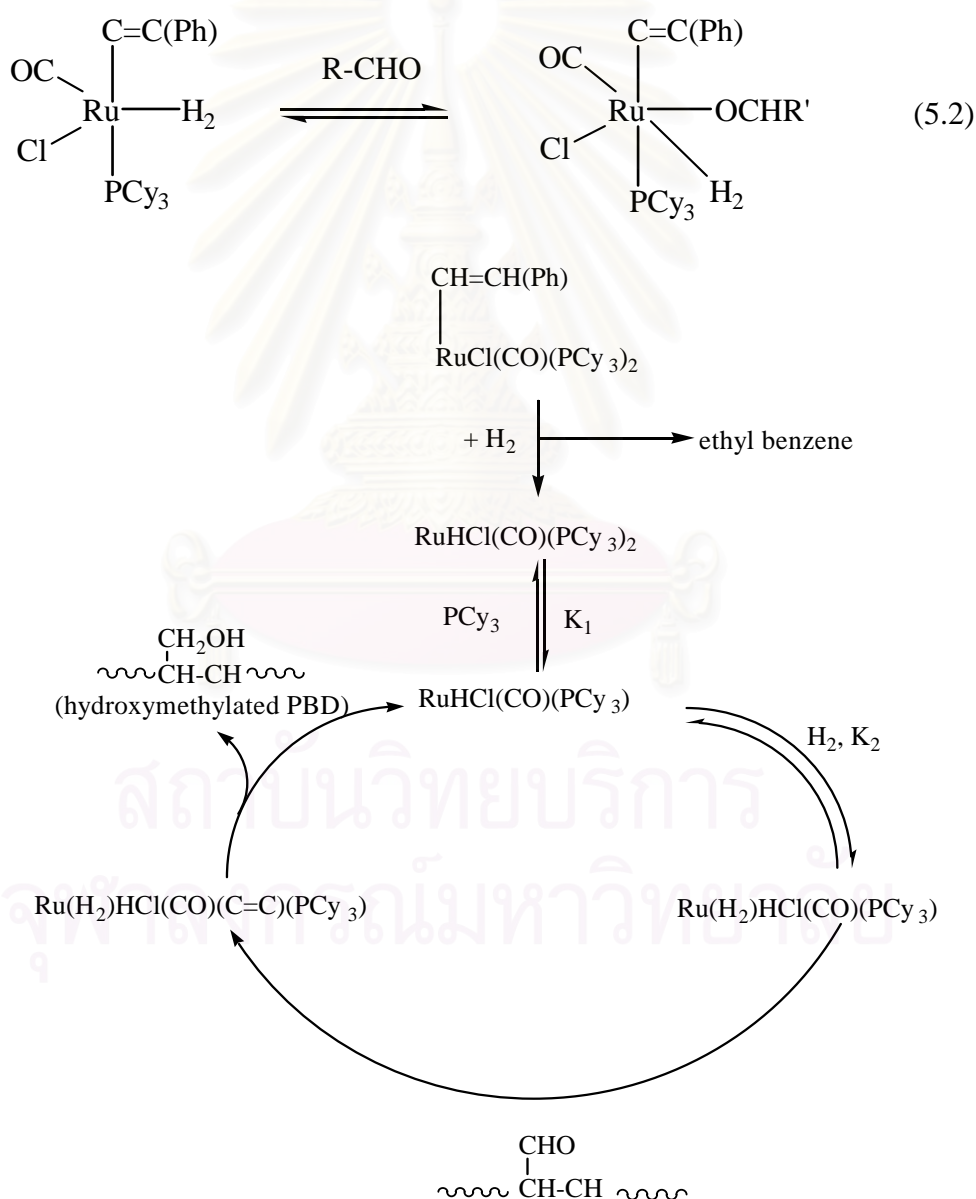
**Scheme 5.1** Mechanism for NBR hydrogenation catalyzed by  $\text{Ru}(\text{CH}=\text{CH}(\text{Ph}))\text{Cl}(\text{CO})(\text{PCy}_3)_2$  (Martin et al., 1997).



**Scheme 5.2** Mechanism for CPIP hydrogenation catalyzed by  $\text{Ru}(\text{CH}=\text{CH}(\text{Ph}))\text{Cl}(\text{CO})(\text{PCy}_3)_2$  (Tangtongkul et al., 2003).



Since hydroxymethylation of PBD can afford both hydrogenated and hydroxymethylated PBD, the possible mechanism in this step could involve two catalytic cycles: hydrogenation of residual C=C double bonds and hydrogenation of polyaldehyde. For hydrogenation of the remaining C=C double bonds, the mechanism also can be expressed as Scheme 5.1 and 5.2. For hydrogenation of polyaldehyde, the formation of  $\text{Ru}(\text{H}_2)\text{HCl}(\text{CO})(\text{C}=\text{C})(\text{PCy}_3)$  species in order to provide site needed for activation of the formyl group of polyaldehyde coordinated as shown by Eq. 5.2. Thus, the mechanism for PBD hydroxymethylation can be proposed as shown in Scheme 5.3.



**Scheme 5.3** Mechanism for PBD hydroxymethylation catalyzed by  $\text{Ru}(\text{CH}=\text{CH}(\text{Ph}))\text{Cl}(\text{CO})(\text{PCy}_3)_2$ .

## CHAPTER VI

### PHYSICAL PROPERTIES OF HYDROFORMYLATED AND HYDROXYMETHYLATED POLYBUTADIENE

The physical properties of polymers usually are investigated to observe the performance of polymers in their applications. One of the most used analyses for physical properties is thermal analysis. Thermal methods of analysis may be broadly defined as methods of analysis in which the effect of heat on a sample is studied to provide qualitative or quantitative analytic information. The temperatures at which physical transitions occur are important to the first criterion to determine how the state of polymers are related to the temperature. Polymers are generally considered to have a nearly constant thermal expansion rate as a function of temperature over their entire usable temperature range. The value of the expansion rate is useful for the design in processing polymers under the observed condition.

The thermal properties of polymers may be investigated by differential thermal analysis (DTA), differential scanning calorimeter (DSC), dynamic mechanical thermal analysis (DMTA), and thermal gravimetric analysis (TGA). Generally, DTA and TGA are broadly used to analyze the thermal properties of polymers with respect to enthalpy and entropy changes. DMTA is used to measure the dynamic mechanical properties such as storage modulus or loss tangent with respect to a change of temperature. TGA is used to determine the degradation temperature by measuring the weight loss of polymers related to temperature change (Campbell and White, 1989).

Thermal analyses have some advantages over other analytical methods as follows: (i) the analysis can be done over a wide range of temperature and different temperature profiles (ii) any physical form such as solid, liquid, or gel can be accommodated by using various sample vessels (iii) a small amount of sample is required (iv) as a standard condition the analysis can be operated at atmospheric pressure (v) the operating time can be varied (vi) the price for thermal analyses is reasonable.

Some reports on the physical properties of the hydroformylated and hydroxymethylated products were not attempted since they were used as

intermediates for further reactions (Sanui et al., 1974; Tremont et al., 1990; Mill et al., 1990; Chen et al., 1997). However, thermal property of hydroxymethylated product was investigated in the form of a substrate as for polyurethane (Martin et al., 1995). The thermal stability of polyurethane films made from EPDM and polybutadiene polyols were studied by using TGA and compared with polyurethane made from polyether-based polyols. The results showed that polyurethane made from EPDM and polybutadiene polyols exhibit a higher thermal stability than that made from polyester-based polyols. The higher the level of hydroxyl group in polyurethane, the higher the thermal stability.

The purpose of this chapter is to report on an investigation of the thermal properties of hydroformylated and hydroxymethylated *cis*-1,4-PBD. The differential scanning calorimetry (DSC) and the thermogravimetric analysis (TGA) were used to determine the glass transition temperature ( $T_g$ ) and the thermal degradation temperature ( $T_d$ ) of the products, respectively. Since the hydroformylated polymers can possibly be used as membranes (Ogata et al, 1976; Mertzweiller, 1969), an interesting property is the swelling in solvents which are affected by the presence of the hydrophilic groups in the structure of the polymer.

## 6.1 Differential Scanning Calorimetry (DSC)

Differential scanning calorimetry (DSC) is a technique for determining the glass transition temperature ( $T_g$ ) of elastomers. The glass transition temperature is the temperature at which the amorphous domain of a polymer takes on the characteristic properties of glassy state-brittleness, stiffness, and rigidity (Odian, 1991). DSC is based on the measurement of the temperature difference ( $\Delta T$ ) between the sample and a reference. In principle, the DSC is similar to DTA, but the sample and a reference are heated separately with separate electrical heaters in DSC. The heaters are programmed to ensure that the temperatures of both sample and reference advance at exactly the same rate. It follows that when endotherms or exotherms occur in the sample, the power to the heater needs to be varied in order to maintain  $\Delta T = 0$ . Thus by monitoring the difference in power supplied to the heaters, the process can be followed (Rodriguez, 1970; Fifield and Kealey, 1995).

The DSC thermogram for PBD and hydroformylated PBD are presented in Figure 6.1. The glass transition temperature ( $T_g$ ) of the polymer was determined from the middle point of the incline portion of the DSC curve. The glass transition temperatures of PBD and hydroformylated PBD having various levels of aldehyde group content (0-75% CHO) are presented in Figure 6.2 and Table 6.1. The glass transition temperatures increased with increasing %CHO contents in the range of 0 to 10%.

According to the appearance of PBD and hydroformylated PBD (Appendix IV), PBD is in a rubbery form, having  $T_g$  about  $-100^\circ\text{C}$  whereas hydroformylated PBD is in a film form, having  $T_g$  about  $48^\circ\text{C}$  (see Table 6.1). This implies that the hydroformylation causes a change from an amorphous state of PBD to a highly crystalline state due to the addition of CHO groups in the polymer chain. Also, the strength of hydroformylated film is expected to be high due to the high molecular weight of the starting polymers.

Hydroformylation can increase  $T_g$  since the CHO groups in hydroformylated PBD are crosslinked due to their polarity. Between 10%-75% CHO content in PBD,  $T_g$  increased slightly with increasing %CHO. It can be explained that complexity of high MW PBD is obstacle to coordinate crosslinking in CHO groups.

For hydroxymethylation, the appearance of hydroxymethylated PBD is also shown in Appendix IV. The glass transition temperature of the hydroxymethylated PBD with %OH content in the range of 2% to 20% was determined. The thermogram of 20% hydroxymethylated PBD is shown in Figure 6.3. The hydroxymethylated PBD with 2% and 20% hydroxyl group had glass transition temperature of  $38^\circ\text{C}$  and  $44^\circ\text{C}$ , respectively. This suggests that the hydroxymethylated PBD exhibits amorphous properties compared with the hydroformylated PBD. This can be rationalized in that the hydrogenated portion of PBD forms amorphous regions while the hydroxymethylated portion of PBD forms crystalline regions. Thus,  $T_g$  increases with increasing %OH group in the polymer chain.

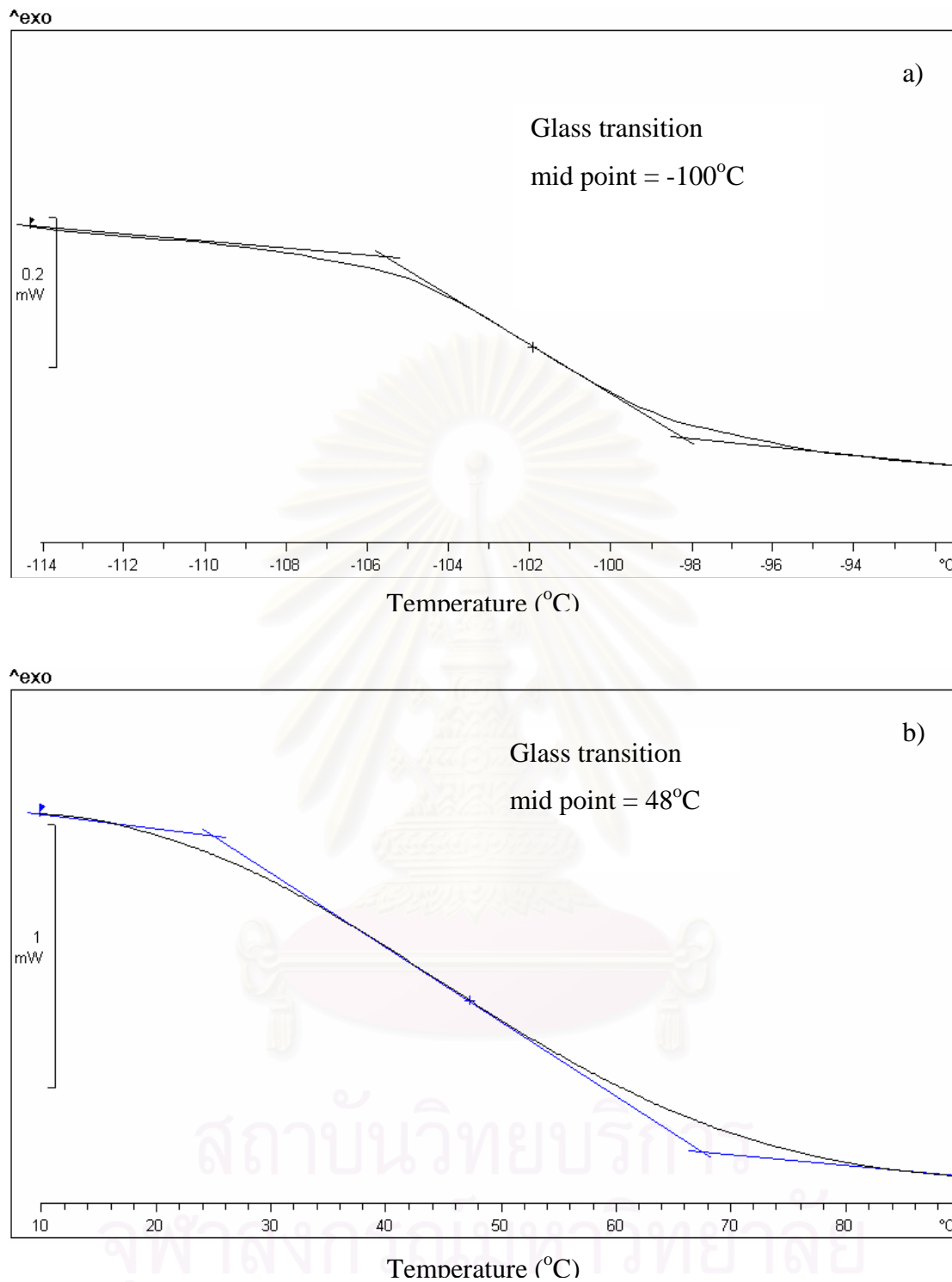


**Figure 6.1** DSC thermograms of a) PBD and b) 20% hydroformylated PBD.

**Table 6.1** DSC and TGA results of PBD, hydroformylated PBD, and hydroxymethylated PBD.

Polymer	%Conversion	T <sub>g</sub> (°C)	T <sub>id</sub> (°C)	T <sub>max</sub> (°C)
PBD	0	-100	431	472
Hydroformylated PBD	5	45	428	453
	18	47	405	455
	20	48	403	449
	43	51	401	447
	56	53	396	444
	75	54	389	440
Hydroxymethylated PBD	2	38	437	476
	20	44	453	477

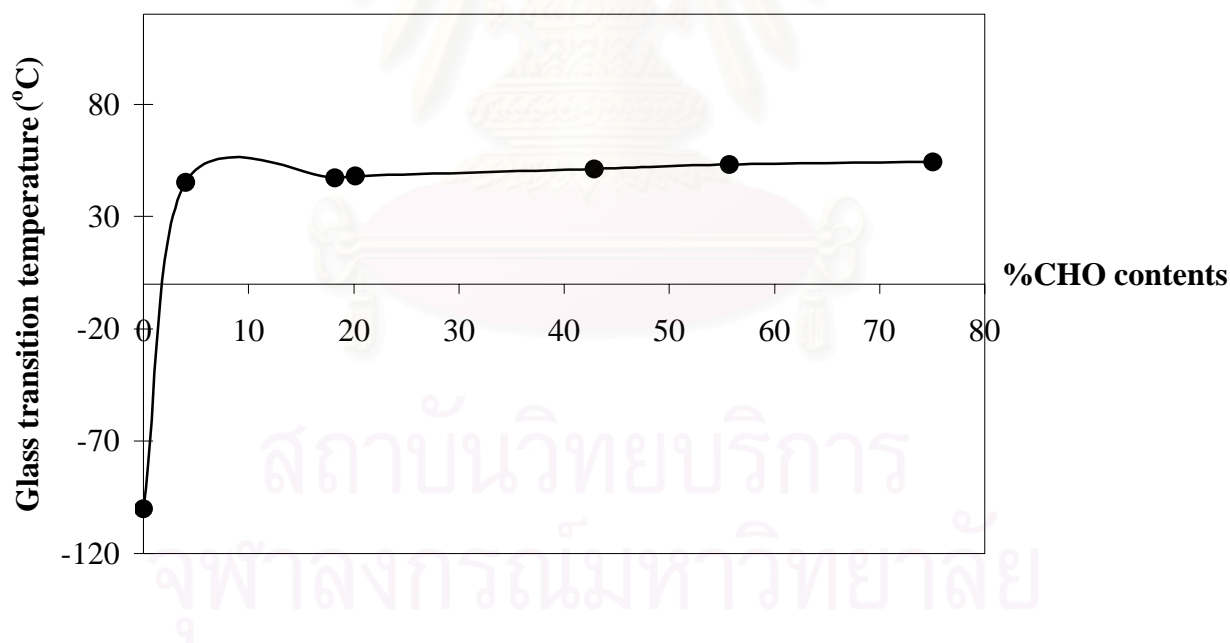


**Figure 6.2** Glass transition temperature of high molecular weight *cis*-1,4-PBD and hydroformylated PBD at various %CHO contents.

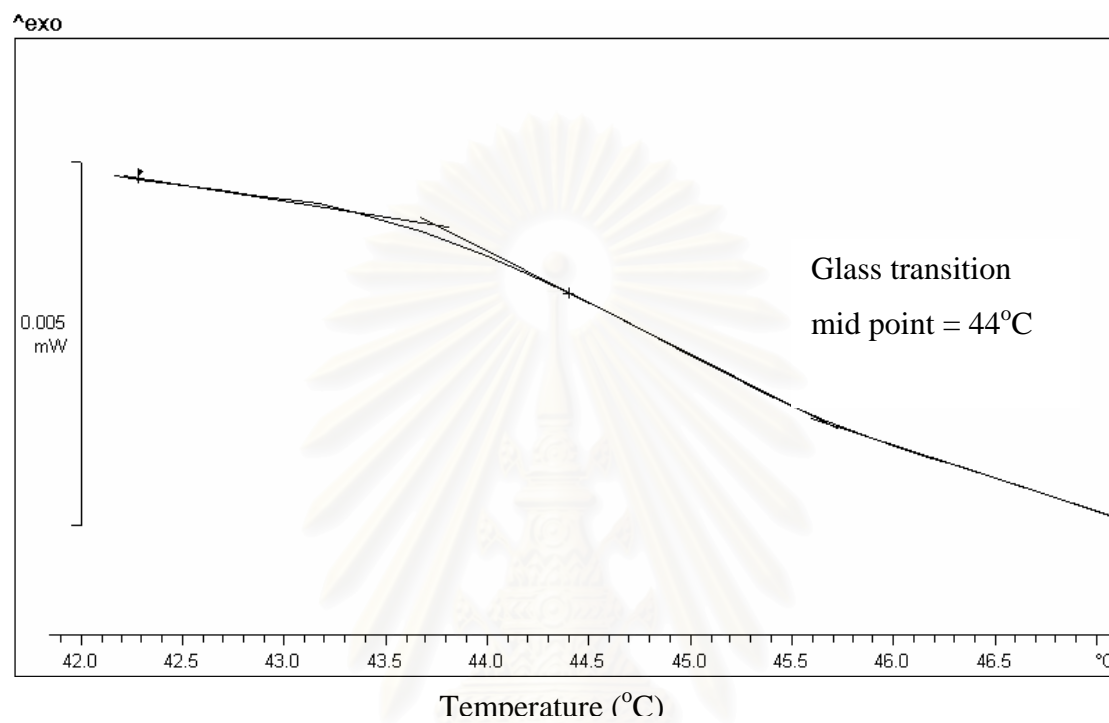


**Figure 6.3** DSC thermograms of 20% hydroxymethylated PBD.

สถาบันวิทยบริการ  
จุฬาลงกรณ์มหาวิทยาลัย

## 6.2 Thermogravimetric Analysis (TGA)

Thermogravimetric analysis (TGA) is based on the simple principle of monitoring the change in weight of a sample as the temperature is varied. When heated at high temperature, many materials undergo weight changes that can be linked to a particular thermal event such as oxidation or loss of water or crystallization. In this study, the experiments were achieved under a  $N_2$  atmosphere to observe the weight change due to degradation and to prevent other reactions caused by oxidation. The obtained characteristic curves were used for quantitative analysis. The initial decomposition temperature ( $T_{id}$ ) was determined from the intersection of two tangents at the onset of the decomposition temperature. The maximum decomposition temperature ( $T_{max}$ ) was obtained from the peak maximum of the derivative of the TGA curve.

The characteristic curves of TGA for PBD and hydroformylated PBD are presented in Figure 6.4. For PBD, there is no weight loss up to  $325^\circ C$  indicating its stability over this temperature range. The weight loss occurred over the temperature range of  $325$  to  $500^\circ C$  due to the decomposition of the polymer. The high temperature degradation of the hydroformylated PBD at %CHO content over the range of 0% to 75% was studied. The  $T_{id}$  and  $T_{max}$  of hydroformylated PBD at various %CHO content are shown in Figure 6.5.

For 5% hydroformylated PBD (Figure 6.5b), the weight loss of the polymer sample starts at a temperature of  $100^\circ C$ . This may be caused by the instability of aldehyde group in the polymer. Although crosslinking can yield crystalline properties of hydroformylated PBD, the crosslinking which occurred seems to be temporary. The observed  $T_{id}$  and  $T_{max}$  of hydroformylated PBD were lower than that of PBD. In addition,  $T_{id}$  and  $T_{max}$  slightly decrease with increasing %CHO content in PBD as shown in Figure 6.4. This may be due to the instability of aldehyde groups on the backbone of the polymer or remaining solvent in the polymer as well.

The decomposition temperature of the hydroxymethylated PBD was also studied. The TG curve for hydroformylated PBD is presented in Figure 6.6. The results show some small-improved thermal properties of hydroxymethylated PBD which is caused by the loss of crystalline region in polymer.



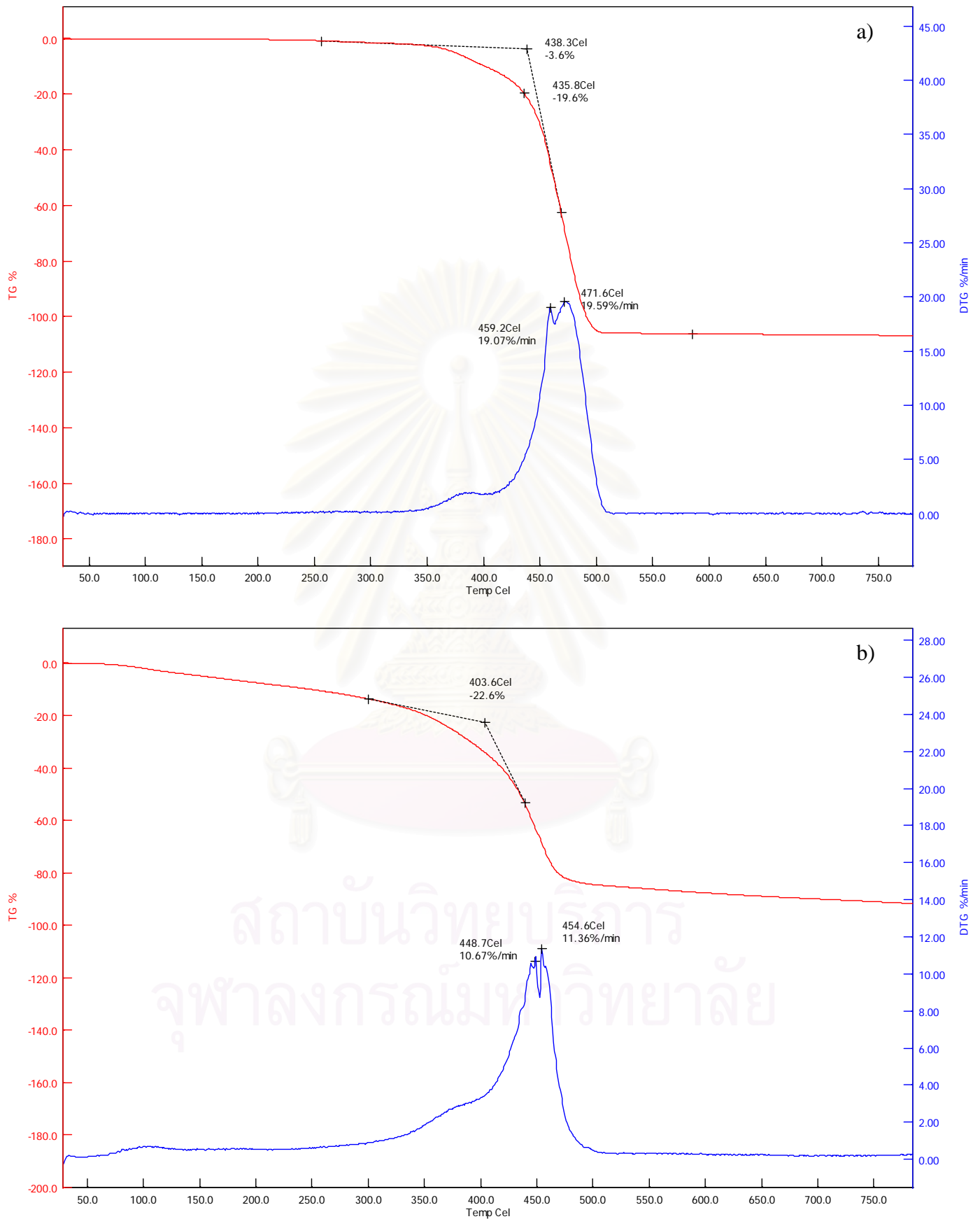


**Figure 6.4** TG curves of a) PBD and b) 18% hydroformylated PBD.

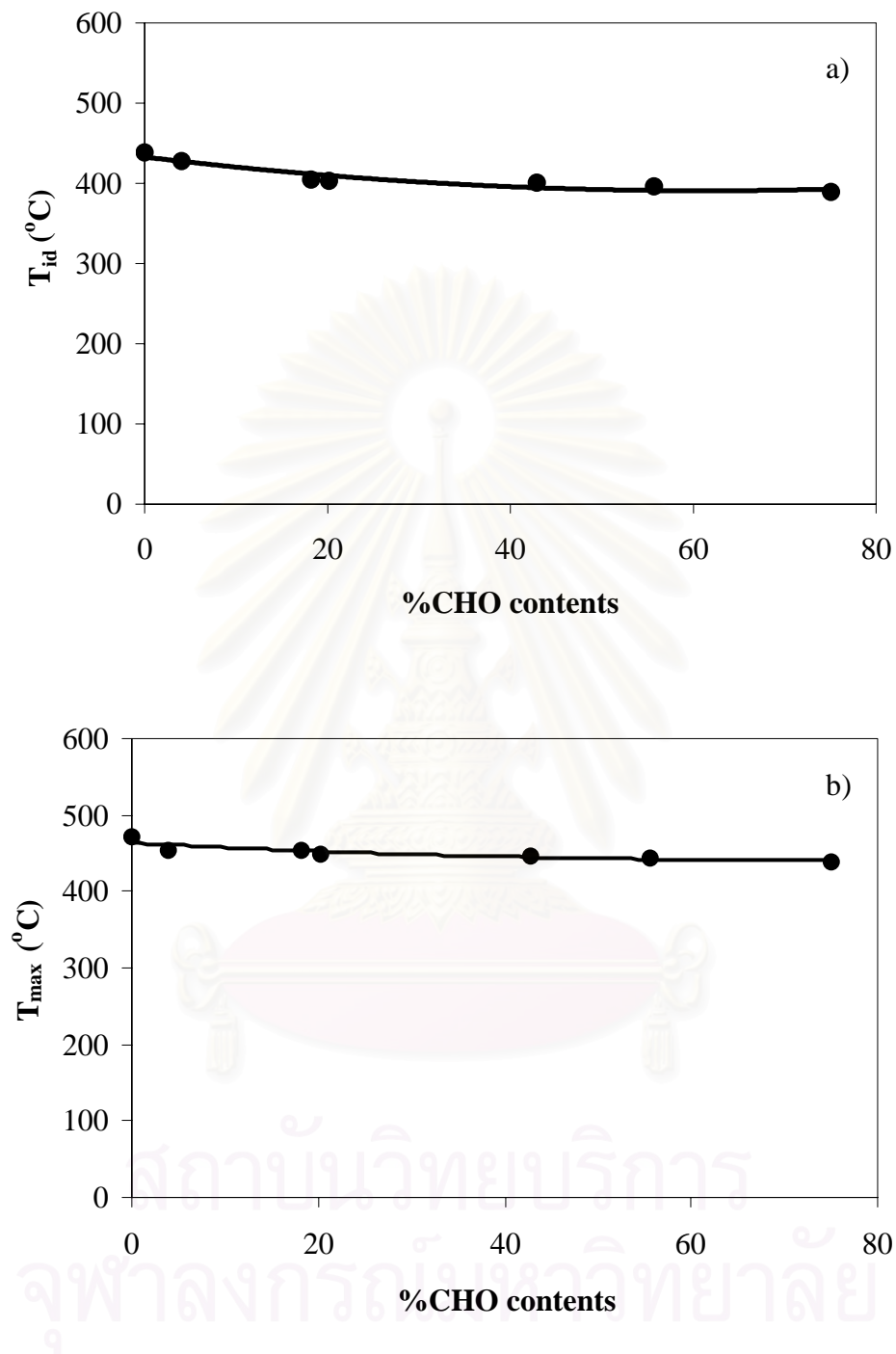


**Figure 6.5** a) The initial decomposition temperature ( $T_{id}$ ) and b) the maximum decomposition temperature ( $T_{max}$ ) with various %CHO contents in PBD.

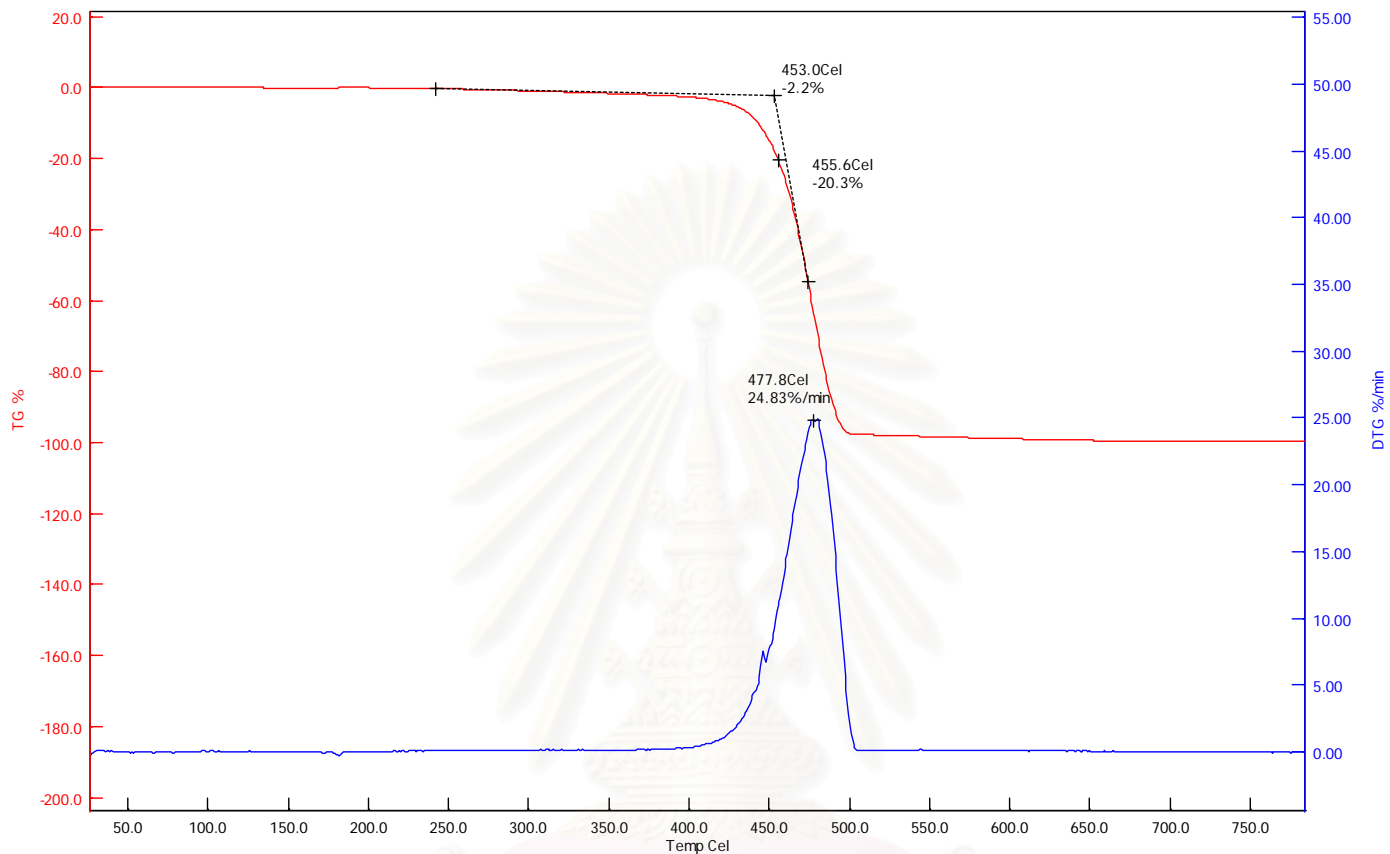


**Figure 6.6** TG curves of a) PBD and b) 20% hydroxymethylated PBD.

สถาบันวิทยบริการ  
จุฬาลงกรณ์มหาวิทยาลัย

### 6.3 Swelling Properties of Hydroformylated PBD Film

Regarding the possible use of hydroformylated PBD as a membrane (Ogata et al, 1976; Mertzweiller, 1969), swelling measurements are a basic method to investigate their permeation with respect to solvent. The membrane swelling is affected by the presence of hydrophilic groups, i.e., aldehyde groups, in the polymer structure.

The observed swelling properties of hydroformylated PBD in various types of solvent were determined from the weight increase after solvent absorption. The solvents used in this study were water, ethanol, monochlorobenzene, and tetrahydrofuran. %Swelling is defined as follows:

$$\% \text{ Swelling} = \frac{(B - A)}{A} \times 100 \quad (6.1)$$

where        A        =        Initial weight of film  
                   B        =        Final weight of film after absorption

The observation on the solvent resistance of hydroformylated PBD film with various %CHO are provided in Table 6.2. The results show that hydroformylated PBD film has high resistance in the solvent of MCB and water and the films are very stable over 4 days of swelling. For swelling in ethanol and THF, cracking of the hydroformylated PBD film was observed after 6 and 2 hours, respectively.

The %swelling with respect to time of the hydroformylated PBD film with 75% CHO is shown in Figure 6.7. It can be seen that %swelling of the film in solvent increased in the order: THF > Ethanol > Water > MCB. Thus, the permeability of hydroformylated PBD to these solvents increased in this order as well.

The change of %swelling of hydroformylated PBD film with various %CHO is shown in Figure 6.8. The appearance of the film is not affected by an increase in %CHO in PBD film. The %swelling in water and ethanol increases with increasing %CHO. The %swelling in MCB decreases with increasing %CHO because MCB is a better solvent for hydrophobic polymers.

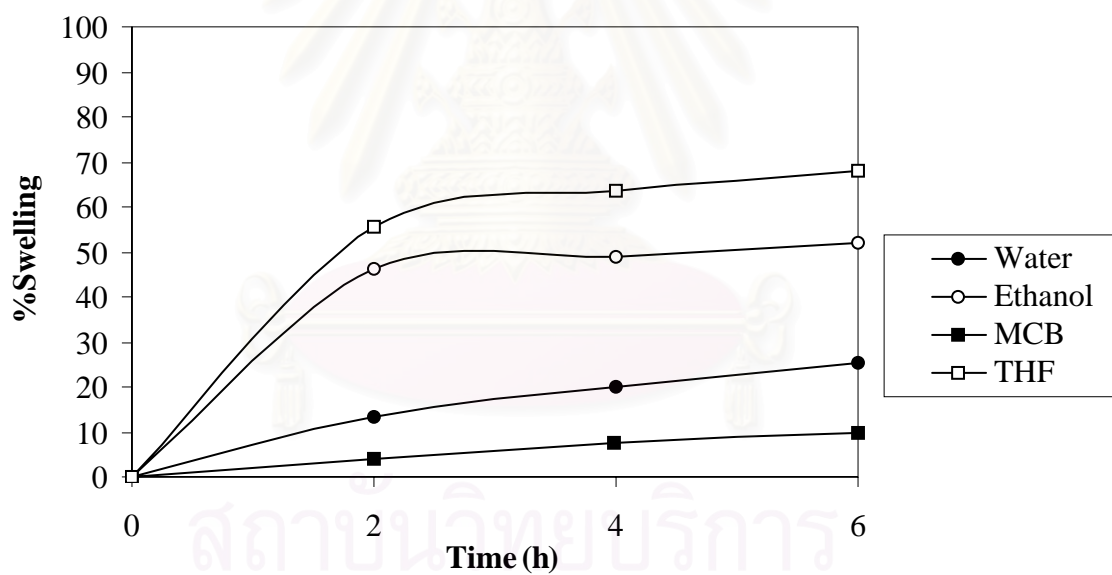
**Table 6.2** The solvent resistance of hydroformylated PBD film with various %CHO

%CHO in PBD film	MCB <sup>a</sup>	Water <sup>a</sup>	Ethanol <sup>b</sup>	THF <sup>c</sup>
5	good	good	Crack	Crack
20	good	good	Crack	Crack
55	good	good	Crack	Crack
75	good	good	Crack	Crack

<sup>a</sup> Swelling time = 4 days

<sup>b</sup> Swelling time = 6 hours

<sup>c</sup> Swelling time = 2 hours

**Figure 6.7** %Swelling of hydroformylated PBD film (75% CHO) with time.

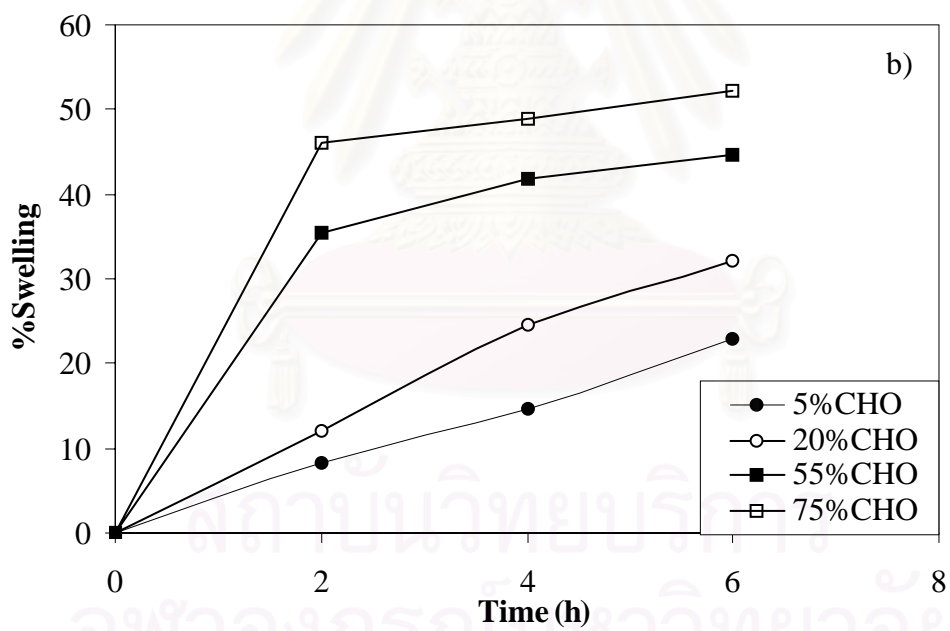
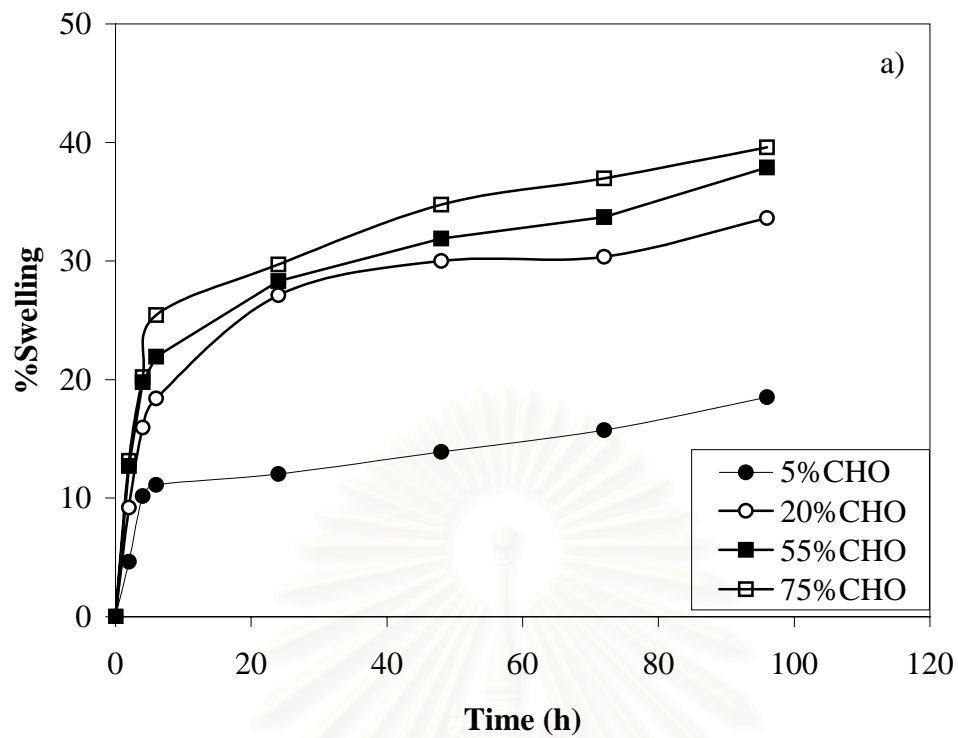


**Figure 6.8** %Swelling of hydroformylated PBD film with various %CHO in (a) water, (b) ethanol, and (c) MCB.

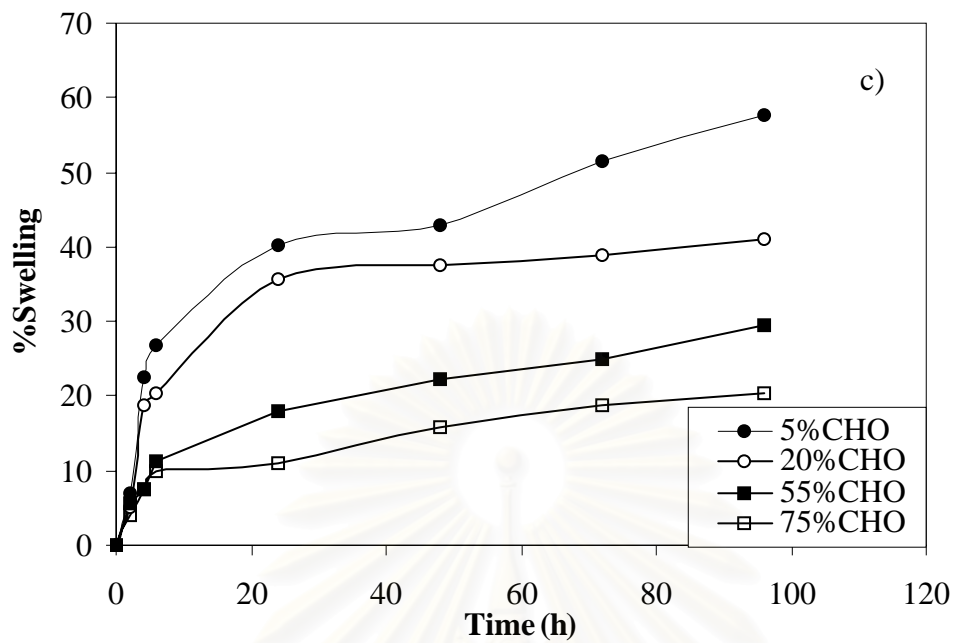


Figure 6.8 (continued)

สถาบันวิทยบริการ  
จุฬาลงกรณ์มหาวิทยาลัย

## CHAPTER VII

### CONCLUSION AND RECOMMENDATIONS

#### 7.1 Conclusion

Homogeneous catalytic chemical modification reaction on unsaturated polymers represents a feasible method for the synthesis of new polymers. Based on previous studies, low molecular weight polymers can be modified by reacting with a reaction gas in the presence of transition metal complexes as homogeneous catalysts. Thus, the obtained products have certain desirable functional groups on the polymer chain. This experimental investigation has revealed that hydroformylation and hydroxymethylation of high molecular weight of polybutadiene can also be achieved. A summary of the results obtained in the present study is as follows:

##### 7.1.1 Hydroformylation of High Molecular Weight *Cis*-1,4-PBD in a Parr Batch Reactor

Catalytic hydroformylation of high molecular weight *cis*-1,4-polybutadiene can be achieved in the presence of using  $\text{HRh}(\text{CO})(\text{PPh}_3)_3$  in monochlorobenzene to obtain a conversion of nearly 80% under fairly high pressure and moderate temperature. The hydroformylated product showed some selectivity toward 1,2-polybutadiene, which was present at about 2% in the substrates as seen in FT-IR and  $^1\text{H}$  NMR analysis. A  $2^4$  factorial experimental design was used to determine the significant parameters for the hydroformylation reaction. The resultant normal probability plot clearly indicated that temperature, catalyst concentration and total pressure of synthesis gas were important factors. Kinetic studies showed that the reaction rate is first order with respect each of catalyst concentration, and carbon-carbon double bond concentration. From the experiments, the first-order behavior with respect to total pressure was observed over the range of 13.8 to 41.3 bar. Also, an inverse first order rate with respect to triphenyl phosphine concentration and %CO in synthesis gas mixture was found. The apparent activation energy was estimated to be 41 kJ/mol over the temperature range of 60°C to 80°C. From this, it can be concluded that the reaction is preliminary under chemical reaction control.



### 7.1.2 Hydroformylation of High Molecular Weight *Cis*-1,4-PBD using a Computer Controlled Batch Reactor

In order to study the precise kinetics for the hydroformylation of *cis*-1,4-polybutadiene catalyzed by  $\text{HRh}(\text{CO})(\text{PPh}_3)_3$ , a gas uptake apparatus was used to detect the reaction gas consumption with respect to reaction time. The reaction was carried out over 2 h and the final product was sampled to determine the degree of conversion by  $^1\text{H}$  NMR analysis. The PBD hydroformylation was studied by using various rhodium complexes as  $\text{HRh}(\text{CO})(\text{PPh}_3)_3$ ,  $\text{Rh}_4(\text{CO})_{12}$ , and  $[\text{Rh}(\text{COD})\text{Cl}]_2$ .  $\text{HRh}(\text{CO})(\text{PPh}_3)_3$  was found to be the most efficient catalyst for PBD hydroformylation.  $\text{Rh}_4(\text{CO})_{12}$  and  $[\text{Rh}\{\text{COD}\}\text{Cl}]_2$  had low activity with respect to the catalytic hydroformylation of PBD. Kinetic studies show that the reaction rate is first order with respect to  $[\text{C}=\text{C}]$ , catalyst concentration, and total pressure of synthesis gas in the pressure range of 13.8 to 30 bar which is a shorter range with that observed for the Parr reactor due to the higher superior mixing in the autoclave of gas uptake apparatus.

The reaction rate is also independent of polymer concentration and inverse first order with respect to %CO in synthesis gas mixture and added triphenyl phosphine concentration. The apparent activation energy was estimated to be 66 kJ/mol over the temperature range of 60°C to 80°C. The reaction rate obtained when using the gas uptake apparatus was somewhat higher than that of the Parr reactor due to the configuration of the impeller and mixing and L/D ratio which provided superior mixing and completely overcame any transport limitation of the reaction. Furthermore, it was found that the rate constant and % conversion at 2 h increased with increasing solvating power of the solvent in the order: monochlorobenzene > benzene > toluene.

### 7.1.3 Hydroxymethylation of High Molecular Weight *Cis*-1,4-PBD

Hydroxymethylation of PBD can be carried out by a two-step process of controlled hydroformylation and subsequent hydrogenation. The hydroformylation of PBD was carried out in the presence of  $\text{HRh}(\text{CO})(\text{PPh}_3)_3$  in MCB using a 1:1 mixture of  $\text{H}_2$  and CO. The hydroformylated PBD was directly subjected to a subsequent hydrogenation reaction step by using  $\text{Ru}(\text{CH}=\text{CH}(\text{Ph}))\text{Cl}(\text{CO})(\text{PCy}_3)_2$  to produce hydroxymethylated PBD. The hydroxymethylated PBD was characterized using FT-IR and  $^1\text{H}$ -NMR spectroscopy. The result showed that only hydroformylated PBD

solution with less than 40% formyl loading could be used for subsequent hydrogenation. The crosslinking in hydroxymethylated PBD increases with increasing formyl loading or hydroxyl loading. At high formyl loading (40%), the polymer became gel like due to the increase in the hydrophilic nature of the –OH group in the hydroxymethylated PBD. In addition, hydrogenation of residual C=C double bonds was achieved. However, the calculated conversion results for hydroxymethylation were not consistent with a comparison of the conversion results for hydroformylation. This may be caused by only partial solubility of the hydroxymethylated product in the NMR solvent,  $\text{CDCl}_3$ .

### **7.1.3 Physical Properties of Hydroformylated and Hydroxymethylated PBD**

The thermal properties of hydroformylated and hydroxymethylated polybutadiene were characterized by differential scanning calorimetry and thermogravimetric analysis. The results show that hydroformylation increases the glass transition temperature ( $T_g$ ) of the polymer. PBD is rubbery in form, having a  $T_g$  of about  $-100^\circ\text{C}$  whereas hydroformylated PBD is in film form, having a  $T_g$  of about  $48^\circ\text{C}$ . However, hydroformylation tends to slightly decrease the initial decomposition temperature ( $T_{id}$ ) and the maximum decomposition temperature ( $T_{max}$ ). Thus, it can be concluded that the functional group, aldehyde group, is not very stable. Therefore, the hydroformylated PBD has less thermal stability. As the degree of hydroformylation increased,  $T_{id}$  and  $T_{max}$  do not seem to be dependent on %CHO content. In addition,  $T_{id}$  and  $T_{max}$  of hydroxymethylated PBD do not significantly change with respect to %OH contents in polymer.

The hydroformylated PBD can be formed as a film which potentially could be used as a membrane. Swelling measurements are basic method to investigate the permeation of solvent as influenced by the presence of hydrophilic groups, such as aldehyde groups, in the polymer structure. The observed swelling properties in various types of solvent were achieved by determining the weight change after solvent absorption of hydroformylated PBD. The results show the permeability of hydroformylated PBD to solvent increased in this order: THF > ethanol > water > MCB.

## 7.2 Recommendations

Further investigation on the hydroformylation and hydroxymethylation of unsaturated polymers should take into account with the following aspects:

### 1. Hydroformylation and Hydroxymethylation for other diene polymers

Modification of natural rubber can improve its properties and also provide alternative specialty polymers as new valued added products. The hydroformylation and hydroxymethylation of synthetic *cis*-1,4-polyisoprene and natural rubber should be carried out.

### 2. Catalyst Study on Hydroformylation and Hydroxymethylation

It was found that  $\text{HRh}(\text{CO})(\text{PPh}_3)_3$  and  $\text{Ru}(\text{CH}=\text{CHPh})\text{Cl}(\text{CO})(\text{PCy}_3)_2$  were efficient catalysts for the hydroformylation and hydrogenation, respectively. Further investigation with respect to the catalyst selectivity for internal C=C and a study of other hydroformylation catalysts are imperative to obtain insight into this behavior.

### 3. Quantitative Treatments or Hydroformylated and Hydroxymethylation Products

A more quantitative treatment of the data should be attempted in order to observe more insight into side reactions such as, crosslinking and degradation, which may be accompanying the desirable modification reaction. This information can be used further to modify the catalyst and reaction conditions so as to minimize the side reactions.

### 4. Properties of Hydroformylated and Hydroxymethylated Polymers

Some properties such as chemical, physical, and mechanical properties of hydroformylated and hydroxymethylated products are changed. In addition, other properties regarding possible membrane applications should be also investigated in detail.

## REFERENCES

- Ahmad, N.; Levison, J. J., Robinson, S. D., and Uttey, M. F. Triphenylphosphine complexes of transition metals. Inorg. Syn. 15 (1974): 45-63.
- Azuma, C., Mituboshi, T., Sanui, K., and Ogata, N. Synthesis and properties of polydiene and polypentenamer having formyl or hydroxymethyl groups and their photosensitive derivations. J. Polym. Sci., Polym. Chem. Ed. 18 (1980): 781-797.
- Barlow, F. W. Rubber compounding: principles, materials, and techniques. 2<sup>nd</sup> ed. New York: Dekker, 1993: pp. 41-47.
- Bhaburi, S., and Mukesh, D. Homogeneous catalysis: mechanisms and industrial applications New York: Wiley, 1979: pp. 86-103.
- Bhattacharjee, S., Bhowmick, A. K., and Avasthi, B. N. Hydroformylation of nitrile rubber and its characterization. Angew. Makromol. Chem. 198 (1992): 1-14.
- Charmondusit, K., Prasassarakich, P., McManus, N. T., and Rempel, G. L. Hydrogenation of *cis*-1,4-poly(isoprene) catalyzed by OsHCl(CO)(O<sub>2</sub>)(PCy<sub>3</sub>)<sub>2</sub>. J. Appl. Polym. Sci. 89 (2003): 142-152.
- Chamondusit, K. Hydrogenation of *cis*-1,4-poly(isoprene) and natural rubber catalyzed by OsCl(CO)(O<sub>2</sub>)(PCy<sub>3</sub>)<sub>2</sub> and [Ir(COD)py(PCy<sub>3</sub>)]PF<sub>6</sub>. Doctoral dissertation, Department of Chemical Technology, Faculty of Science, Chulalongkorn University, 2001.
- Chatt, J., and Venanzi, L. M. Olefin co-ordination compounds. Part IV. Diene complexes of rhodium (I). J. Chem. Soc. (1957): 4735-4741.

- Chen, J., Ajjou, A. N., Chanthateyanonth, R., and Alper, H. Catalytic hydroformylation of styrene-butadiene copolymers. Macromolecules 30 (1997): 2897-2901.
- Crabtree, R. H. The Organometallic Chemistry of the Transition Metal New York: Wiley, 1988: pp. 200 – 202.
- Cull, N. L., and Mertzweiler, J. K. Flexible oxygen containing polybutadiene surface coating composition. U.S. Patent 3 337 489 (1967).
- Cull, N. L. Colloidal silica containing lattices of hydroformylated polymers of conjugated dienes. U.S. Patent 3 314 911 (1967).
- Fifield, F. W., and Kealey, Principle and practice of analytical chemistry. 4<sup>th</sup> ed. London: Chapman&Hall, 1995: pp. 475-492.
- Hinchiran, N., Prasassarakich, P., and Rempel, G. L. Preparation of hydrogenated natural rubber using  $\text{OsHCl}(\text{CO})(\text{O}_2)(\text{PCy}_3)_2$ : Kinetics and its characterizations. . J. Appl. Polym. Sci. (Impress).
- Jardine, F. H. Carbonylhydrido*tris*(triphenylphosphine)rhodium(I). Polyhedron, 1, (1982): 569-605.
- Jongsma, T., Challa, G., Van Leeuwen, P. W. N. M. A. A mechanistic study of rhodium tri(*o*-*t*-butylphenyl)phosphite complexes as hydroformylation catalysts. J. Org. Chem. 421 (1991): 121-128.
- Jongsma, T., Kimkes, P. Challa, G., and Van Leeuwen, P. W. N. M. A new type of highly active polymer-bound rhodium hydroformylation catalyst. Polymer 33, (1991): 161-165.

- Martinengo, S., Giordano, G., and Chini, P. Metal cluster complexes. Inorg. Synth. 20 (1980): 209-212.
- McGrath, M. P., Sall, E. D., Forster, D., Tremont, S. J., Sendijarevic, A., Sendijarevic, V., Promer, D., Jiang, J., Iyer, K., Klempner, D., and Frisch, K. C. Novel polymeric alcohols by controlled catalytic polymer fictionalization. J. Appl. Polym. Sci. 56 (1995): 533-543.
- McManus, N. T., and Rempel, G. L. Chemical modification of polymers: catalytic hydrogenation and related Reactions. Rev. Macromol. Chem. Phys. C35(2) (1995): 239 - 285.
- Mertzweiller, J. K., and Cull, N. L. Composition containing a hydroformylated-hydrogenated reaction product of an unsaturated hydrocarbon polymer and an epoxidized polyolefin. U.S. Patent 3 318 972 (1967).
- Mertzweiller, J. K., Segura, M. A., and Cull, N. L. Coating composition containing a blend of modified polybutadiene. U.S. Patent 3 365 411 (1968).
- Mertzweiller, J. K., Cull, N. L., and Hawley, R. S. Glass fibers sized with hydroformylated polymer and laminate therefrom. U.S. Patent 3 425 895 (1965).
- Mills, P. L., Tremont, S. J., and Remsen, E. E. Synthesis, characterization, and kinetics of functionalized polybutadiene using a homogenous rhodium hydroformylation catalyst. Ind. Eng. Chem. Res. 29 (1990): 1443-1454.
- Mohammadi, N. A. Catalytic hydrogenation, hydroformylation and hydroxymethylation of diene polymers. Doctoral dissertation, Department of Chemical Engineering, University of Waterloo, 1987.

- Mohammadi, N. A. and Rempel, G. L. Control, data acquisition and analysis of catalytic gas-liquid mini slurry reactors using a personal computer. Comput. Chem. Eng. 11 (1987): 27-35.
- Ogata, N., Sanui, K., Shimozato, Y., and Munemuro S. Syntheses of functional condensation polymer. I. Polyesters having pendant functional groups such as hydroxyl, formyl, aldoxime, aminomethyl and hydroxymethyl. J. Polym. Sci., Polym. Chem. Ed. 14 (1976): 2969-2981.
- Parkinson, L. E. Application of oxygenated  $\text{Rh}_6(\text{CO})_{16}$  for the catalytic hydrogenation of anthracene: An exploratory investigation Doctoral dissertation, Department of Chemical Engineering, University of Waterloo, 1987.
- Ramp, F. L., Dewitt, E. J., and Trapasso, L. E. Hydroformylation of high polymers. J. Polym. Sci. 4 (1966): 2267-2279.
- Sanchez-Delgado, R. A., Bradiev, J. S., and Wilkinson, G. Further studies on the homogenous hydroformylation of alkenes by use of ruthenium complex catalysts. J. Chem. Soc. (A) (1976): 399-404.
- Sanui, K., MacKnight, W. J., and Lenz, R. W. Hydroformylation of a polybutadiene and preparation of derivatives therefrom Macromolecules. 7 (1974): 952-956.
- Scott, P. J., and Rempel, G. L. Homogeneous catalytic hydroformylation of styrene-butadiene copolymers in the presence of  $\text{HRh}(\text{CO})(\text{PPh}_3)_3$ . Macromolecules. 25 (1992): 2811-2819.
- Sibtain, F., and Rempel, G. L. Chemical modification of polymers: Catalytic hydroformylation and hydroxymethylation of styrene-butadiene copolymers. J. Polym. Sci., Polym. Chem. Ed. 29 (1991): 629-635.

Spessard, G. O., Miessler, G. L. Organometallic Chemistry. New Jersey: Prentice-Hall, 1996: pp. 255-265.

Tangthongkul, R., Prasassarakich, P., N. T., McManus, Rempel, G. L. Hydrogenation of *cis*-1,4-polyisoprene catalyzed by  $\text{Ru}(\text{CH}=\text{CH}(\text{Ph}))\text{Cl}(\text{CO})(\text{PCy}_3)_2$ . J. Polym. Sci. 91 (2004): 3259-3273.

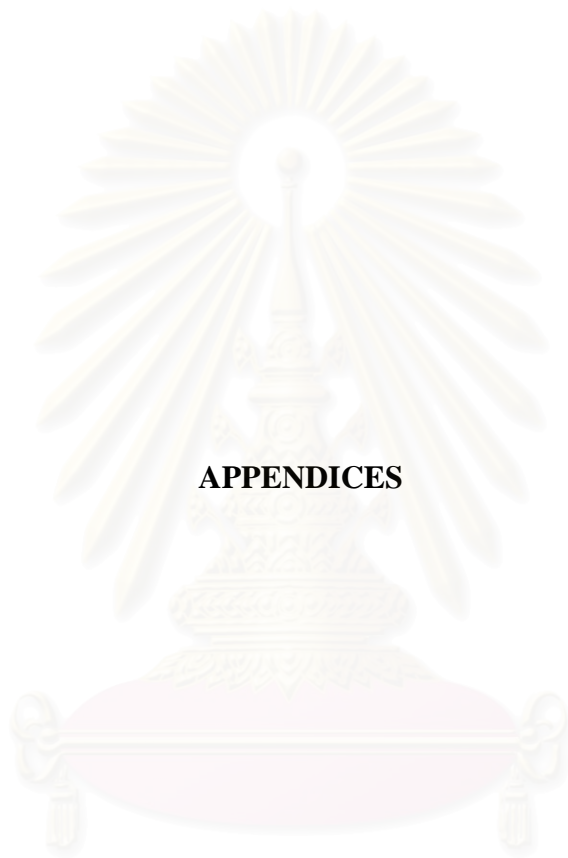
Tremont, S. J., Remsen, E. E., Mills, P. L. An experiment and modeling study of polybutadiene functionalization to polyaldehyde using a homogenous rhodium catalyst. Chem. Eng. Sci. 45 (1990): 2801-2808.

Tremont, S. J., Remsen, E. E., Mills, P. L. Hydroformylation of 1,2- and 1,4-polybutadiene and their mixtures with hydroformyltris (triphenylphosphine) rhodium (I) catalyst and excess triphenylphosphine Macromolecules. 23 (1990): 1984-1993.

Trzeciak, A. M., and Ziolkowski, J. J. Perspective of rhodium organometallic catalysis. Fundamental and applied aspects of hydroformylation, Coord. Chem. Rev. 190-192 (1999): 883-900.

สถาบันวิทยบริการ  
จุฬาลงกรณ์มหาวิทยาลัย





**APPENDICES**

สถาบันวิทยบริการ  
จุฬาลงกรณ์มหาวิทยาลัย

## Appendix I: Elemental Analysis of Rhodium Complexes

### Catalyst

HRh(CO)(PPh <sub>3</sub> ) <sub>3</sub>	Calcd. from C <sub>55</sub> H <sub>46</sub> OP <sub>3</sub> Rh: C = 71.90%; H = 5.05%; P = 10.11%
	Found*: C = 71.90%; H = 5.04%
Rh <sub>4</sub> (CO) <sub>12</sub>	Calcd. from C <sub>12</sub> O <sub>12</sub> Rh <sub>4</sub> : Rh = 55.08%
Rh <sub>6</sub> (CO) <sub>16</sub>	Calcd. from C <sub>16</sub> O <sub>16</sub> Rh <sub>6</sub> : C = 18.04%; Rh = 57.94%
[RhCl(COD)] <sub>2</sub>	Calcd. from C <sub>16</sub> H <sub>24</sub> Cl <sub>2</sub> Rh <sub>2</sub> : C = 38.97% ; H = 4.91%; Cl = 14.38%
Rh(COD)acac	Calcd. from C <sub>13</sub> H <sub>19</sub> O <sub>2</sub> Rh <sub>2</sub> : C = 50.34%; H = 6.17%; Rh = 33.17%

\*Analyzed by elemental analysis at Glueph Laboratories, Ltd (Canada)



สถาบันวิทยบริการ  
จุฬาลงกรณ์มหาวิทยาลัย

## Appendix II: Calculation of %Conversion of Hydroformylation and Hydroxymethylation

### a) Hydroformylation of High Molecular Weight *Cis*-1,4-PBD

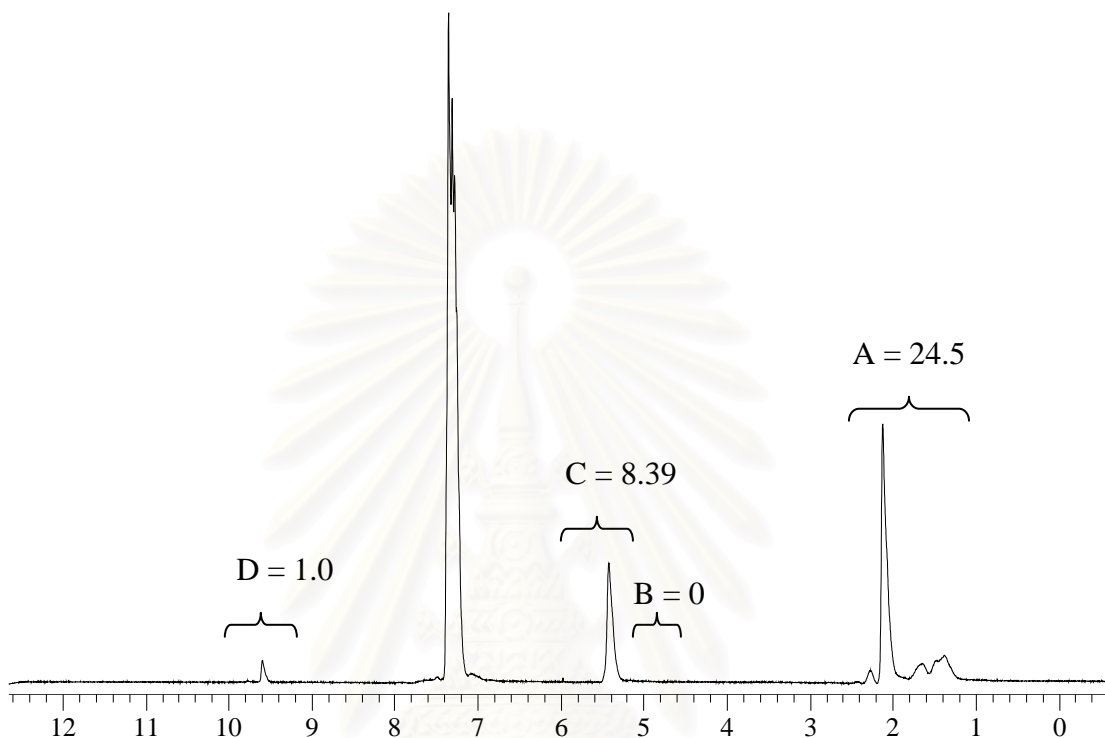


**Figure AII-A**  $^1\text{H-NMR}$  spectrum of partial hydroformylated *cis*-1,4-PBD

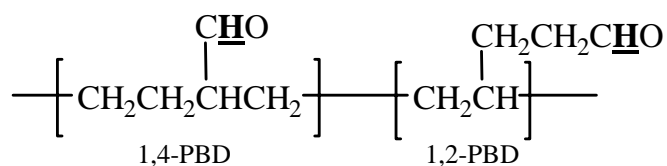
Where

- A = area of paraffinic proton signals
- B = area of  $-\text{CH}_2\text{OH}$  groups
- C = area of olefinic proton signals due to  $\text{C}=\text{C}$  in 1,2-PBD
- D = area of olefinic proton signals due to  $\text{C}=\text{C}$  in 1,4- and 1,2-PBD
- E = area of two aldehydic proton signals

For *cis*-1,4-PBD, the obtained possible products from hydroformylation are as follows:

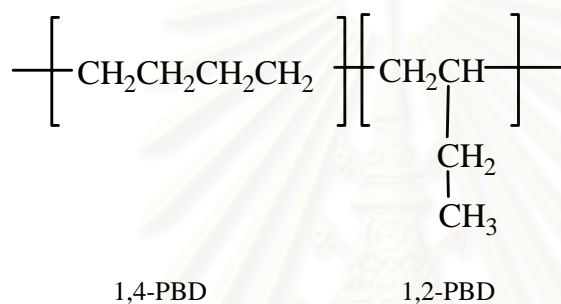
1. Hydroformylated PBD
2. Hydrogenated PBD
3. Residual  $\text{C}=\text{C}$  double bonds

## 1. Hydroformylated PBD



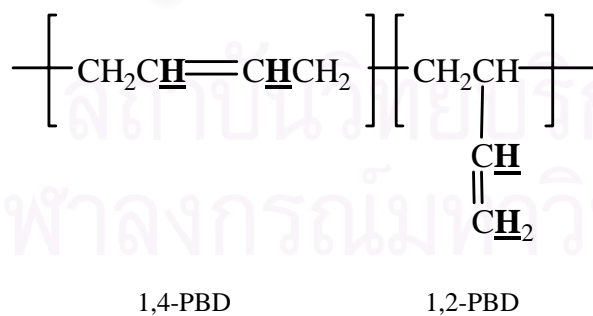
	<u>1,4-PBD</u>	<u>1,2-PBD</u>
CHO protons:	1	1
paraffin protons:	7	7

## 2. Hydrogenated PBD



	<u>1,4-PBD</u>	<u>1,2-PBD</u>
paraffin protons:	8	8

## 3. The remaining C=C double bond



	<u>1,4-PBD</u>	<u>1,2-PBD</u>
HC=CH and CH=CH <sub>2</sub> protons:	2	3
paraffin protons:	4	3

From all above, we can write the following equations.

$$\begin{aligned}
 A &= \text{paraffin content in hydroformylation, hydrogenation, and} \\
 &\quad \text{remaining C=C bonds of PBD} \\
 &= 7*[\text{HDF}] + 8*[\text{HDG}] + 4*[1,4] + 3*[1,2] \\
 B &= 3*[1,2] \\
 C &= 2*[1,4] + 3*[1,2] \\
 D &= 1*[\text{HDF}]
 \end{aligned}$$

where

$$\begin{aligned}
 [\text{HDF}] &= \text{mole fraction of hydroformylation} \\
 [\text{HDG}] &= \text{mole fraction of hydrogenation} \\
 [1,4] &= \text{mole fraction of 1,4-PBD} \\
 [1,2] &= \text{mole fraction of 1,2-PBD}
 \end{aligned}$$

Therefore, we can summarize that

$$\% \text{ Hydroformylation} = \frac{D}{\frac{1}{2}(C - \frac{B}{2}) + \frac{B}{2} + D + \frac{1}{8}(A - \frac{B}{2} - 2C - 7D)} \quad (2.1)$$

$$\% \text{ Hydrogenation} = \frac{\frac{1}{8}(A - \frac{B}{2} - 2C - 7D)}{\frac{1}{2}(C - \frac{B}{2}) + \frac{B}{2} + D + \frac{1}{8}(A - \frac{B}{2} - 2C - 7D)} \quad \text{AII-A}$$

$$\% [\text{C} = \text{C}] = \frac{\frac{1}{2}(C - \frac{B}{2}) + \frac{B}{2}}{\frac{1}{2}(C - \frac{B}{2}) + \frac{B}{2} + D + \frac{1}{8}(A - \frac{B}{2} - 2C - 7D)} \quad \text{AII-B}$$

From Figure AII-A,

A	B	C	D
24.5	0	8.3	1.0

The calculation examples for hydroformylation, hydrogenation, and residual [C=C] double bonds are presented as follows:

$$\begin{aligned} \% \text{ Hydroformylation} &= \frac{1}{\frac{1}{2}(8.3 - 0) + 0 + 1 + \frac{1}{8}(24.5 - 0 - 2 * 8.3 - 7 * 1)} \\ &= 19\% \end{aligned}$$

$$\begin{aligned} \% \text{ Hydrogenation} &= \frac{\frac{1}{8}(A - \frac{B}{2} - 2C - 7D)}{\frac{1}{2}(C - \frac{B}{2}) + \frac{B}{2} + D + \frac{1}{8}(A - \frac{B}{2} - 2C - 7D)} \\ &= 2\% \end{aligned}$$

$$\begin{aligned} \% [C=C] &= \frac{\frac{1}{2}(C - \frac{B}{2}) + \frac{B}{2}}{\frac{1}{2}(C - \frac{B}{2}) + \frac{B}{2} + D + \frac{1}{8}(A - \frac{B}{2} - 2C - 7D)} \\ &= 79\% \end{aligned}$$

Based on this calculation, all experimental results from Parr reactor and Gas Uptake Apparatus are presented in Table AII-A and Table AII-B.

สถาบันวิทยบริการ  
จุฬาลงกรณ์มหาวิทยาลัย

**Table AII-A** The results of %hydroformylation of PBD in Parr batch reactor

(For Table 3.3).

Expt.	Integral Area of Spectra				% [HDF]	% [HDG ]	% [C=C]
	A	B	C	D			
1	5.277	0.000	1.000	0.412	42.9	5.1	52.0
2	5.460	0.000	1.000	0.430	43.6	5.7	50.7
3	6.714	0.000	1.000	0.531	45.9	10.8	43.3
4	7.200	0.000	1.000	0.581	47.5	11.6	40.9
5	10.219	0.000	1.364	1.000	57.4	3.5	39.1
6	8.938	0.000	0.804	1.000	69.3	2.9	27.9
7	8.491	0.000	0.516	1.000	76.0	4.4	19.6
8	8.222	0.000	0.322	1.001	81.1	5.8	13.1
9	8.152	0.000	0.336	1.000	81.4	4.9	13.7
10	8.126	0.000	0.039	1.004	87.2	11.1	1.7
11	8.558	0.000	0.199	1.000	80.4	11.7	8.0
12	8.074	0.000	0.355	1.000	81.8	3.7	14.5
13	8.680	0.000	0.394	1.000	76.4	8.5	15.1
14	8.816	0.000	0.692	1.000	71.4	3.9	24.7
15	9.478	0.000	0.797	1.000	66.3	7.3	26.4
16	14.547	0.000	3.443	1.000	35.7	2.9	61.4
17	3.432	0.000	1.000	0.197	28.0	0.9	71.1
18	12.377	0.000	2.089	1.000	45.6	6.8	47.6
19	9.905	0.000	1.209	1.000	60.0	3.7	36.3
20	3.903	0.000	1.000	0.238	31.0	3.9	65.1
21	9.240	0.000	0.755	1.000	68.1	6.2	25.7
22	8.558	0.000	0.199	1.000	80.4	11.7	8.0
23	8.084	0.000	1.000	0.691	51.3	11.6	37.1
24	8.274	0.000	0.474	1.000	78.3	3.2	18.5
25	9.463	0.000	1.000	0.862	56.0	11.6	32.5
26	11.970	0.000	1.955	1.000	47.4	6.3	46.3
27	7.651	0.000	1.000	0.517	40.7	20.0	39.3
28	10.926	0.000	1.682	1.000	52.3	3.7	44.0
29	9.922	0.000	0.792	1.000	64.0	10.7	25.3
30	8.277	0.000	1.000	0.680	49.7	13.8	36.5
31	8.558	0.000	0.199	1.000	80.4	11.7	8.0
32	8.084	0.000	1.000	0.691	51.3	11.6	37.1
33	8.491	0.000	0.516	1.000	76.0	4.4	19.6
34	7.145	0.000	1.000	0.582	47.8	11.0	41.1
35	8.588	0.000	0.700	1.000	72.8	1.7	25.5
36	5.104	0.000	1.000	0.331	35.6	10.6	53.8
37	9.035	0.000	0.723	1.000	69.7	5.1	25.2
38	9.298	0.000	0.878	1.000	66.4	4.5	29.1
39	11.246	0.000	1.865	1.065	53.1	0.4	46.5
40	13.288	0.001	2.689	1.000	40.7	4.6	54.7

**Table AII-B** The results of %hydroformylation of PBD in Gas Uptake Apparatus  
(For Table 4.3).

Expt.	Integral Area of Spectra				% [HDF]	% [HDG]	% [C=C]
	A	B	C	D			
1	16.291	0.000	3.819	1.000	32.1	6.6	61.3
2	363.100	0.000	84.400	22.451	32.4	6.7	60.9
3	395.900	0.000	89.100	24.466	32.7	7.8	59.5
4	363.100	0.000	84.400	22.235	32.1	7.0	60.9
5	15.476	0.000	3.263	0.911	31.8	11.2	57.0
6	576.580	0.000	133.190	35.238	32.1	7.2	60.7
7	16.005	0.000	3.797	0.990	32.2	6.0	61.8
8	16.069	0.000	3.886	1.010	32.5	5.0	62.5
9	428.600	0.000	94.800	26.430	32.8	8.4	58.8
10	558.000	0.000	222.400	11.500	9.1	3.2	87.7
11	473.200	0.000	160.400	15.700	15.5	5.2	79.2
12	456.300	0.000	120.800	19.643	21.9	10.8	67.3
13	294.600	0.000	83.100	14.865	25.0	5.1	69.9
14	224.020	0.000	55.080	13.290	30.6	6.0	63.4
15	16.291	0.000	3.819	1.000	32.1	6.6	61.3
16	273.700	0.000	62.100	18.422	35.4	4.9	59.7
17	14.945	0.000	3.384	0.899	31.8	8.3	59.9
18	22.197	0.000	6.896	0.989	21.4	4.0	74.6
19	28.279	0.000	9.669	0.953	15.7	4.7	79.6
20	33.107	0.000	12.078	0.916	12.6	4.4	83.0
21	24.355	0.000	7.401	0.901	18.0	8.1	73.9
22	20.070	0.000	5.655	1.000	24.7	5.4	69.9
23	15.209	0.000	3.113	0.870	31.2	13.0	55.8
24	208.210	0.000	34.428	16.592	45.2	7.9	46.9
25	11.929	0.000	1.685	0.994	48.8	9.8	41.4
26	18.609	0.000	4.823	0.987	27.0	7.0	66.0
27	16.004	0.000	3.705	0.919	30.2	8.9	60.9
28	15.935	0.000	3.825	0.944	30.8	6.8	62.4
29	15.210	0.000	3.286	0.905	31.9	10.2	57.9
30	17.367	0.000	4.068	1.073	32.3	6.5	61.2
31	12.485	0.000	1.880	0.993	46.1	10.3	43.6
32	15.673	0.000	2.773	1.000	36.0	14.1	49.9
33	15.782	0.000	2.811	0.895	32.1	17.5	50.4
34	59.960	0.000	22.070	0.985	7.5	8.5	84.0



**b) Hydroxymethylation of High Molecular Weight *Cis*-1,4-PBD**

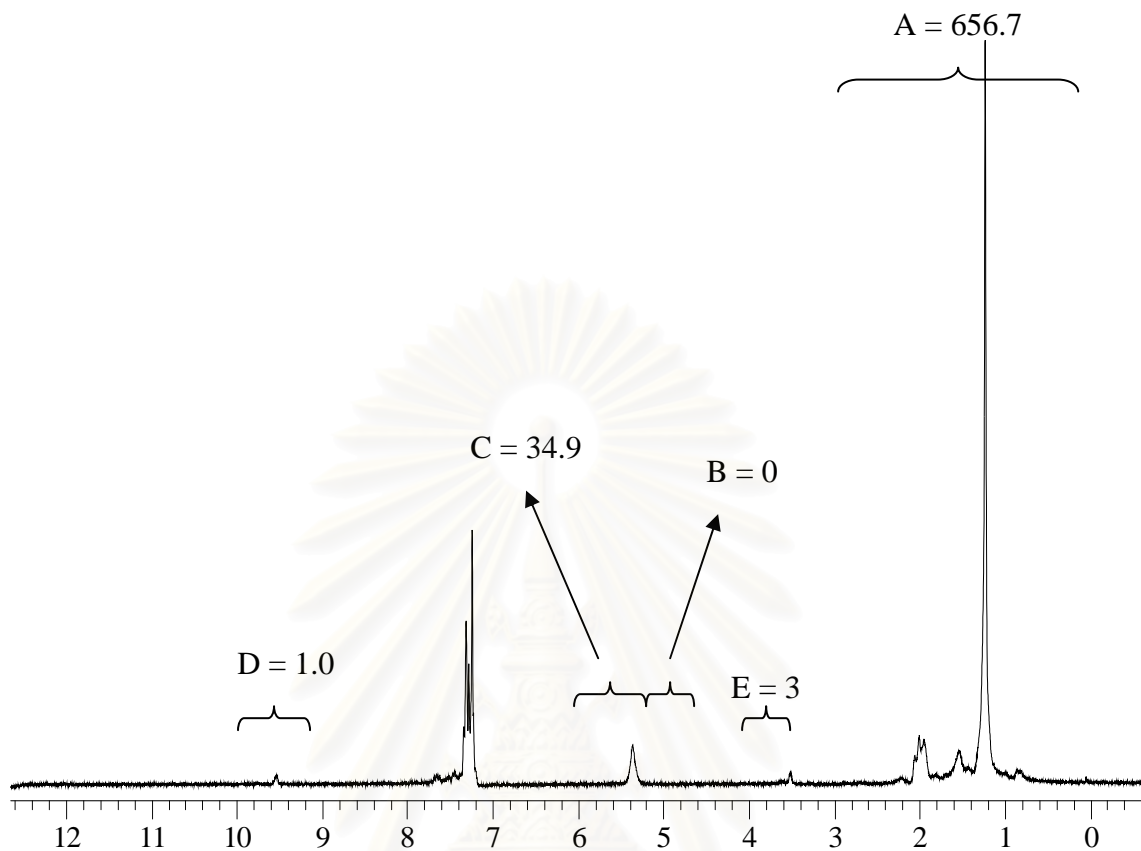


**Figure AII-B**  $^1\text{H}$ -NMR spectrum of partial hydroformylated and hydroxymethylated *cis*-1,4-PBD

Where

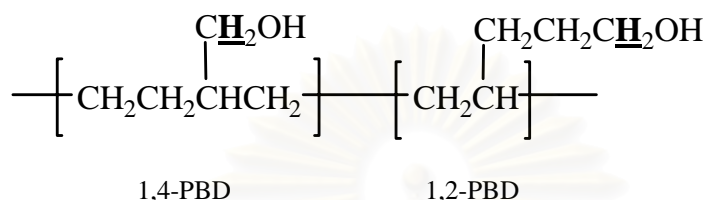
- A = area of paraffinic proton signals  
 B = area of olefinic proton signals due to C=C in 1,2-PBD  
 C = area of olefinic proton signals due to C=C in 1,4- and 1,2-PBD  
 D = area of two aldehydic proton signals  
 E = area of  $-\text{CH}_2\text{OH}$  groups

For *cis*-1,4-PBD, the obtained possible products from hydroformylation and hydroxymethylation are as follows:

1. Hydroformylated PBD
2. Hydrogenated PBD
3. Residual C=C double bonds
4. Hydroxymethylated PBD

As mentioned above, the possible products of hydroformylation are hydroformylated PBD, hydrogenated PBD, and residual C=C double bonds. The subsequent hydrogenation or hydroxymethylation produced hydroxymethylated PBD as follows:

#### Hydroxymethylated PBD



	<u>1,4-PBD</u>	<u>1,2-PBD</u>
CH <sub>2</sub> OH protons:	2	2
paraffin protons:	9	9

From all above, we can write the following equations.

$$\begin{aligned} A &= \text{paraffin content in hydroformylation, hydrogenation, remaining} \\ &\quad \text{C=C bonds of PBD, and hydroxymethylation} \\ &= 7*[\text{HDF}] + 8*[\text{HDG}] + 4*[1,4] + 3*[1,2] + E/2 \\ B &= 3*[1,2] \\ C &= 2*[1,4] + 3*[1,2] \\ D &= 1*[\text{HDF}] \\ E &= E/2 \end{aligned}$$

where

$$\begin{aligned} [\text{HDF}] &= \text{mole fraction of hydroformylation} \\ [\text{HDG}] &= \text{mole fraction of hydrogenation} \\ [1,4] &= \text{mole fraction of 1,4-PBD} \\ [1,2] &= \text{mole fraction of 1,2-PBD} \\ [\text{HDX}] &= \text{mole fraction of hydroxymethylation} \end{aligned}$$

Therefore, %hydroformylation, %hydroxymethylation, %hydrogenation, and %residual double bond can be calculated from the following equations:

$$\% \text{ Hydroxymet hylation} = \frac{\frac{E}{2}}{\frac{1}{2}(C - \frac{B}{2}) + \frac{B}{2} + D + \frac{1}{8}(A - \frac{B}{2} - 2C - 7D - \frac{7}{2}E) + \frac{E}{2}} \quad (2.2)$$

$$\% \text{ Hydroformy lation} = \frac{D}{\frac{1}{2}(C - \frac{B}{2}) + \frac{B}{2} + D + \frac{1}{8}(A - \frac{B}{2} - 2C - 7D - \frac{7}{2}E) + \frac{E}{2}} \quad (\text{AII-C})$$

$$\% \text{ Hydrogenat ion} = \frac{\frac{1}{8}(A - \frac{B}{2} - 2C - 7D - \frac{7}{2}E)}{\frac{1}{2}(C - \frac{B}{2}) + \frac{B}{2} + D + \frac{1}{8}(A - \frac{B}{2} - 2C - 7D - \frac{7}{2}E) + \frac{E}{2}} \quad (\text{AII-D})$$

$$\% [C = C] = \frac{\frac{1}{2}(C - \frac{B}{2}) + \frac{B}{2}}{\frac{1}{2}(C - \frac{B}{2}) + \frac{B}{2} + D + \frac{1}{8}(A - \frac{B}{2} - 2C - 7D - \frac{7}{2}E) + \frac{E}{2}} \quad (\text{AII-E})$$

From Figure AII-B,

A	B	C	D	E
656.7	0	34.9	1	3

The %hydroformylation and %hydroxymethylation are calculated as follows:

$$\% \text{ Hydroxymet hylation} = \frac{\frac{3}{2}}{\frac{1}{2}(34.9 - 0) + 0 + 1 + \frac{1}{8}(656.7 - 0 - 2 * 34.9 - 7 * 1 - \frac{7}{2} * 3) + \frac{3}{2}}$$

$$= 1.6\%$$

$$\% \text{ Hydroformy lation} = \frac{1}{\frac{1}{2}(34.9 - 0) + 0 + 1 + \frac{1}{8}(656.7 - 0 - 2 * 34.9 - 7 * 1 - \frac{7}{2} * 3) + \frac{3}{2}}$$

$$= 1.1\%$$

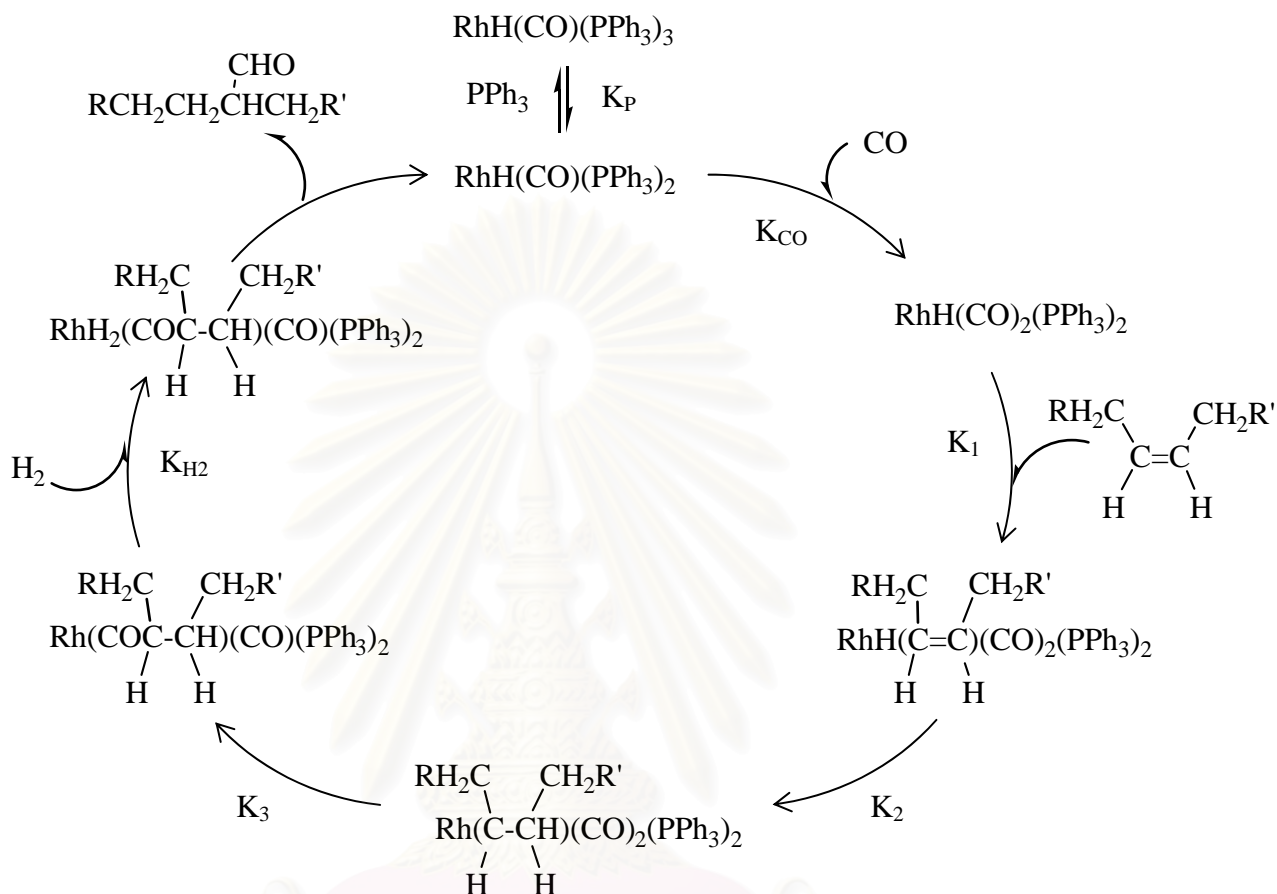
$$\begin{aligned} \% \text{Hydrogenat ion} &= \frac{\frac{1}{8}(656.7 - 0 - 2 * 34.9 - 7 * 1 - \frac{7}{2} * 3)}{\frac{1}{2}(34.9 - 0) + 0 + 1 + \frac{1}{8}(656.7 - 0 - 2 * 34.9 - 7 * 1 - \frac{7}{2} * 3) + \frac{3}{2}} \\ &= 78.1\% \end{aligned}$$

$$\begin{aligned} \%[C = C] &= \frac{\frac{1}{2}(34.9 - 0) + 0}{\frac{1}{2}(34.9 - 0) + 0 + 1 + \frac{1}{8}(656.7 - 0 - 2 * 34.9 - 7 * 1 - \frac{7}{2} * 3) + \frac{3}{2}} \\ &= 19.1\% \end{aligned}$$



สถาบันวิทยบริการ  
จุฬาลงกรณ์มหาวิทยาลัย

### Appendix III: Derivation of the Expression from the Proposed Kinetic Model for PBD Hydroformylation



Using the steady state assumption for reaction intermediates, the following equilibria define the concentrations of each may be related to the rate determining step as shown in Eg. 3.10:

$$\frac{-d[\text{C}=\text{C}]}{dt} = \frac{[\text{Rh}]_T K_1 K_2 K_3 K_{\text{H}_2} K_{\text{CO}} K_P [\text{H}_2] [\text{CO}] [\text{C}=\text{C}]}{\alpha} \quad (3.10)$$

where

$$\alpha = [\text{PPh}_3] + K_P(1 + K_{\text{CO}}[\text{CO}]) + K_1 K_{\text{CO}} K_P [\text{C}=\text{C}](1 + K_2) + K_1 K_2 K_3 K_{\text{CO}} K_P [\text{CO}][\text{C}=\text{C}](1 + K_{\text{H}_2}[\text{H}_2])$$

Thus, the functional relationship between the observed first order reaction constant,  $k$  and the studied parameter can be written as follows:

$$k = \frac{K_1 K_2 K_3 K_{H_2} K_{CO} K_P [Rh]_T [H_2] [CO] [C = C]}{A} \quad (\text{AIII-A})$$

where

$$\begin{aligned} A &= [PPh_3] + K_P (1 + K_{CO} [CO]) + K_1 K_{CO} K_P [C = C] (1 + K_2) + K_1 K_2 K_3 K_{CO} K_P [CO] [C = C] (1 + K_{H_2} [H_2]) \\ &= [PPh_3] + K_P + K_P K_{CO} [CO] + K_1 K_{CO} K_P [C = C] + K_1 K_2 K_{CO} K_P [C = C] + K_1 K_2 K_3 K_{CO} K_P [CO] [C = C] \\ &\quad + K_1 K_2 K_3 K_{CO} K_{H_2} K_P [CO] [H_2] [C = C] \\ &= [PPh_3] + K_P + K_P K_{CO} [CO] + (K_1 K_{CO} K_P + K_1 K_2 K_{CO} K_P) [C = C] + K_1 K_2 K_3 K_{CO} K_P [CO] [C = C] \\ &\quad + K_1 K_2 K_3 K_{CO} K_{H_2} K_P [CO] [H_2] [C = C] \end{aligned}$$

According to Henry's Law constant for hydrogen and carbonmonoxide in monochlorobenzene, we can rearrange Eq. AIII-B as:

$$k = \frac{K_1 K_2 K_3 K_{H_2} K_{CO} K_P K_{H,H_2} K_{H,CO} [Rh]_T [H_2] [CO] [C = C]}{A} \quad (\text{AIII-B})$$

where

$$\begin{aligned} A &= [PPh_3] + K_P + K_P K_{CO} K_{H,CO} P_{CO} + (K_1 K_{CO} K_P + K_1 K_2 K_{CO} K_P) [C = C] \\ &\quad + K_1 K_2 K_3 K_{CO} K_P K_{CO} K_{H,CO} P_{CO} [C = C] + K_1 K_2 K_3 K_{CO} K_{H_2} K_P K_{H,CO} K_{H,H_2} P_{CO} P_{H_2} [C = C] \end{aligned}$$

For derivation of PBD hydroformylation on the model, the coefficients from Eq. AIII-B are given as follows:

$$\begin{aligned} K_A &= K_1 K_2 K_3 K_{H_2} K_{CO} K_P K_{H,H_2} K_{H,CO} \\ K_B &= K_P \\ K_C &= K_P K_{CO} K_{H,CO} \\ K_D &= K_1 K_{CO} K_P + K_1 K_2 K_{CO} K_P \\ K_E &= K_1 K_2 K_3 K_{CO} K_P K_{H,CO} \\ K_F &= K_1 K_2 K_3 K_{CO} K_{H_2} K_P K_{H,H_2} K_{H,CO} \end{aligned}$$

Therefore, the first order equation for modeling can be written as Eq. AIII-C.

$$k = \frac{K_A [Rh]_T P_{H_2} P_{CO} [C = C]}{[PPh_3] + K_B + K_C P_{CO} + K_D [C = C] + K_E P_{CO} [C = C] + K_F P_{CO} P_{H_2} [C = C]} \quad (4.1)$$

**Appendix IV: The appearance of hydroformylated PBD (film) and hydroxymethylated PBD**

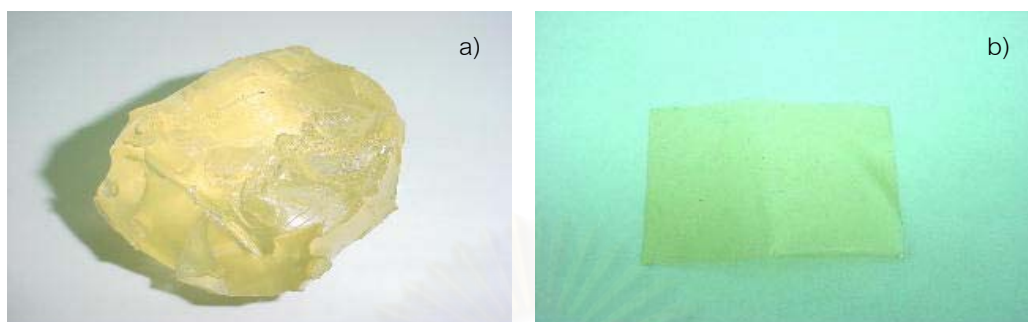


**Figure AIV-A** High Molecular weight of (a) polybutadiene and (b) hydroformylated polybutadiene.

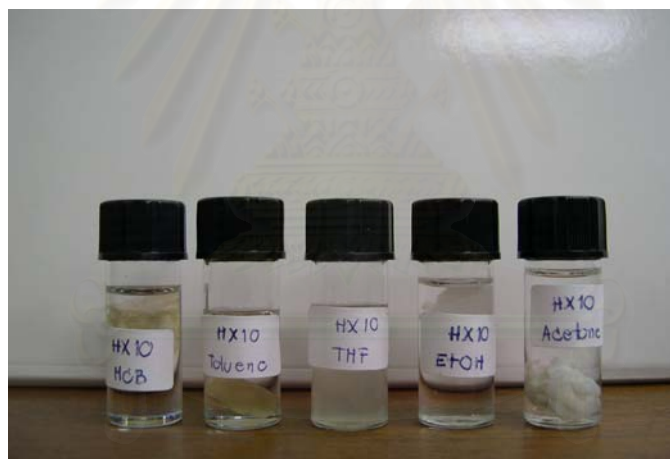


**Figure AIV-B** Hydroxymethylated polybutadiene in various solvent types: MCB, toluene, THF, ethanol, and acetone.

### Appendix V: %Swelling of Hydroformylated Polybutadiene Film in Various Types of Solvent

**Table AV-A** The experimental data for swelling of hydroformylated polybutadiene film in various types of solvent.

<b>Solvent:</b>	Water			
Time (h)	Weight (g)			
	5%CHO	20%CHO	55%CHO	75%CHO
0	0.0108	0.0163	0.01668	0.0495
2	0.0113	0.0178	0.0188	0.05601
4	0.0119	0.0189	0.01998	0.0595
6	0.012	0.0193	0.02034	0.0621
24	0.0121	0.02072	0.0214	0.0642
48	0.0123	0.02119	0.022	0.0667
72	0.0125	0.02125	0.0223	0.0678
96	0.0128	0.02178	0.023	0.0691

<b>Solvent:</b>	Ethanol			
Time (h)	Weight (g)			
	5%CHO	20%CHO	55%CHO	75%CHO
0	0.0144	0.0446	0.0215	0.0339
2	0.0156	0.05	0.0291	0.0495
4	0.0165	0.0556	0.0305	0.0505
6	0.0177	0.0589	0.0311	0.0516

<b>Solvent:</b>	THF			
Time (h)	Weight (g)			
	5%CHO	20%CHO	55%CHO	75%CHO
0	0.0135	0.0668	0.0335	0.0373
2	0.0157	0.125	0.0464	0.058



**Table AV-A (continued)**

Time (h)	Weight (g)			
	5%CHO	20%CHO	55%CHO	75%CHO
0	0.0142	0.0294	0.0509	0.0352
2	0.0152	0.0309	0.0538	0.0366
4	0.0174	0.0349	0.0547	0.0378
6	0.018	0.0354	0.0567	0.0387
24	0.0199	0.0399	0.0601	0.0391
48	0.0203	0.0404	0.0622	0.0408
72	0.0215	0.0408	0.0636	0.0418
96	0.0224	0.0415	0.0659	0.0424

**Table AV-B** %The experimental data for swelling of hydroformylated polybutadiene film in various types of solvent

Time (h)	Weight (g)			
	5%CHO	20%CHO	55%CHO	75%CHO
0	0	0	0	0
2	4.63	9.20	12.71	13.15
4	10.19	15.95	19.78	20.20
6	11.11	18.40	21.94	25.45
24	12.04	27.12	28.30	29.70
48	13.89	30.00	31.89	34.75
72	15.74	30.37	33.69	36.97
96	18.52	33.62	37.89	39.60

**Table AV-B (continued)**

<b>Solvent:</b>		Ethanol			
Time (h)	Weight (g)				
	5%CHO	20%CHO	55%CHO	75%CHO	
0	0	0	0	0	
2	8.33	12.11	35.35	46.02	
4	14.58	24.66	41.86	48.97	
6	22.92	32.06	44.65	52.21	

<b>Solvent:</b>		THF			
Time (h)	Weight (g)				
	5%CHO	20%CHO	55%CHO	75%CHO	
0	0	0	0	0	
2	16.30	87.13	38.51	55.50	

<b>Solvent:</b>		MCB			
Time (h)	Weight (g)				
	5%CHO	20%CHO	55%CHO	75%CHO	
0	0	0	0	0	
2	7.04	5.10	5.70	3.98	
4	22.54	18.71	7.47	7.39	
6	26.76	20.41	11.39	9.94	
24	40.14	35.71	18.07	11.08	
48	42.96	37.41	22.20	15.91	
72	51.41	38.78	24.95	18.75	
96	57.75	41.16	29.47	20.45	

## VITA

Miss Sasisom Im-erbsin was born on August 4, 1978 in Bangkok, Thailand. On her education background, she attended private elementary and secondary schools, including nine years at St. Joseph Bangna School in Samutprakarn and two years at Traim Udom Suksa School in Bangkok. Afterward, she entered Chulalongkorn University and began her four years study in Department of Chemical Technology, Faculty of Science. She received her Bachelor degree of Science with the second class honor in 1999. She has continued her study in Ph.D. program at the Department of Chemical Technology, Faculty of Science, Chulalongkorn University and also received the Royal Golden Jubilee scholarship.

During 2001-2002, she had opportunity to go to University of Waterloo in Canada to work on her dissertation in the Applied Catalysis Laboratory. During her study, she presented the paper on “Hydroformylation of High Molecular Weight *Cis*-1,4-Polybutadiene Catalyzed by  $\text{HRh}(\text{CO})(\text{PPh}_3)_3$  in two conferences, the 39<sup>th</sup> IUPAC Congress and 86<sup>th</sup> Conference of the Canadian Society on 10 - 15 August 2003 at Ottawa Congress Centre, Ottawa, Canada and the 8<sup>th</sup> Pacific Polymer Conference during 24 - 26 November 2003 at Queen Sirikit Convention Center, Bangkok

In 2004, she published an article entitled “Hydroformylation of High Molecular Weight *Cis*-1,4-Polybutadiene Catalyzed by  $\text{HRh}(\text{CO})(\text{PPh}_3)_3$ ” in the Journal of Applied Polymer Science. She graduated with Ph.D. in Chemical Technology in March 2004.

สถาบันวิทยบริการ  
จุฬาลงกรณ์มหาวิทยาลัย